POLSKA AKADEMIA NAUK
INSTYTUT FIZYKI

ACTA PHYSICA POLONICA

DWUMIESIĘCZNIK

Vol. XVII — Fasc. 6

WARSZAWA 1958

First reprint by PWN — Polish Scientific Publishers 1969

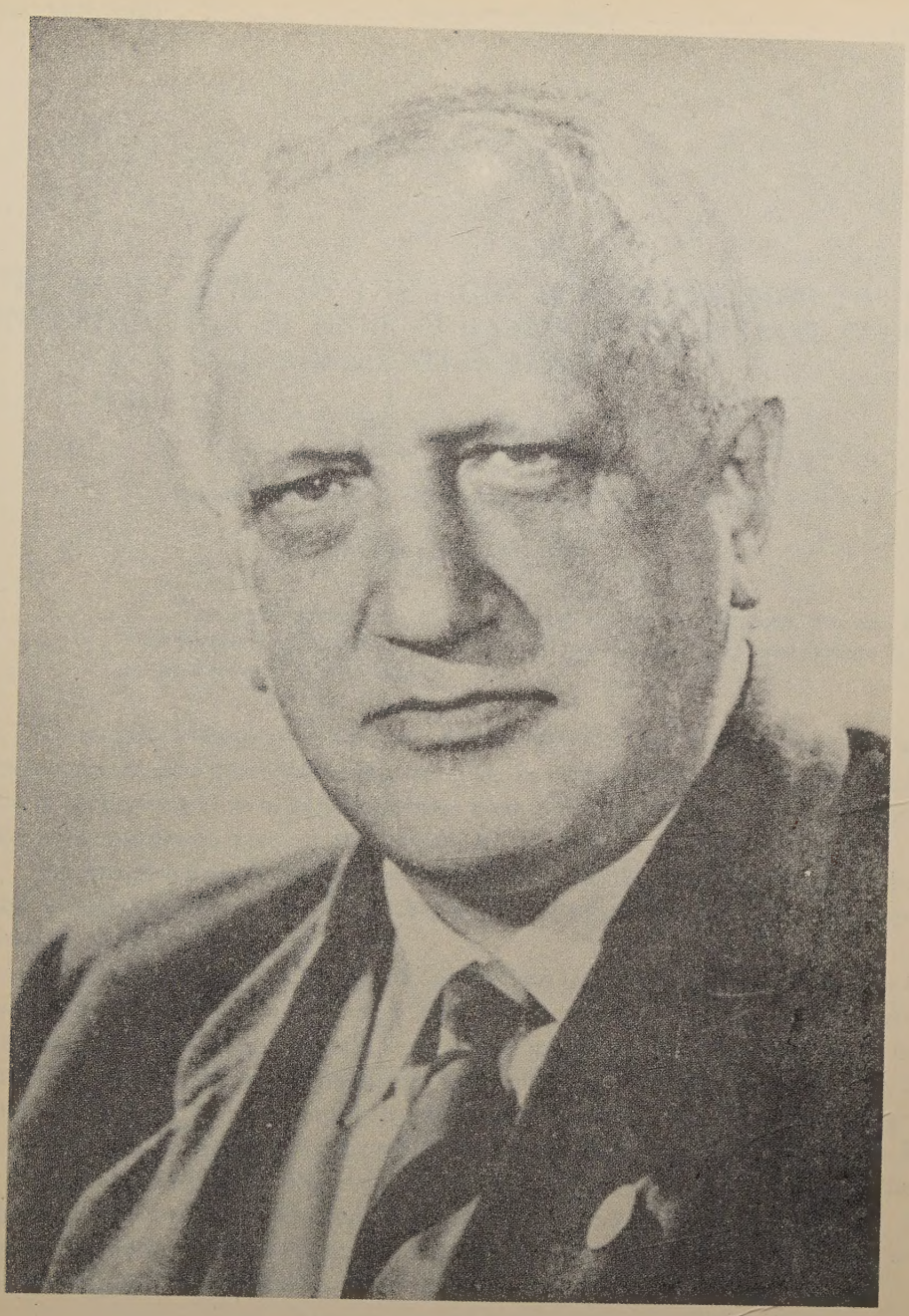

LEOPOLD INFELD

AUGUST 20, 1898 — AUGUST 20, 1958

With best wishes for continued success in his scientific work

The Editorial Staff

THE APPLICATION OF THE TIGHT BINDING METHOD TO THE INVESTIGATION OF ENERGY BANDS IN HEXAGONAL CLOSE-PACKED STRUCTURE. III

By Maria Miąsek

Institute of Theoretical Physics University of Warsaw, Warsaw

(Received July 16, 1957)

The matrix components of energy in the close-packed hexagonal structure have been calculated taking into account the interactions of further neighbours of order 2, 3, 4 in the two-centre approximation.

The tight-binding approximation for hexagonal close-packed structure with further neighbours interaction has been given in part II (1957) of this work and has the validity irrespective of approximations used in computing of the energy integrals. We have taken into account the neighbours of order 2, 3, 4-th.

For completeness we shall now summarize the formulas for two-centre approximation, though it is obvious that for further neighbour interactions the two-centre approximation may be not reliable.

The results of the calculations are summarized in two tables. Table I contains the matrix components of energy $(m/n)_{11}$ expressed in terms of the two-centre integrals. Because the second neighbours of the zero atom in lattice 1 in hexagonal close-packed lattice are only in the simple hexagonal lattice 2, we have in the components $(m/n)_{11}$ only the integrals for 3-rd and 4-th neighbours. Therefore the two-centre integrals $(ss\sigma)$, $(sp\sigma)$ etc. have here the indices "3" for the centre $\boldsymbol{R}_2$ and "4" for the centre $\boldsymbol{R}_3$.

In Table II are given the components $(m/n)_{12}$ in the two-centre approximation. The indices in two-centre integrals are here "2" for the centre I_2 and "4" for the centre I_3. Index "3" does not appear in Table II since the third neighbours are only in the simple lattice 1.

TABLE I

The elements $(m/n)_{11}$ in terms of two-centre integrals — the neighbours of the order 3, 4.

$$(s/yz) = (s/xz) = (x/z) = (x/yz) = (y/z) = (y/xz) = (z/xy) = (z/x^2 - y^2) = (xy/yz) = (xy/xz)$$
$$= (yz/x^2 - y^2) = (yz/3z^2 - r^2) = (xz/x^2 - y^2) = (xz/3z^2 - r^2) = 0$$

$(s|s)$ $2\,(ss\,\sigma)_3 \cos 2\zeta + 2\,(ss\,\sigma)_4\,(2\cos\xi\cos\eta + \cos 2\eta)$

$(s|x)$ $2\sqrt{3}\,i\,(sp\,\sigma)_4 \sin 3\xi \cos\eta$

$(s|y)$ $2i\,(sp\,\sigma)_4\,(\sin 2\eta + \cos 3\xi \sin\eta)$

$(s|z)$ $2i\,(sp\,\sigma)_3 \sin 2\zeta$

$(s|xy)$ $-3\,(sd\,\sigma)_4 \sin 3\xi \sin\eta$

$(s|x^2-y^2)$ $-\sqrt{3}\,(sd\,\sigma)_4\,(\cos 2\eta - \cos 3\xi\cos\eta)$

$(s|3z^2-r^2)$ $2\,(sd\,\sigma)_3 \cos 2\zeta - (sd\,\sigma)_4\,(2\cos 3\xi\cos\eta + \cos 2\eta)$

$(x|x)$ $2\,(pp\,\pi)_3 \cos 2\zeta + [3\,(pp\,\sigma)_4 + (pp\,\pi)_4] \cos 3\xi\cos\eta + 2\,(pp\,\pi)_4 \cos 2\eta$

$(x|y)$ $-\sqrt{3}\,[(pp\,\sigma)_4 - (pp\,\pi)_4] \sin 3\xi \sin\eta$

$(x|xy)$ $\frac{1}{2}\,i\,\{[3\sqrt{3}\,(pd\,\sigma)_4 - 2\,(pd\,\pi)_4] \cos 3\xi \sin\eta + 4\,(pd\,\pi)_4 \sin 2\eta\}$

$(x|xz) = (y|yz)$ $2i\,(pd\,\pi)_3 \sin 2\zeta$

$(x|x^2-y^2) = (y|xy)$ $\frac{1}{2}\,i\,[3\,(pd\,\sigma)_4 + 2\sqrt{3}\,(pd\,\pi)_4] \sin 3\xi\cos\eta$

$(x|3z^2-r^2)$ $-\sqrt{3}i(pd\,\sigma)_4 \sin 3\xi\cos\eta$

$(y|y)$ $2\,(pp\,\pi)_3 \cos 2\zeta + [(pp\,\sigma)_4 + 3\,(pp\,\pi)_4] \cos 3\xi\cos\eta + 2\,(pp\,\sigma)_4 \cos 2\eta$

$(y|x^2-y^2)$ $\frac{1}{2}\,i\,\{[\sqrt{3}\,(pd\,\sigma)_4 - 6\,(pd\,\pi)_4] \cos 3\xi \sin\eta - 2\sqrt{3}\,(pd\,\sigma)_4 \sin 2\eta\}$

$(y|3z^2-r^2)$ $-i\,(pd\,\sigma)_4\,(\sin 2\eta + \cos 3\xi \sin\eta)$

$(z|z)$ $2\,(pp\,\sigma)_3 \cos 2\zeta + 2\,(pp\,\pi)_4\,(2\cos 3\xi\cos\eta + \cos 2\eta)$

$(z|yz)$ $2i\,(pd\,\pi)_4\,(\sin 2\eta + \cos 3\xi \sin\eta)$

$(z|xz)$ $2\sqrt{3}\,i\,(pd\,\pi)_4 \sin 3\xi\cos\eta$

$(z|3z^2-r^2)$ $2i\,(pd\,\sigma)_3 \sin 2\zeta$

$(xy|xy)$ $2\,(dd\,\delta)_3 \cos 2\zeta + \frac{1}{4}\,[9\,(dd\,\sigma)_4 + 4\,(dd\,\pi)_4 + 3\,(dd\,\delta)_4] \cos 3\xi\cos\eta + 2\,(dd\,\pi)_4 \cos 2\eta$

$(xy|x^2-y^2)$ $-\frac{1}{4}\sqrt{3}\,[3\,(dd\,\sigma)_4 - 4\,(dd\,\pi)_4 + (dd\,\delta)_4] \sin 3\xi \sin\eta$

$(xy|3z^2-r^2)$ $\frac{3}{2}\,[(dd\,\sigma)_4 - (dd\,\delta)_4] \sin 3\xi \sin\eta$

$(yz|yz)$ $2\,(dd\,\pi)_3 \cos 2\zeta + [(dd\,\pi)_4 + 3\,(dd\,\delta)_4] \cos 3\xi\cos\eta + 2\,(dd\,\pi)_4 \cos 2\eta$

$(yz|xz)$ $-\sqrt{3}\,[(dd\,\pi)_4 - (dd\,\delta)_4] \sin 3\xi \sin\eta$

(xz/xz) $\quad 2\,(dd\,\pi)_3 \cos 2\zeta + [3\,(dd\,\pi)_4 + (dd\,\delta)_4] \cos 3\xi \cos \eta + 2\,(dd\,\delta)_4 \cos 2\eta$

$(x^2 - y^2/x^2 - y^2)$ $\quad 2\,(dd\,\delta)_3 \cos 2\zeta + \frac{1}{4}\,[3\,(dd\,\sigma)_4 + 12\,(dd\,\pi)_4 + (dd\,\delta)_4] \cos 3\xi \cos \eta +$

$$+ \frac{1}{2}\,[3\,(dd\,\sigma)_4 + (dd\,\delta)_4] \cos 2\eta$$

$(x^2 - y^2/3z^2 - r^2)$ $\quad \frac{1}{2}\sqrt{3}\,[(dd\,\sigma)_4 - (dd\,\delta)_4]\,(\cos 2\eta - \cos 3\xi \cos \eta)$

$(3z^2 - r^2/3z^2 - r^2)$ $\quad 2\,(dd\,\sigma)_3 \cos 2\zeta + \frac{1}{2}\,[(dd\,\sigma)_4 + 3\,(dd\,\delta)_4]\,(2 \cos 3\xi \cos \eta + \cos 2\eta)$

TABLE II

The elements $(m/n)_{12}$ in terms of two-centre integrals — the neighbours of the order 2, 3, 4.

(s/s) $\quad 2\,(ss\,\sigma)_2 \cos \zeta \left[\left(\cos \frac{4}{3}\eta + 2 \cos 2\xi \cos \frac{2}{3}\eta\right) + i\left(\sin \frac{4}{3}\eta - 2 \cos 2\xi \times \right.\right.$

$\left.\left. \times \sin \frac{2}{3}\eta\right)\right] + 4\,(ss\,\sigma)_4 \cos \zeta \left[\left(\cos 3\xi \cos \frac{1}{3}\eta + \cos 2\xi \cos \frac{4}{3}\eta + \right.\right.$

$\left.\left. + \cos \xi \cos \frac{5}{3}\eta\right) + i\left(\cos 3\xi \sin \frac{1}{3}\eta + \cos 2\xi \sin \frac{4}{3}\eta - \cos \xi \sin \frac{5}{3}\eta\right)\right]$

(s/x) $\quad 2\sqrt{2}\,(sp\,\sigma)_2 \sin 2\xi \cos \zeta \left(\sin \frac{2}{3}\eta + i \cos \frac{2}{3}\eta\right) - \frac{2}{3}\sqrt{3}\,(sp\,\sigma)_4 \cos \zeta \times$

$\times \left[\left(3 \sin 3\xi \sin \frac{1}{3}\eta + 2 \sin 2\xi \sin \frac{4}{3}\eta - \sin \xi \sin \frac{5}{3}\eta\right) - \right.$

$\left. - i\left(3 \sin 3\xi \cos \frac{1}{3}\eta + 2 \sin 2\xi \cos \frac{4}{3}\eta + \sin \xi \cos \frac{5}{3}\eta\right)\right]$

(s/y) $\quad 2\sqrt{\frac{2}{3}}\,(sp\,\sigma)_2 \cos \zeta \left[\left(\cos \frac{4}{3}\eta - \cos 2\xi \cos \frac{2}{3}\eta\right) + i\left(\sin \frac{4}{3}\eta + \cos 2\xi \times \right.\right.$

$\left.\left. \times \sin \frac{2}{3}\eta\right)\right] + \frac{2}{3}\,(sp\,\sigma)_4 \cos \zeta \left[\left(\cos 3\xi \cos \frac{1}{3}\eta + 4 \cos 2\xi \cos \frac{4}{3}\eta - \right.\right.$

$\left.\left. - 5 \cos \xi \cos \frac{5}{3}\eta\right) + i\left(\cos 3\xi \sin \frac{1}{3}\eta + 4 \cos 2\xi \sin \frac{4}{3}\eta + \right.\right.$

$\left.\left. + 5 \cos \xi \sin \frac{5}{3}\eta\right)\right]$

(s/z) $\quad \frac{2}{3}\sqrt{3}\,(sp\,\sigma)_2 \sin \zeta \left[\left(2 \cos 2\xi \sin \frac{2}{3}\eta - \sin \frac{4}{3}\eta\right) + i\left(2 \cos 2\xi \cos \frac{2}{3}\eta + \right.\right.$

$$+\cos\frac{4}{3}\eta\Big)\Big]-\frac{4}{3}\sqrt{2}\,(sp\,\sigma)_4\sin\zeta\Big[\Big(\cos 3\xi\sin\frac{1}{3}\eta+\cos 2\xi\sin\frac{4}{3}\eta-$$

$$-\cos\xi\sin\frac{5}{3}\eta\Big)-i\Big(\cos 3\xi\cos\frac{1}{3}\eta+\cos 2\xi\cos\frac{4}{3}\eta+$$

$$+\cos\xi\cos\frac{5}{3}\eta\Big)\Big]$$

$(s|xy)$

$$-2\,(sd\,\sigma)_2\sin 2\xi\cos\zeta\Big(\sin\frac{2}{3}\eta+\mathrm{i}\cos\frac{2}{3}\eta\Big)-\frac{1}{3}\,(sd\,\sigma)_4\cos\zeta\times$$

$$\times\Big[\Big(3\sin 3\xi\sin\frac{1}{3}\eta+8\sin 2\xi\sin\frac{4}{3}\eta+5\sin\xi\sin\frac{5}{3}\eta\Big)-$$

$$-i\Big(3\sin 3\xi\cos\frac{1}{3}\eta+8\sin 2\xi\cos\frac{4}{3}\eta-5\sin\xi\cos\frac{5}{3}\eta\Big)\Big]$$

$(s|yz)$

$$-2\sqrt{\frac{2}{3}}\,(sd\,\sigma)_2\sin\zeta\Big[\Big(\sin\frac{4}{3}\eta+\cos 2\xi\sin\frac{2}{3}\eta\Big)-i\Big(\cos\frac{4}{3}\eta-$$

$$-\cos 2\xi\cos\frac{2}{3}\eta\Big)\Big]-\frac{2}{3}\sqrt{\frac{2}{3}}\,(sd\,\sigma)_4\sin\zeta\Big[\Big(\cos 3\xi\sin\frac{1}{3}\eta+$$

$$+4\cos 2\xi\sin\frac{4}{3}\eta+5\cos\xi\sin\frac{5}{3}\eta\Big)-i\Big(\cos 3\xi\cos\frac{1}{3}\eta+$$

$$+4\cos 2\xi\cos\frac{4}{3}\eta-5\cos\xi\cos\frac{5}{3}\eta\Big)\Big]$$

$(s|xz)$

$$-2\sqrt{2}\,(sd\,\sigma)_2\sin 2\xi\sin\zeta\Big(\cos\frac{2}{3}\eta-i\sin\frac{2}{3}\eta\Big)-\frac{2}{3}\sqrt{2}\,(sd\,\sigma)_4\sin\zeta\times$$

$$\times\Big[\Big(3\sin 3\xi\cos\frac{1}{3}\eta+2\sin 2\xi\cos\frac{4}{3}\eta+\sin\xi\cos\frac{5}{3}\eta\Big)+$$

$$+i\Big(3\sin 3\xi\sin\frac{1}{3}\eta+2\sin 2\xi\sin\frac{4}{3}\eta-\sin\xi\sin\frac{5}{3}\eta\Big)\Big]$$

$(s|x^2-y^2)$

$$-\frac{2}{3}\sqrt{3}\,(sd\,\sigma)_2\cos\zeta\Big[\Big(\cos\frac{4}{3}\eta-\cos 2\xi\cos\frac{2}{3}\eta\Big)+i\Big(\sin\frac{4}{3}\eta+$$

$$+\cos 2\xi\sin\frac{2}{3}\eta\Big)\Big]+\frac{1}{9}\sqrt{3}\,(sd\,\sigma)_4\cos\zeta\Big[\Big(13\cos 3\xi\cos\frac{1}{3}\eta-$$

$$-2\cos 2\xi\cos\frac{4}{3}\eta-11\cos\xi\cos\frac{5}{3}\eta\Big)+i\Big(13\cos 3\xi\sin\frac{1}{3}\eta-$$

$$-2\cos 2\xi\sin\frac{4}{3}\eta+11\cos\xi\sin\frac{5}{3}\eta\Big)\Big]$$

$(s/3z^2 - r^2)$

$$- \frac{2}{3} (sd\,\sigma)_4 \cos\zeta \left[\left(\cos 3\xi \cos \frac{1}{3}\eta + \cos 2\xi \cos \frac{4}{3}\eta + \cos\xi \cos \frac{5}{3}\eta \right) + \right.$$

$$\left. + i \left(\cos 3\xi \sin \frac{1}{3}\eta + \cos 2\xi \sin \frac{4}{3}\eta - \cos\xi \sin \frac{5}{3}\eta \right) \right]$$

(x/x)

$$2 \cos\zeta \left\{ \left((\mathrm{pp}\,\pi)_2 \cos \frac{4}{3}\eta + [(pp\,\sigma)_2 + (pp\,\pi)_2] \cos 2\xi \cos \frac{2}{3}\eta \right) + \right.$$

$$\left. + i \left((pp\,\pi)_2 \sin \frac{4}{3}\eta - [(pp\,\sigma)_2 + (pp\,\pi)_2] \cos 2\xi \sin \frac{2}{3}\eta \right) \right\} +$$

$$+ \frac{1}{3} \cos\zeta \left\{ \left(3\,[3(pp\,\sigma)_4 + (pp\,\pi)_4] \cos 3\xi \cos \frac{1}{3}\eta + 4\,[(pp\,\sigma)_4 + \right. \right.$$

$$\left. + 2\,(pp\,\pi)_4] \cos 2\xi \cos \frac{4}{3}\eta + [(pp\,\sigma)_4 + 11\,(pp\,\pi)_4] \cos\xi \times \right.$$

$$\left. \times \cos \frac{5}{3}\eta \right) + i \left(3\,[3(pp\,\sigma)_4 + (pp\,\pi)_4] \cos 3\xi \sin \frac{1}{3}\eta + \right.$$

$$\left. + 4[(pp\,\sigma)_4 + 2\,(pp\,\pi)_4] \cos 2\xi \sin \frac{4}{3}\eta - [(pp\,\sigma)_4 + \right.$$

$$\left. \left. + 11\,(pp\,\pi)_4] \cos\xi \sin \frac{5}{3}\eta \right) \right\}$$

(x/y)

$$- \frac{2}{3} \sqrt{3}\,[(pp\,\sigma)_2 - (pp\,\pi)_2] \cos\zeta \sin 2\xi \left(\sin \frac{2}{3}\eta + i \cos \frac{2}{3}\eta \right) -$$

$$- \frac{1}{9} \sqrt{3}\,[(pp\,\sigma)_4 - (pp\,\pi)_4] \cos\zeta \left[\left(3 \sin 3\xi \sin \frac{1}{3}\eta + \right. \right.$$

$$\left. + 8 \sin 2\xi \sin \frac{4}{3}\eta + 5 \sin\xi \sin \frac{5}{3}\eta \right) - i \left(3 \sin 3\xi \cos \frac{1}{3}\eta + \right.$$

$$\left. \left. + 8 \sin 2\xi \cos \frac{4}{3}\eta - 5 \sin\xi \cos \frac{5}{3}\eta \right) \right].$$

(x/z)

$$-2 \sqrt{\frac{2}{3}}\,[(pp\,\sigma)_2 - (pp\,\pi)_2] \sin 2\xi \sin\zeta \left(\cos \frac{2}{3}\eta - i \sin \frac{2}{3}\eta \right)$$

$$- \frac{2}{3} \sqrt{\frac{2}{3}}\,[(pp\,\sigma)_4 - (pp\,\pi)_4] \sin\zeta \left[\left(3 \sin 3\xi \cos \frac{1}{3}\eta + \right. \right.$$

$$\left. + 2 \sin 2\xi \cos \frac{4}{3}\eta + \sin\xi \cos \frac{5}{3}\eta \right) + i \left(3 \sin 3\xi \sin \frac{1}{3}\eta + \right.$$

$$\left. \left. + 2 \sin 2\xi \sin \frac{4}{3}\eta - \sin\xi \sin \frac{5}{3}\eta \right) \right]$$

$$(x|xy) \qquad \sqrt{\frac{2}{3}}\cos\zeta\left\{\left(2\,(pd\pi)_2\cos\frac{4}{3}\eta-\sqrt{3}\,(pd\sigma)_2\cos 2\xi\cos\frac{2}{3}\eta\right)+\right.$$

$$\left.+\,i\left(2\,(pd\pi)_2\sin\frac{4}{3}\eta+\sqrt{3}\,(pd\sigma)_2\cos 2\xi\sin\frac{2}{3}\eta\right)\right\}+$$

$$+\frac{1}{18}\cos\zeta\left\{\left(3\left[3\sqrt{3}\,(pd\sigma)_4-2\,(pd\pi)_4\right]\cos 3\xi\cos\frac{1}{3}\eta+\right.\right.$$

$$+16\left[\sqrt{3}\,(pd\sigma)_4+(pd\pi)_4\right]\cos 2\xi\cos\frac{4}{3}\eta-5\left[\sqrt{3}\,(pd\sigma)_4+\right.$$

$$\left.\left.+10\,(pd\pi)_4\right]\cos\xi\cos\frac{5}{3}\eta\right)+i\left(3\left[3\sqrt{3}\,(pd\sigma)_4-2\,(pd\pi)_4\right]\times\right.$$

$$\times\cos 3\xi\sin\frac{1}{3}\eta+16\left[\sqrt{3}\,(pd\sigma)_4+(pd\pi)_4\right]\cos 2\xi\sin\frac{4}{3}\eta+$$

$$\left.+5\left[\sqrt{3}\,(pd\sigma)_4+10\,(pd\pi)_4\right]\cos\xi\sin\frac{5}{3}\eta\right)\Big\}$$

$$(x|yz)= \qquad \frac{2}{9}\sqrt{3}\left[3\,(pd\sigma)_2-2\sqrt{3}\,(pd\pi)_2\right]\sin 2\xi\sin\zeta\left(\cos\frac{2}{3}\eta-i\sin\frac{2}{3}\eta\right)-$$

$$=(y|xz)= \qquad -\frac{1}{9}\sqrt{\frac{2}{3}}\left[\sqrt{3}\,(pd\sigma)_4-2\,(pd\pi)_4\right]\sin\zeta\left[\left(3\sin 3\xi\cos\frac{1}{3}\eta+\right.\right.$$

$$=(z|xy) \qquad \left.+8\sin 2\xi\cos\frac{4}{3}\eta-5\sin\xi\cos\frac{5}{3}\eta\right)+i\left(3\sin 3\xi\sin\frac{1}{3}\eta+\right.$$

$$\left.\left.+8\sin 2\xi\sin\frac{4}{3}\eta+5\sin\xi\sin\frac{5}{3}\eta\right)\right]$$

$$(x|xz) \qquad \frac{2}{3}\sin\zeta\left\{\left(3(pd\sigma)_2\cos 2\xi\sin\frac{2}{3}\eta-\sqrt{3}\,(pd\pi)_2\sin\frac{4}{3}\eta\right)+i\left[3\,(pd\sigma)_2\times\right.\right.$$

$$\left.\left.\times\cos 2\zeta\cos\frac{2}{3}\eta+\sqrt{3}(pd\pi)_2\cos\frac{4}{3}\eta\right]\right\}-\frac{1}{9}\sqrt{2}\sin\zeta\times$$

$$\times\left\{\left(3\left[3\sqrt{3}\,(pd\sigma)_4-2\,(pd\pi)_4\right]\cos 3\xi\sin\frac{1}{3}\eta+4\left[\sqrt{3}\,(pd\sigma)_4+\right.\right.\right.$$

$$\left.+(pd\pi)_4\right]\cos 2\xi\sin\frac{4}{3}\eta-\left[\sqrt{3}\,(pd\sigma)_4+10\,(pd\pi)_4\right]\cos\xi\times$$

$$\left.\times\sin\frac{5}{3}\eta\right)-i\left(3\left[3\sqrt{3}\,(pd\sigma)_4-2\,(pd\pi)_4\right]\cos 3\xi\cos\frac{1}{3}\eta+\right.$$

$$+4\left[\sqrt{3}\,(pd\sigma)_4+(pd\pi)_4\right]\cos 2\xi\cos\frac{4}{3}\eta+\left[\sqrt{3}\,(pd\sigma)_4+\right.$$

$$\left.\left.+10\,(pd\pi)_4\right]\cos\xi\cos\frac{5}{3}\eta\right)\Big\}$$

$(x|x^2-y^2)$

$$\frac{1}{3}\sqrt{\frac{2}{3}}\left[3(pd\sigma)_2+4\sqrt{3}(pd\pi)_2\right]\sin 2\xi\cos\zeta\left(\sin\frac{2}{3}\eta+i\cos\frac{2}{3}\eta\right)-$$

$$-\frac{1}{54}\cos\zeta\left\{\left(3\left[39(pd\sigma)_4+10\sqrt{3}(pd\pi)_4\right]\sin 3\xi\sin\frac{1}{3}\eta-\right.\right.$$

$$-4\left[3(pd\sigma)_4-20\sqrt{3}(pd\pi)_4\right]\sin 2\xi\sin\frac{4}{3}\eta+\left[33(pd\sigma)_4-\right.$$

$$\left.-58\sqrt{3}(pd\pi)_4\right]\sin\xi\sin\frac{5}{3}\eta\Big)-i\Big(3\left[39(pd\sigma)_4+10\sqrt{3}(pd\pi)\right]\times$$

$$\times\sin 3\xi\cos\frac{1}{3}\eta-4\left[3(pd\sigma)_4-20\sqrt{3}(pd\pi)_4\right]\sin 2\xi\cos\frac{4}{3}\eta-$$

$$\left.-\left[33(pd\sigma)_4-58\sqrt{3}(pd\pi)_4\right]\sin\xi\cos\frac{5}{3}\eta\Big)\right\}$$

$(x|3z^2-r^2)$

$$-2\sqrt{\frac{2}{3}}(pd\pi)_2\sin 2\xi\cos\zeta\left(\sin\frac{2}{3}\eta+i\cos\frac{2}{3}\eta\right)+\frac{1}{9}\left[\sqrt{3}(pd\sigma)_4+\right.$$

$$+4(pd\pi)_4\cos\zeta\left[\left(3\sin 3\xi\sin\frac{1}{3}\eta+2\sin 2\xi\sin\frac{4}{3}\eta-\sin\xi\times\right.\right.$$

$$\left.\left.\times\sin\frac{5}{3}\eta\right)-i\left(3\sin 3\xi\cos\frac{1}{3}\eta+2\sin 2\xi\cos\frac{4}{3}\eta+\sin\xi\cos\frac{5}{3}\eta\right)\right]$$

$(y|y)$

$$\frac{2}{3}\cos\zeta\left\{\left(\left[2(pp\sigma)_2+(pp\pi)_2\right]\cos\frac{4}{3}\eta+\left[(pp\sigma)_2+5(pp\pi)_2\right]\times\right.\right.$$

$$\times\cos 2\xi\cos\frac{2}{3}\eta\Big)+i\left(\left[2(pp\sigma)_2+(pp\pi)_2\right]\sin\frac{4}{3}\eta-\right.$$

$$\left.\left.-\left[(pp\sigma)_2+5(pp\pi)_2\right]\cos 2\xi\sin\frac{2}{3}\eta\Big)\right\}+\frac{1}{9}\cos\zeta\left\{\left(\left[(pp\sigma)_4+\right.\right.\right.$$

$$35(pp\pi)_4\cos 3\xi\cos\frac{1}{3}\eta+4\left[4(pp\sigma)_4+5(pp\pi)_4\right]\cos 2\xi\times$$

$$\times\cos\frac{4}{3}\eta+\left[25(pp\sigma)_4+11(pp\pi)_4\right]\cos\xi\cos\frac{5}{3}\eta\Big)+$$

$$+i\left(\left[(pp\sigma)_4+35(pp\pi)_4\right]\cos 3\xi\sin\frac{1}{3}\eta+4\left[4(pp\sigma)_4+\right.\right.$$

$$\left.\left.+5(pp\pi)_4\right]\cos 2\xi\sin\frac{4}{3}\eta-\left[25(pp\sigma)_4+11(pp\pi)_4\right]\cos\xi\sin\frac{5}{3}\eta\Big)\right\}$$

$(y|z)$

$$-\frac{2}{3}\sqrt{2}\left[(pp\sigma)_2-(pp\pi)_2\right]\sin\zeta\left[\left(\sin\frac{4}{3}\eta+\cos 2\xi\sin\frac{2}{3}\eta\right)-\right.$$

$$- i\left(\cos\frac{4}{3}\eta - \cos 2\xi\cos\frac{2}{3}\eta\right)\Big] - \frac{2}{9}\sqrt{2}\,[(pp\sigma)_4 - (pp\pi)_4]\times$$

$$\times \sin\zeta\left[\left(\cos 3\xi\sin\frac{1}{3}\eta + 4\cos 2\xi\sin\frac{4}{3}\eta + 5\cos\xi\sin\frac{5}{3}\eta\right) -\right.$$

$$\left. - i\left(\cos 3\xi\cos\frac{1}{3}\eta + 4\cos 2\xi\cos\frac{4}{3}\eta - 5\cos\xi\cos\frac{5}{3}\eta\right)\right]$$

$(y|xy)$

$$\frac{1}{3}\sqrt{\frac{2}{3}}\,[3(pd\sigma)_2 + 4\sqrt{3}(pd\pi)_2]\sin 2\xi\cos\zeta\left(\sin\frac{2}{3}\eta + i\cos\frac{2}{3}\eta\right) -$$

$$- \frac{1}{54}\cos\zeta\left\{\left(3\,[3\,(pd\sigma)_4 + 34\sqrt{3}\,(pd\pi)_4]\sin 3\xi\sin\frac{1}{3}\eta +\right.\right.$$

$$+ 8\,[12\,(pd\sigma)_4 + \sqrt{3}\,(pd\pi)_4]\sin 2\xi\sin\frac{4}{3}\eta - [75\,(pd\sigma)_4 -$$

$$\left. - 14\sqrt{3}\,(pd\pi)_4]\sin\xi\sin\frac{5}{3}\eta\right) - i\left(3\,[3\,(pd\sigma)_4 + 34\sqrt{3}\,(pd\pi)_4]\times\right.$$

$$\times \sin 3\xi\cos\frac{1}{3}\eta + 8\,[12\,(pd\sigma)_4 + \sqrt{3}\,(pd\pi)_4]\sin 2\xi\cos\frac{4}{3}\eta +$$

$$\left.\left. + [75\,(pd\sigma)_4 - 14\sqrt{3}\,(pd\pi)_4]\sin\xi\cos\frac{5}{3}\eta\right)\right\}$$

$(y|yz)$

$$- \frac{2}{9}\sin\zeta\left\{\left([6(pd\sigma)_2 - \sqrt{3}(pd\pi)_2]\sin\frac{4}{3}\eta - [3\,(pd\sigma)_2 +\right.\right.$$

$$+ 4\sqrt{3}\,(pd\pi)_2]\cos 2\xi\sin\frac{2}{3}\eta\Big) - i\left([6\,(pd\sigma)_2 - \sqrt{3}\,(pd\pi)_2]\times\right.$$

$$\left.\left.\times\cos\frac{4}{3}\eta + [3\,(pd\sigma)_2 + 4\sqrt{3}\,(pd\pi)_2]\cos 2\xi\cos\frac{2}{3}\eta\right)\right\} -$$

$$- \frac{1}{27}\sqrt{2}\sin\zeta\left\{\left([\sqrt{3}\,(pd\sigma)_4 + 34(pd\pi)_4]\cos 3\xi\sin\frac{1}{3}\eta +\right.\right.$$

$$+ 4\,[4\sqrt{3}\,(pd\sigma)_4 + (pd\pi)_4]\cos 2\xi\sin\frac{4}{3}\eta - [25\sqrt{3}\,(pd\sigma)_4 -$$

$$- 14\,(pd\pi)_4]\cos\xi\sin\frac{5}{3}\eta\Big) - i\left([\sqrt{3}\,(pd\sigma)_4 + 34\,(pd\pi)_4]\times\right.$$

$$\times\cos 3\xi\cos\frac{1}{3}\eta + 4\,[4\sqrt{3}\,(pd\sigma)_4 + (pd\pi)_4]\cos 2\xi\cos\frac{4}{3}\eta +$$

$$\left.\left. + [25\sqrt{3}\,(pd\sigma)_4 - 14(pd\pi)_4]\cos\xi\cos\frac{5}{3}\eta\right)\right\}$$

(y/x^2-y^2)

$$-\frac{1}{3}\sqrt{\frac{2}{3}}\cos\zeta\left\{\left(2\left[\sqrt{3}\,(pd\,\sigma)_2+(pd\,\pi)_2\right]\cos\frac{4}{3}\eta+\left[\sqrt{3}\,(pd\,\sigma)_2-\right.\right.\right.$$

$$\left.-8(pd\,\pi)_2\right]\cos 2\xi\cos\frac{2}{3}\eta\Big)+i\left(2\left[\sqrt{3}\,(pd\,\sigma)_2+(pd\,\pi)_2\right]\times\right.$$

$$\left.\times\sin\frac{4}{3}\eta-\left[\sqrt{3}\,(pd\,\sigma)_2-8(pd\,\pi)_2\right]\cos 2\xi\sin\frac{2}{3}\eta\right)\Big\}+$$

$$+\frac{1}{54}\cos\zeta\left\{\left(\left[13\sqrt{3}\,(pd\,\sigma)_4-62(pd\,\pi)_4\right]\cos 3\xi\cos\frac{1}{3}\eta-\right.\right.$$

$$-8\left[\sqrt{3}(pd\,\sigma)_4+16\,(pd\,\pi)_4\right]\cos 2\xi\cos\frac{4}{3}\eta+5\left[11\sqrt{3}\,(pd\,\sigma)_4+\right.$$

$$\left.+14\,(pd\,\pi)_4\right]\cos\xi\cos\frac{5}{3}\eta\Big)+i\left(\left[13\sqrt{3}\,(pd\,\sigma)_4-62\,(pd\,\pi)_4\right]\times\right.$$

$$\times\cos 3\xi\sin\frac{1}{3}\eta-8\left[\sqrt{3}\,(pd\,\sigma)_4+16\,(pd\,\pi)_4\right]\cos 2\xi\sin\frac{4}{3}\eta-$$

$$\left.\left.-5\left[11\sqrt{3}\,(pd\,\sigma)_4+14\,(pd\,\pi)_4\right]\cos\xi\sin\frac{5}{3}\eta\right)\right\}$$

$(y/3z^2-r^2)$

$$-\frac{2}{3}\sqrt{2}\,(pd\,\pi)_2\cos\zeta\left[\left(\cos\frac{4}{3}\eta-\cos 2\xi\cos\frac{2}{3}\eta\right)+i\left(\sin\frac{4}{3}\eta+\right.\right.$$

$$\left.+\cos 2\xi\sin\frac{2}{3}\eta\right)\Big]-\frac{1}{27}\left[3(pd\,\sigma)_4+4\sqrt{3}\,(pd\,\pi)_4\right]\cos\zeta\times$$

$$\times\left[\left(\cos 3\xi\cos\frac{1}{3}\eta+4\cos 2\xi\cos\frac{4}{3}\eta-5\cos\xi\cos\frac{5}{3}\eta\right)+\right.$$

$$\left.+i\left(\cos 3\xi\sin\frac{1}{3}\eta+4\cos 2\xi\sin\frac{4}{3}\eta+5\cos\xi\sin\frac{5}{3}\eta\right)\right]$$

(z/z)

$$\frac{2}{3}\left[(pp\,\sigma)_2+2(pp\,\pi)_2\right]\cos\xi\left[\left(\cos\frac{4}{3}\eta+2\cos 2\xi\cos\frac{2}{3}\eta\right)+\right.$$

$$\left.+i\left(\sin\frac{4}{3}\eta-2\cos 2\xi\sin\frac{2}{3}\eta\right)\right]+\frac{4}{9}\left[2(pp\,\sigma)_4+7(pp\,\pi)_4\right]\times$$

$$\times\cos\zeta\left[\left(\cos 3\xi\cos\frac{1}{3}\eta+\cos 2\xi\cos\frac{4}{3}\eta+\cos\xi\cos\frac{5}{3}\eta\right)+\right.$$

$$\left.+i\left(\cos 3\xi\sin\frac{1}{3}\eta+\cos 2\xi\sin\frac{4}{3}\eta-\cos\xi\sin\frac{5}{3}\eta\right)\right]$$

(z/yz)

$$\frac{2}{3}\sqrt{\frac{2}{3}}\left[\sqrt{3}\,(pd\,\sigma)_2+(pd\,\pi)_2\right]\cos\zeta\left[\left(\cos\frac{4}{3}\eta-\cos 2\xi\cos\frac{2}{3}\eta\right)+\right.$$

$$+ i\left(\sin\frac{4}{3}\eta + \cos 2\xi \sin\frac{2}{3}\eta\right)\Big] + \frac{1}{27}\,[4\sqrt{3}\,(pd\,\sigma)_4 +$$

$$+ 10\,(pd\,\pi)_4]\cos\zeta\Big[\Big(\cos 3\xi\cos\frac{1}{3}\eta + 4\cos 2\xi\cos\frac{4}{3}\eta -$$

$$- 5\cos\xi\cos\frac{5}{3}\eta\Big) + i\Big(\cos 3\xi\sin\frac{1}{3}\eta + 4\cos 2\xi\sin\frac{4}{3}\eta +$$

$$+ 5\cos\xi\sin\frac{5}{3}\eta\Big)\Big]$$

$(z|xz)$

$$\frac{2}{3}\sqrt{\frac{2}{3}}\,[3(pd\,\sigma)_2 + \sqrt{3}\,(pd\,\pi)_2]\sin 2\xi\cos\zeta\left(\sin\frac{2}{3}\eta + i\cos\frac{2}{3}\eta\right) -$$

$$- \frac{2}{27}\,[6\,(pd\,\sigma)_4 + 5\sqrt{3}\,(pd\,\pi)_4]\cos\zeta\Big[\Big(3\sin 3\xi\sin\frac{1}{3}\eta +$$

$$+ 2\sin 2\xi\sin\frac{4}{3}\eta - \sin\xi\sin\frac{5}{3}\eta\Big) - i\Big(3\sin 3\xi\cos\frac{1}{3}\eta +$$

$$+ 2\sin 2\xi\cos\frac{4}{3}\eta + \sin\xi\cos\frac{5}{3}\eta\Big)\Big]$$

$(z|x^2 - y^2)$

$$\frac{2}{9}\,[3(pd\,\sigma)_2 - 2\sqrt{3}\,(pd\,\pi)_2]\sin\zeta\Big[\Big(\sin\frac{4}{3}\eta + \cos 2\xi\sin\frac{2}{3}\eta\Big) -$$

$$- i\Big(\cos\frac{4}{3}\eta - \cos 2\xi\cos\frac{2}{3}\eta\Big)\Big] - \frac{1}{27}\sqrt{2}\,[\sqrt{3}\,(pd\,\sigma)_4 -$$

$$- 2\,(pd\,\pi)_4]\sin\zeta\Big[\Big(13\cos 3\xi\sin\frac{1}{3}\eta - 2\cos 2\xi\sin\frac{4}{3}\eta +$$

$$+ 11\cos\xi\sin\frac{5}{3}\eta\Big) - i\Big(13\cos 3\xi\cos\frac{1}{3}\eta - 2\cos 2\xi\cos\frac{4}{3}\eta -$$

$$- 11\cos\xi\cos\frac{5}{3}\eta\Big)\Big]$$

$(z|3z^2 - r^2)$

$$\frac{4}{3}\,(pd\,\pi)_2\sin\zeta\Big[\Big(2\cos 2\xi\sin\frac{2}{3}\eta - \sin\frac{4}{3}\eta\Big) + i\Big(2\cos 2\xi\cos\frac{2}{3}\eta +$$

$$+ \cos\frac{4}{3}\eta\Big)\Big[+ \frac{2}{27}\sqrt{2}\,[3\,(pd\,\sigma)_4 - 14\sqrt{3}\,(pd\,\pi)_4]\sin\zeta\Big[\Big(\cos 3\xi \times$$

$$\times \sin\frac{1}{3}\eta + \cos 2\xi\sin\frac{4}{3}\eta - \cos\xi\sin\frac{5}{3}\eta\Big) - i\,(\cos 3\xi\cos\frac{1}{3}\eta +$$

$$+ \cos 2\xi\cos\frac{4}{3}\eta + \cos\xi\cos\frac{5}{3}\eta\Big)\Big]$$

$(xy|xy)$

$$\frac{1}{3}\cos\zeta\left\{\left(2\left[2\,(dd\,\pi)_2+(dd\,\delta)_2\right]\cos\frac{4}{3}\,\eta+\left[3\,(dd\,\sigma)_2+\right.\right.\right.$$

$$4\,(dd\,\pi)_2+5\,(dd\,\delta)_2\left.\right]\cos 2\xi\cos\frac{2}{3}\,\eta\Big)+i\left(2\left[2\,(dd\,\pi)_2+\right.\right.$$

$$\left.\left.+\,(dd\,\delta)_2\right]\sin\frac{4}{3}\,\eta-\left[3\,(dd\,\sigma)_2+4\,(dd\,\pi)_2+5\,(dd\,\delta)_2\right]\times\right.$$

$$\left.\times\cos 2\xi\sin\frac{2}{3}\,\eta\right)+\frac{1}{108}\cos\zeta\left\{\left(3\left[9\,(dd\,\sigma)_4+100\,(dd\,\pi)_4+\right.\right.\right.$$

$$\left.+\,35\,(dd\,\delta)_4\right]\cos 3\xi\cos\frac{1}{3}\,\eta+16\left[12\,(dd\,\sigma)_4+5\,(dd\,\pi)_4+\right.$$

$$\left.+\,10\,(dd\,\delta)_4\right]\cos 2\xi\cos\frac{4}{3}\,\eta+\left[75\,(dd\,\sigma)_4+236\,(dd\,\pi)_4+\right.$$

$$\left.+\,121\,(dd\,\delta)_4\right]\cos\xi\cos\frac{5}{3}\,\eta\Big)+i\left(3\left[9(dd\sigma)_4+100\,(dd\,\pi)_4+\right.\right.$$

$$\left.+\,35(dd\,\delta)_4\right]\cos 3\xi\sin\frac{1}{3}\,\eta+16\left[12\,(dd\,\sigma)_4+5\,(dd\,\pi)_4+\right.$$

$$\left.+\,10\,(dd\,\delta)_4\right]\cos 2\xi\sin\frac{4}{3}\,\eta-\left[75\,(dd\,\sigma)_4+236\,(dd\,\pi)_4+\right.$$

$$\left.\left.+\,121\,(dd\,\delta)_4\right]\cos\xi\sin\frac{5}{3}\,\eta\right)\Big\}$$

$(xy|yz)$

$$-\frac{1}{3}\sqrt{\frac{2}{3}}\left[3\,(dd\,\sigma)_2+2\,(dd\,\pi)_2-5\,(dd\,\delta)_2\right]\sin 2\xi\sin\zeta\left(\cos\frac{2}{3}\,\eta-\right.$$

$$\left.i\sin\frac{2}{3}\,\eta\right)-\frac{1}{54}\sqrt{\frac{2}{3}}\sin\zeta\left\{\left(3\left[3\,(dd\,\sigma)_4+32\,(dd\,\pi)_4-\right.\right.\right.$$

$$\left.-\,35\,(dd\,\delta)_4\right]\sin 3\xi\cos\frac{1}{3}\,\eta+8\left[12\,(dd\,\sigma)_4-7\,(dd\,\pi)_4-\right.$$

$$\left.-\,5\,(dd\,\delta)_4\right]\sin 2\xi\cos\frac{4}{3}\,\eta+\left[75\,(dd\sigma)_4-64\,(dd\,\pi)_4-\right.$$

$$\left.-\,11\,(dd\,\delta)_4\right]\sin\xi\cos\frac{5}{3}\,\eta\Big)+i\left(3\left[3\,(dd\,\sigma)_4+32\,(dd\,\pi)_4-\right.\right.$$

$$\left.-\,35\,(dd\,\delta)_4\right]\sin 3\xi\sin\frac{1}{3}\,\eta+8\left[12\,(dd\,\sigma)_4-7\,(dd\,\pi)_4-\right.$$

$$\left.-\,5\,(dd\,\delta)_4\right]\sin 2\xi\sin\frac{4}{3}\,\eta-\left[75\,(dd\,\sigma)_4-64\,(dd\,\pi)_4-\right.$$

$$\left.\left.-\,11\,(dd\,\delta)_4\right]\sin\xi\sin\frac{5}{3}\,\eta\right)\Big\}$$

$(xy|xz)$

$$-\frac{1}{3}\sqrt{2}\sin\zeta\left\{\left(2\left[(dd\pi)_2-(dd\delta)_2\right]\sin\frac{4}{3}\eta+\left[3(dd\sigma)_2-\right.\right.\right.$$

$$\left.\left.\left.-2(dd\pi)_2-(dd\delta)_2\right]\cos 2\xi\sin\frac{2}{3}\eta\right)-i\left(2\left[(dd\pi)_2-\right.\right.\right.$$

$$\left.\left.\left.-(dd\delta)_2\right]\cos\frac{4}{3}\eta-\left[3(dd\sigma)_2-2(dd\pi)_2-(dd\delta)_2\right]\times\right.\right.$$

$$\left.\left.\times\cos 2\xi\cos\frac{2}{3}\eta\right)\right\}-\frac{1}{54}\sqrt{2}\sin\zeta\left\{\left(3\left[9(dd\sigma)_4-8(dd\pi)_4-\right.\right.\right.$$

$$\left.\left.\left.-(dd\delta)_4\right]\cos 3\xi\sin\frac{1}{3}\eta+16\left[3(dd\sigma)_4-(dd\pi)_4-\right.\right.\right.$$

$$\left.\left.\left.-2(dd\delta)_4\right]\cos 2\xi\sin\frac{4}{3}\eta+5\left[3(dd\sigma)_4+8(dd\pi)_4-\right.\right.\right.$$

$$\left.\left.\left.-11(dd\delta)_4\right]\cos\xi\sin\frac{5}{3}\eta\right)-i\left(3\left[9(dd\sigma)_4-8(dd\pi)_4-\right.\right.\right.$$

$$\left.\left.\left.-(dd\delta)_4\right]\cos 3\xi\cos\frac{1}{3}\eta+16\left[3(dd\sigma)_4-(dd\pi)_4-\right.\right.\right.$$

$$\left.\left.\left.-2(dd\delta)_4\right]\cos 2\xi\cos\frac{4}{3}\eta-5\left[3(dd\sigma)_4+8(dd\pi)_4-\right.\right.\right.$$

$$\left.\left.\left.-11(dd\delta)_4\right]\cos\xi\cos\frac{5}{3}\eta\right)\right\}$$

$(xy|x^2-y^2)$

$$-\frac{1}{9}\sqrt{3}\left[3(dd\sigma)_2-4(dd\pi)_2+(dd\delta)_2\right]\sin 2\xi\cos\zeta\left(\sin\frac{2}{3}\eta+\right.$$

$$\left.+i\cos\frac{2}{3}\eta\right)-\frac{1}{324}\sqrt{3}\left[3(dd\sigma)_4-4(dd\pi)_4+(dd\delta)_4\right]\times$$

$$\times\cos\zeta\left[\left(39\sin 3\xi\sin\frac{1}{3}\eta-16\sin 2\xi\sin\frac{4}{3}\eta-55\sin\xi\times\right.\right.$$

$$\left.\left.\times\sin\frac{5}{3}\eta\right)-i\left(39\sin 3\xi\cos\frac{1}{3}\eta-16\sin 2\xi\cos\frac{4}{3}\eta+\right.\right.$$

$$\left.\left.+55\sin\xi\cos\frac{5}{3}\eta\right)\right]$$

$(xy|3z^2-r^2)$

$$\frac{4}{3}\left[(dd\pi)_2-(dd\delta)_2\right]\sin 2\xi\cos\zeta\left(\sin\frac{2}{3}\eta+i\cos\frac{2}{3}\eta\right)+$$

$$+\frac{1}{54}\left[3(dd\sigma)_4+8(dd\pi)_4-11(dd\delta)_4\right]\cos\zeta\left[\left(3\sin 3\xi\times\right.\right.$$

$$\times \sin\frac{1}{3}\eta + 8\sin 2\xi \sin\frac{4}{3}\eta + 5\sin\xi\sin\frac{5}{3}\eta\Big) - i\Big(3\sin 3\xi \times$$

$$\times \cos\frac{1}{3}\eta + 8\sin 2\xi\cos\frac{4}{3}\eta - 5\sin\xi\cos\frac{5}{3}\eta\Big)\Big]$$

$(yz|yz)$

$$\frac{2}{9}\cos\zeta\Big\{\Big(\Big[6\,(dd\,\sigma)_2 + (dd\,\pi)_2 + 2\,(dd\,\delta)_2\Big]\cos\frac{4}{3}\eta +$$

$$+ \Big[3\,(dd\,\sigma)_2 + 5\,(dd\,\pi)_2 + 10\,(dd\,\delta)_2\Big]\cos 2\xi\cos\frac{2}{3}\eta\Big) +$$

$$+ i\Big(\Big[6\,(dd\,\sigma)_2 + (dd\,\pi)_2 + 2(dd\,\delta)_2\Big]\sin\frac{4}{3}\eta - \Big[3\,(dd\,\sigma)_2 +$$

$$+ 5\,(dd\,\pi)_2 + 10\,(dd\,\delta)_2\Big]\cos 2\xi\sin\frac{2}{3}\eta\Big)\Big\} + \frac{1}{81}\cos\zeta \times$$

$$\times\Big\{\Big(\Big[6\,(dd\,\sigma)_4 + 73\,(dd\,\pi)_4 + 245\,(dd\,\delta)_4\Big]\cos 3\xi\cos\frac{1}{3}\eta +$$

$$+ 4\Big[24\,(dd\,\sigma)_4 + 22\,(dd\,\pi)_4 + 35\,(dd\,\delta)_4\Big]\cos 2\xi\cos\frac{4}{3}\eta +$$

$$+ \Big[150\,(dd\,\sigma)_4 + 97\,(dd\,\pi)_4 + 77\,(dd\,\delta)_4\Big]\cos\xi\cos\frac{5}{3}\eta\Big) +$$

$$+ i\Big(\Big[6\,(dd\,\sigma)_4 + 73\,(dd\,\pi)_4 + 245\,(dd\,\delta)_4\Big]\cos 3\xi\sin\frac{1}{3}\eta +$$

$$+ 4\Big[24\,(dd\,\sigma)_4 + 22\,(dd\,\pi)_4 + 35\,(dd\,\delta)_4\Big]\cos 2\xi\sin\frac{4}{3}\eta -$$

$$- \Big[150\,(dd\,\sigma)_4 + 97\,(dd\,\pi)_4 + 77\,(dd\,\delta)_4\Big]\cos\xi\sin\frac{5}{3}\eta\Big)\Big\}$$

$(yz|xz)$

$$-\frac{2}{9}\sqrt{3}\Big[3\,(dd\,\sigma)_2 - (dd\,\pi)_2 - 2\,(dd\,\delta)_2\Big]\sin 2\xi\cos\zeta\Big(\sin\frac{2}{3}\eta +$$

$$+ i\cos\frac{2}{3}\eta\Big) - \frac{1}{81}\sqrt{3}\cos\zeta\Big[6\,(dd\,\sigma)_4 + (dd\,\pi)_4 -$$

$$- 7\,(dd\,\delta)_4\Big]\Big[\Big(3\sin 3\xi\sin\frac{1}{3}\eta + 8\sin 2\xi\sin\frac{4}{3}\eta + 5\sin\xi\sin\frac{5}{3}\eta\Big) -$$

$$- i\Big(3\sin 3\xi\cos\frac{1}{3}\eta + 8\sin 2\xi\cos\frac{4}{3}\eta - 5\sin\xi\cos\frac{5}{3}\eta\Big)\Big]$$

$(yz|x^2-y^2)$

$$\frac{1}{9}\sqrt{2}\sin\zeta\Big\{\Big(2\Big[3\,(dd\,\sigma)_2 - (dd\,\pi)_2 - 2\,(dd\,\delta)_2\Big]\sin\frac{4}{3}\eta -$$

$$- \left[3\,(dd\,\sigma)_2 - 10\,(dd\,\pi)_2 + 7\,(dd\,\delta)_2\right] \cos 2\xi \sin \frac{2}{3}\,\eta \Big) -$$

$$- i \left(2\left[3\,(dd\,\sigma)_2 - (dd\,\pi)_2 - 2\,(dd\,\delta)_2\right] \cos \frac{4}{3}\,\eta + \left[3\,(dd\,\sigma)_2 - \right.\right.$$

$$\left.\left. - 10(dd\,\pi)_2 + 7(dd\,\delta)_2\right] \cos 2\xi \cos \frac{2}{3}\,\eta \right) \Big\} - \frac{1}{162}\sqrt{2} \sin\zeta \times$$

$$\times \Big\{ \Big(\left[39\,(dd\,\sigma)_4 - 88\,(dd\,\pi)_4 + 49\,(dd\,\delta)_4\right] \cos 3\xi \sin \frac{1}{3}\,\eta -$$

$$- 8\left[3\left[dd\,\sigma)_4 + 14\,(dd\,\pi)_4 - 17\,(dd\,\delta)_4\right] \cos 2\xi \sin \frac{4}{3}\,\eta -\right.$$

$$\left. - 5\left[33\,(dd\,\sigma)_4 - 8\,(dd\,\pi)_4 - 25\,(dd\,\delta)_4\right] \cos\xi \sin \frac{5}{3}\,\eta \right) -$$

$$- i \Big(\left[39\,(dd\,\sigma)_4 - 88\,(dd\,\pi)_4 + 49\,(dd\,\delta)_4\right] \cos 3\xi \cos \frac{1}{3}\,\eta -$$

$$- 8\left[3(dd\,\sigma)_4 + 14\,(dd\,\pi)_4 - 17\,(dd\,\delta)_4\right] \cos 2\xi \cos \frac{4}{3}\,\eta +$$

$$+ 5\left[33\,(dd\,\sigma)_4 - 8\,(dd\,\pi)_4 - 25\,(dd\,\delta)_4\right] \cos\xi \cos \frac{5}{3}\,\eta \Big) \Big\}$$

$(yz/3z^2 - r^2)$

$$- \frac{2}{3}\sqrt{\frac{2}{3}}\left[(dd\,\pi)_2 - (dd\,\delta)_2\right] \sin\zeta \left[\left(\sin \frac{4}{3}\,\eta + \cos 2\xi \sin \frac{2}{3}\,\eta \right) - \right.$$

$$\left. - i \left(\cos \frac{4}{3}\,\eta - \cos 2\xi \cos \frac{2}{3}\,\eta \right) \right] + \frac{1}{27}\sqrt{\frac{2}{3}}\left[3\,(dd\,\sigma)_4 - \right.$$

$$\left. - 10\,(dd\,\pi)_4 + 7\,(dd\,\delta)_4\right] \sin\zeta \left[\left(\cos 3\xi \sin \frac{1}{3}\,\eta + \right.\right.$$

$$\left.\left. + 4\cos 2\xi \sin \frac{4}{3}\,\eta + 5\cos\xi \sin \frac{5}{3}\,\eta \right) - i \left(\cos 3\xi \cos \frac{1}{3}\,\eta + \right.\right.$$

$$\left.\left. + 4\cos 2\xi \cos \frac{4}{3}\,\eta - 5\cos\xi \cos \frac{5}{3}\,\eta \right) \right]$$

(xz/xz)

$$\frac{2}{3}\cos\zeta \Big\{ \Big(\left[(dd\,\pi)_2 + 2\,(dd\,\delta)_2\right] \cos \frac{4}{3}\,\eta + \left[3\,(dd\,\sigma)_2 + (dd\,\pi)_2 + \right.$$

$$\left. + 2\,(dd\,\delta)_2\right] \cos 2\xi \cos \frac{2}{3}\,\eta \Big) + i \Big(\left[(dd\,\pi)_2 + 2\,(dd\,\delta)_2\right] \times$$

$$\times \sin \frac{4}{3}\,\eta - \left[3\,(dd\,\sigma)_2 + (dd\,\pi)_2 + 2\,(dd\,\delta)_2\right] \cos 2\xi \times$$

$$\times \sin \frac{2}{3}\,\eta \Big) \Big\} + \frac{1}{27}\cos\zeta \Big\{ 3\left[18\,(dd\,\sigma)_4 + 11\,(dd\,\pi)_4 + \right.$$

$$+ 7\,(dd\,\delta)_4]\cos 3\xi\cos\frac{1}{3}\eta + 4\,[6\,(dd\,\sigma)_4 + 7\,(dd\,\pi)_4 +$$

$$+ 14\,(dd\,\delta)_4]\cos 2\xi\cos\frac{4}{3}\eta + [6\,(dd\,\sigma)_4 + 25\,(dd\,\pi)_4 +$$

$$+ 77\,(dd\,\delta)_4]\cos\xi\cos\frac{5}{3}\eta + i\left(3\,[18\,(dd\,\sigma)_4 + 11\,(dd\,\pi)_4 +\right.$$

$$+ 7\,(dd\,\delta)_4]\cos 3\xi\sin\frac{1}{3}\eta + 4\,[6\,(dd\,\sigma)_4 + 7\,(dd\,\pi)_4 +$$

$$\left.+ 14\,(dd\,\delta)_4]\cos 2\xi\sin\frac{4}{3}\eta - [6\,(dd\,\sigma)_4 + 25\,(dd\,\pi)_4 +\right.$$

$$\left.+ 77\,(dd\,\delta)_4]\cos\xi\sin\frac{5}{3}\eta\right)\Bigg\}$$

(xz/x^2-y^2)

$$-\frac{1}{3}\sqrt{\frac{2}{3}}\,[3\,(dd\,\sigma)_2 + 2\,(dd\,\pi)_2 - 5\,(dd\,\delta)_2]\sin\xi\sin\zeta\left(\cos\frac{2}{3}\eta -\right.$$

$$\left.- i\sin\frac{2}{3}\eta\right) - \frac{1}{54}\sqrt{\frac{2}{3}}\sin\zeta\left\{\left(3\,[39\,(dd\,\sigma)_4 - 16\,(dd\,\pi)_4 -\right.\right.$$

$$- 23\,(dd\,\delta)_4]\sin 3\xi\cos\frac{1}{3}\eta - 4\,[3\,(dd\,\sigma)_4 - 22\,(dd\,\pi)_4 +$$

$$+ 19\,(dd\,\delta)_4]\sin 2\xi\cos\frac{4}{3}\eta - [33\,(dd\,\sigma)_4 - 80\,(dd\,\pi)_4 +$$

$$\left.+ 47(dd\,\delta)_4]\sin\xi\cos\frac{5}{3}\eta\right) + i\left(3\,[39\,(dd\,\sigma)_4 - 16\,(dd\,\pi)_4 -\right.$$

$$- 23(dd\,\delta)_4]\sin 3\xi\sin\frac{1}{3}\eta - 4\,[3\,(dd\,\sigma)_4 - 22\,(dd\,\pi)_4 +$$

$$+ 19\,(dd\,\delta)_4]\sin 2\xi\sin\frac{4}{3}\eta + [33\,(dd\,\sigma)_4 - 80\,(dd\,\pi)_4 +$$

$$\left.\left.+ 47\,(dd\,\delta)_4]\sin\xi\sin\frac{5}{3}\eta\right)\right\}$$

$(xz/3z^2-r^2)$

$$-\frac{2}{3}\sqrt{2}\,[(dd\,\pi)_2 - (dd\,\delta)_2]\sin 2\xi\sin\zeta\left(\cos\frac{2}{3}\eta - i\sin\frac{2}{3}\eta\right) +$$

$$+\frac{1}{27}\sqrt{2}\,[3(dd\,\sigma)_4 - 10(dd\,\pi)_4 + 7(dd\,\delta)_4]\sin\zeta\times$$

$$\times\left[\left(3\sin 3\xi\cos\frac{1}{3}\eta + 2\sin 2\xi\cos\frac{4}{3}\eta + \sin\xi\cos\frac{5}{3}\eta\right) +\right.$$

$$\left.+ i\left(3\sin 3\xi\sin\frac{1}{3}\eta + 2\sin 2\xi\sin\frac{4}{3}\eta - \sin\xi\sin\frac{5}{3}\eta\right)\right]$$

(x^2-y^2/x^2-y^2) $\frac{1}{9}\cos\zeta\left\{\left(2\left[3(dd\sigma)_2+2(dd\pi)_2+4(dd\delta)_2\right]\cos\frac{4}{3}\eta+\right.\right.$

$+\left[3(dd\sigma)_2+20(dd\pi)_2+13(dd\delta)_2\right]\cos 2\xi\cos\frac{2}{3}\eta\Big)+$

$+i\left(2\left[3(dd\sigma)_2+2(dd\pi)_2+4(dd\delta)_2\right]\sin\frac{4}{3}\eta-\right.$

$\left.\left.-\left[3(dd\sigma)_2+20(dd\pi)_2+13(dd\delta)_2\right]\cos 2\xi\sin\frac{2}{3}\eta\right)\right\}+$

$+\frac{1}{324}\cos\zeta\left\{\left(\left[507(dd\sigma)_4+332(dd\pi)_4+457(dd\delta)_4\right]\times\right.\right.$

$\times\cos 3\xi\cos\frac{1}{3}\eta+4\left[3(dd\sigma)_4+248(dd\pi)_4+73(dd\delta)_4\right]\times$

$\times\cos 2\xi\cos\frac{4}{3}\eta+\left[363(dd\sigma)_4+524(dd\pi)_4+\right.$

$\left.+409(dd\delta)_4\right]\cos\xi\cos\frac{5}{3}\eta\Big)+i\left(\left[507(dd\sigma)_4+\right.\right.$

$+332(dd\pi)_4+457(dd\delta)_4\Big]\cos 3\xi\sin\frac{1}{3}\eta+4\left[3(dd\sigma)_4+\right.$

$+248(dd\pi)_4+73(dd\delta)_4\Big]\cos 2\xi\sin\frac{4}{3}\eta-\left[363(dd\sigma)_4+\right.$

$\left.\left.+524(dd\pi)_4+409(dd\delta)_4\right]\cos\xi\sin\frac{5}{3}\eta\right)\Big\}$

$(x^2-y^2/3z^2-r^2)$ $\frac{4}{9}\sqrt{3}\left[(dd\pi)_2-(dd\delta)_2\right]\cos\zeta\left[\left(\cos\frac{4}{3}\eta-\cos 2\xi\cos\frac{2}{3}\eta\right)+\right.$

$\left.+i\left(\sin\frac{4}{3}\eta+\cos 2\xi\sin\frac{2}{3}\eta\right)\right]-\frac{1}{162}\sqrt{3}\cos\zeta\left[3(\mathrm{dd}\sigma)_4+\right.$

$+8(dd\pi)_4-11(dd\delta)_4\Big]\left[\left(13\cos 3\xi\cos\frac{1}{3}\eta-2\cos 2\xi\times\right.\right.$

$\times\cos\frac{4}{3}\eta-11\cos\xi\cos\frac{5}{3}\eta\Big)+i\left(13\cos 3\xi\sin\frac{1}{3}\eta-\right.$

$\left.\left.-2\cos 2\xi\sin\frac{4}{3}\eta+11\cos\xi\sin\frac{5}{3}\eta\right)\right]$

$(3z^2-r^2/3z^2-r^2)$ $\frac{2}{3}\left[2(dd\pi)_2+(dd\delta)_2\right]\cos\zeta\left[\left(\cos\frac{4}{3}\eta+2\cos 2\xi\cos\frac{2}{3}\eta\right)+\right.$

$$+ i\left(\sin\frac{4}{3}\eta - 2\cos 2\xi \sin\frac{2}{3}\eta\right)\Big] + \frac{1}{27}\left[3(dd\sigma)_4 + \right.$$

$$\left. + 56(dd\pi)_4 + 49(dd\delta)_4\right]\cos\zeta\left[\left(\cos 3\xi\cos\frac{1}{3}\eta + \cos 2\xi \times\right.\right.$$

$$\times \cos\frac{4}{3}\eta + \cos\xi\cos\frac{5}{3}\eta\Big) + i\left(\cos 3\xi \sin\frac{1}{3}\eta + \cos 2\xi \times\right.$$

$$\left.\left.\times \sin\frac{4}{3}\eta - \cos\xi\sin\frac{5}{3}\eta\right)\right]$$

КРАТКОЕ СОДЕРЖАНИЕ

М. Миончек. *Применение метода сильной связи к исследованию зон энергии для гексагональной структуры с плотной упаковкой.*

В этой работе были расчитанные матричные элементы энергии для гексагональной структуры с плотной упаковкой с учётом влияния дальнейших соседей в сети от второго до четвертого, а также применено двухцентровую апроксимацию.

REFERENCES

Miąsek M., *Acta Phys. Pol.*, **16**, 447 (1957).

STEADY STIMULATION AND QUENCHING OF PHOTOCONDUCTIVITY IN CADMIUM SULFIDE BY INFRARED RADIATION

By M. Bartenbach, B. Buras, H. Rzewuski, Z. Tomczak

Institute for Nuclear Research Polish Academy of Science, Warsaw.

(Received April 17, 1958)

The changes in the steady photocurrent produced by exciting light in CdS single crystals by simultaneous illumination with infrared radiation have been investigated. Many authors have reported quenching of photoconductivity in CdS by infrared and some stimulation phenomena of a transient character. In the present experiments *steady* stimulation has been observed; this occurs when the photocurrent caused by light alone is small compared with the photocurrent caused by infrared alone. For some definite ratio of the light intensity to the infrared intensity the illumination with infrared causes no change in the photocurrent. If the ratio is bigger than that mentioned above the well known quenching phenomena occur. By using X-rays instead of the exciting light similar stimulation and quenching phenomena have been observed. These results can be explained (*i*) using the model proposed by Rose which involves the creation of free holes by infrared radiation and (*ii*) assuming that the current caused by infrared radiation only is associated with holes.

Introduction

Many authors (Frerichs 1947, Fassbender 1950, Kallman et al. 1955) have reported quenching of photoconductivity in CdS single crystals by infrared radiation. After the current produced in a crystal by green light (or light of shorter wavelength) has reached a stationary value, the superposition of infrared light results in general, first in a stimulation, then a quenching of the current (Taft and Hebb 1952, Tutihasi 1956). The observed stimulation has a transient character and is followed immediately by a decay of photoconductivity to the level resulting from the steady quenching of photoconductivity by infrared. The time constant for stimulation is much shorter than that for quenching (Tutihasi 1956). To explain the infrared quenching in CdS Rose (1955) has proposed a model which involves the creation of free holes by infrared radiation. Assuming that the capture cross section of a trapped electron for a free hole is large compared with that of a trapped hole for a free electron (Broser and Warminsky 1950), the infrared light, creating free holes which recombine with trapped electrons, drains off the conduction electrons and thus quenches the photocurrent in the crystal.

In the present experiments the dependence of the quenching effect on the ratio of the intensity of the exciting radiation (light or X-rays) to the infrared intensity has been investigated.

Experimental Arrangement

The single crystals used in this experiment were obtained by the courtesy of the Institut für Festkörperforschung der Deutschen Akademie der Wissenschaften zu Berlin. They are of the type described by Simon (1953). As a source of exciting radiation a Hilger monochromator or an X-ray unit and as a source of infrared radiation a Zeiss monochromator were used. In the case of light excitation the intensity of the exciting radiation was measured by means of a photomultiplier Ф З У 19 and in the case of X-rays with a Roentgen dosimeter. The infrared radiation during one set of measurements was held constant; a measure of its intensity was the photocurrent caused by it in the photocell under investigation. The voltage applied to the CdS-single crystal photocell was 9 V. The photocurrent was measured with a galvanometer.

Results

Curve *a* on figure 1 shows a typical dependence of photocurrent on intensity for green light. Curve *b* in the same figure shows a typical dependence observed of photocurrent on intensity for green light when the photocell was simultaneously illuminated

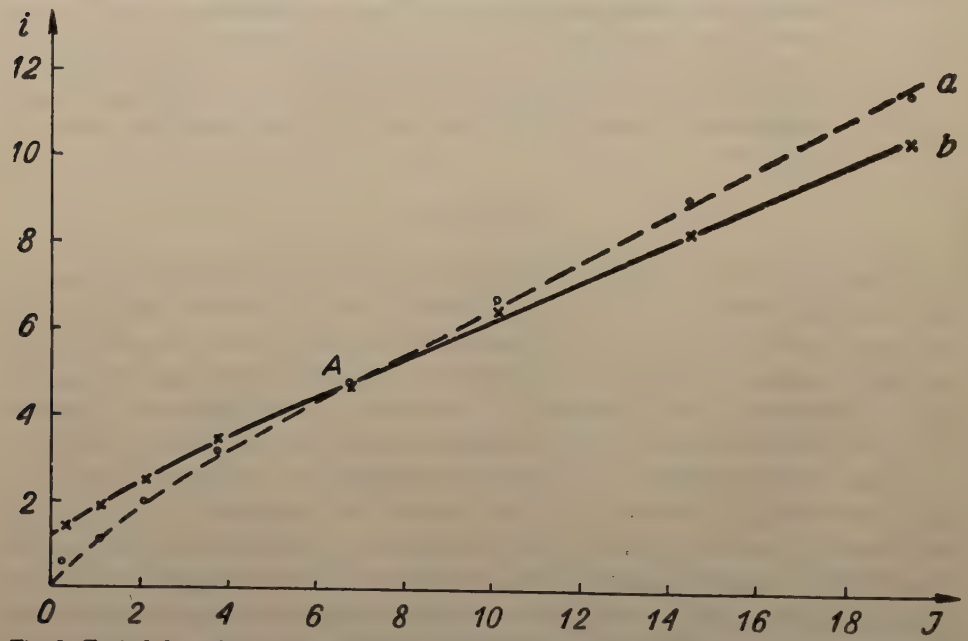

Fig. 1. Typical dependence of photocurrent on intensity: dotted line — green light only, solid line — simultaneous illumination with infrared — 0.86 μ. I — intensity for green light in arbitrary units, i — photocurrent in arbitrary units.

with infrared radiation of wavelength of about 0.86 μ. We see that when the light intensity is small (the photocurrent caused by visible light alone is small compared with the photocurrent caused by infrared) infrared radiation stimulates the electrical current. For some definite ratio (point A on Fig. 1) of the light intensity to the infrared intensity the illumination with infrared causes no change in the photocurrent. If the ratio is bigger than that mentioned above, the well known quenching phenomena occur. We obtain a similar dependence fo- different wavelengths of visible light and infrared radiation (Fig. 2); if the waver

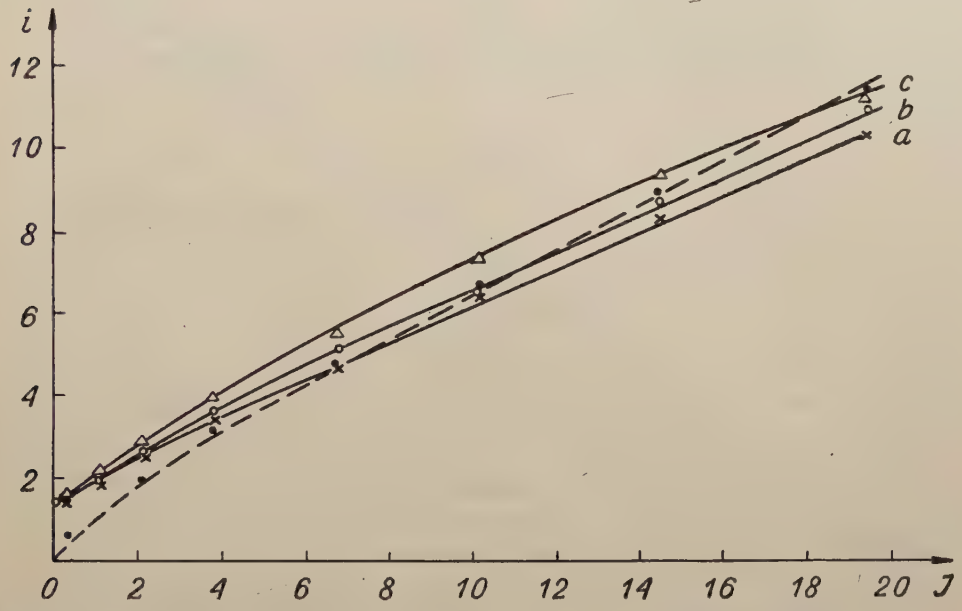

Fig. 2. Dependence of photocurrent on intensity: dotted line — green light only, solid line — simultaneous illumination with radiation of different wavelengths: *a*) 0.86 μ, *b*) 0.82 μ, *c*) 0.78 μ. I — intensity of green light in arbitrary units, i — photocurrent in arbitrary units.

length of the "infrared" radiation is smaller than about 0.7 μ we observe stimulation only. By using X-rays instead of the exciting light similar stimulation and quenching phenomena have been observed (Fig. 3).

Discussion

The results obtained can be explained using the model proposed by Rose (1955) which involves the creation of free holes by infrared radiation. However, it seems also necessary to assume that the photocurrent caused by infrared radiation only is associated with holes. This hole current in CdS single crystals does not manifest itself in usual circumstances because of the small mobility of holes compared with the mobility of electrons (Heerden 1957). Nevertheless, in circumstances when we deal with

infrared radiation only, it seems reasonable that, the holes created (according to Roses model) by infrared radiation give rise to a photocurrent.

Adopting this point of view, we easily see that when a very small electron current caused by green light is flowing in the crystal (few electrons in the conduction band) and we illuminate the crystal simultaneously with infrared radiation of very high

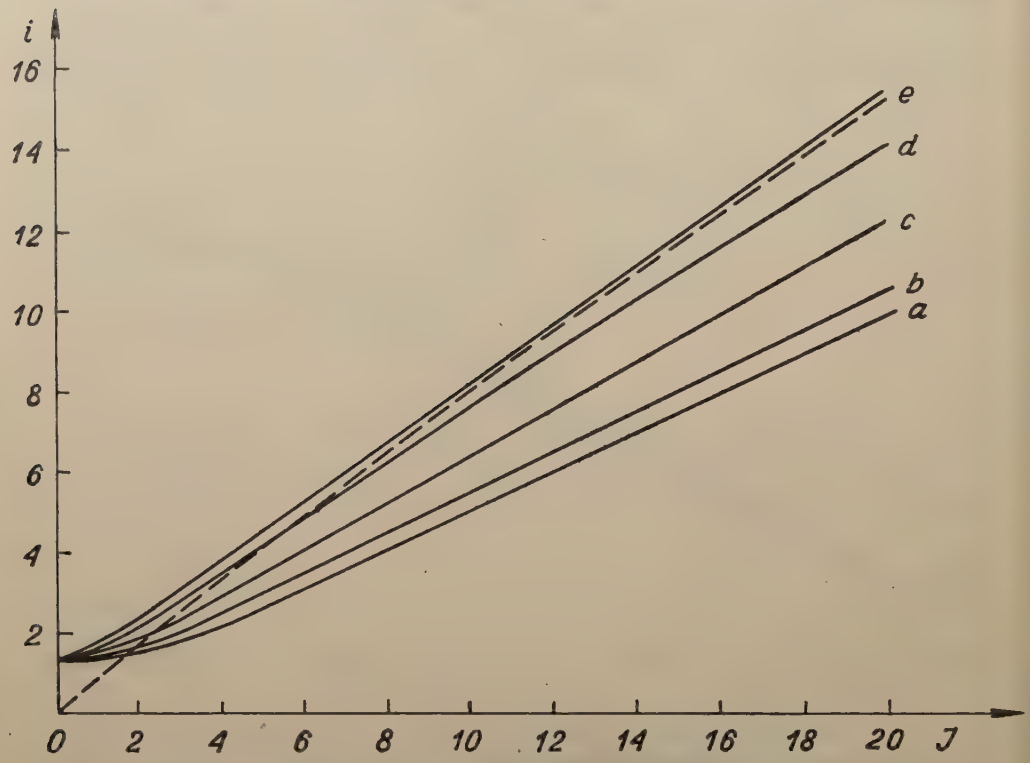

Fig. 3. Dependence of photocurrent on intensity: dotted line — Roentgen radiation only, solid line — simultaneous illumination with radiation of different wavelengths: *a*) 0.86 μ, *b*) 0.80 μ, *c*) 0.76 μ, *d*) 0.72 μ, *e*) 0.70 μ. I — intensity of Roentgen radiation in arbitrary units, i — photocurrent in arbitrary units.

intensity the electrical current should increase. This is so, because, roughly speaking, the hole current caused by the large number of holes created is bigger than the decrease of the electron current due to recombination processes. On the other hand, if a large electron current caused by green light is flowing in the crystal (many electrons in the conduction band) and we illuminate the crystal simultaneously with infrared radiation of comparatively low intensity the electrical current should decrease. This is so, because, simplifying the argument made by Rose, the small number of holes created give only a slight increase in the hole current and a big decrease of electrons in the conduction band due to recombination proposses. This discussion concerning the two extreme cases easily leads to the conclusion that there must be a definite ratio of green

light intensity to infrared intensity for which infrared radiation will cause no change in the photocurrent due to green light. It is possible also to make a very simplified calculation concerning the above mentioned model. As can be seen from the Appendix this calculation leads to a similar dependence as that given in the typical Fig. 1.

The fact that by using X-ray instead of the exciting light similar stimulation and quenching phenomena have been observed lead to the conclusion that in general (whatever may be the mechanism by which the energy of an X-ray photon is transformed into the energy of the electrons) the current caused by X-rays in CdS single crystals has the same character as the photocurrent caused by green light.

The authors are greatly indebed to Prof. L. Sosnowski for helpful discussions. The authors would like also to thank Mr. A. Zawadzki for help in the measure ments.

Appendix

Consider the problem shown in Fig. 4. Green light generates free electrons and holes at identical rates L in the conduction and valence bands. Infrared generates free holes in the valence band and fills the discrete state with electrons at identical rates I. For simplification it is assumed that recombination between electrons in the conduction band and holes in the valence band takes place not via traps but "in flight". Let us denote by n, n_l and p the concentrations in the steady state of electrons in the conduction band, electrons at the discrete levels, and holes in the valence band respectively. Then we can write four equations of which only three are independent:

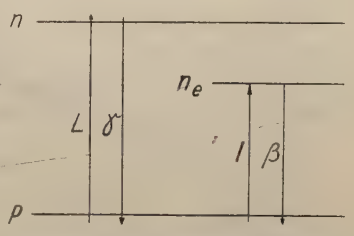

Fig. 4. A simplified model of energy levels.

$$n + n_l = p \tag{1}$$

$$\frac{dn}{dt} = L - \gamma np \tag{2}$$

$$\frac{dp}{dt} = L - \gamma np + I - \beta n_l p \tag{3}$$

$$\frac{dn_l}{dt} = I - \beta n_l p \tag{4}$$

(γ and β are recombination coeficients). For the steady state we have three equations:

$$\begin{aligned} n + n_l &= p \\ L - \gamma np &= o \\ I - \beta n_l p &= o, \end{aligned} \tag{5}$$

from which we obtain

$$p = \sqrt{\frac{I}{\beta} + \frac{L}{\gamma}}, \quad n = \frac{\frac{L}{\gamma}}{\sqrt{\frac{I}{\beta} + \frac{L}{\gamma}}}. \tag{6}$$

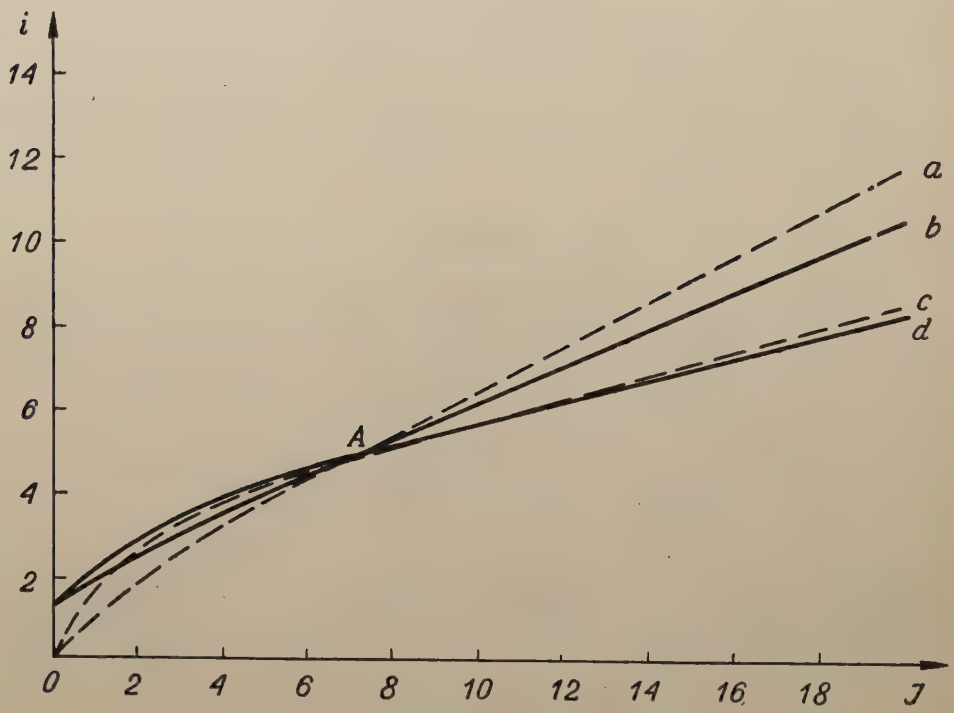

Fig. 5. Dependence of photocurrent on intensity. Experimental curves: a — radiation only, b — simultaneous illumination with infrared; theoretical curves: c — radiation only, d — simultaneous illumination with infrared (normalized for point A).

If we denote by μ^+ and μ^- the mobilities of holes and electrons respectively, we get for the conductivity

$$\sigma = e\left[\mu^+\sqrt{\frac{I}{\beta} + \frac{L}{\gamma}} + \mu^- \frac{\frac{L}{\gamma}}{\sqrt{\frac{I}{\beta} + \frac{L}{\gamma}}}\right]. \tag{7}$$

For $I = o$

$$(\sigma)_{I=0} = e\,(\mu^+ + \mu^-)\sqrt{\frac{L}{\gamma}} \tag{8}$$

Fig. 5 shows the curves $(\sigma)_{I=0}$ *vs* L and σ *vs* L for a definite value of I. It is easy to see that for

$$L = k\frac{\gamma}{\beta} I \tag{9}$$

where k is a simple function of the mobilities μ^+ and μ^-)

$$\sigma = (\sigma)_{I=0} \tag{10}$$

We see that even such a very simplified model is in good semiquantitative agreement with the results of our experiments: it gives the two regions of stimulation and quenching. However, the curvatures of the calculated curves on Fig. 5 are not in good agreement with the experimental curves. This is mainly so because we have assumed that recombination between electrons in the conduction band and holes in the valence band takes place not via traps but "in flight". Adding of traps will lower the curvatures.

КРАТКОЕ СОДЕРЖАНИЕ

М. Ъартенбах, Ъ. Ъурас, Г. Жевуски, Э. Томчак, *Постоянный стимул и гашение фотопроводимости сульфида кадмия инфракрасным излучением.*

Исследовано изменения постоянного фототока в монокристаллах CdS, вызванные возбуждающим светом при одновременном инфракрасном облучении. Многие авторы писали о гашении фотопроводимости в CdS инфраксаным облучением и о некоторых явлениях возбуждения переходного характера. В настоящих опытах замечено постоянное возбуждение. Возникает это тогда, когда фототок, вызванный светом, является малым в сравнении с фототоком, вызванным инфракрасным излучением. Для некоторого отношения интенсивности света к интенсивности инфракрасного излучения инфракрасное облучение не вызывает никаких изменений фототока. Если это отношение является большим, выступает хорошо известное явление гашения. При применении излучения (лучше Рентгеновских лучей) вместо возбуждающего света замечено сходные явления возбуждения и гашения.

Результаты эти могут быть объяснены: 1° на основе модели предположенной Розе охватывающей создание свободных дырок инфракрасными лучами; 2° при предложением, чцо ток вызванный только инфракрасным излучением, появляется в связи с дырками.

REFERENCES

Broser, I. and Warminsky, R., *Ann. Phys.* [*Leipzig*], **7**, 289 (1950).
Fassbender, J., *Ann. Phys.* [*Leipzig*], **5**, 33 (1949).
Frerichs, R., *Phys. Rev.*, **72**, 594 (1947).
Heerden, P. J., *Phys. Rev.*, **106**, 468 (1957).
Kallman, H., Kramer, B., and Perlmutter, A., *Phys. Rev.*, **90**, 391 (1955).
Rose, A., *Phys. Rev.*, **97**, 322 (1955).
Simon, H., *Ann. Phys.* [*Leipzig*], **12**, 45 (1953).
Taft, E. A. and Hebb, M. H., *J, opt. Soc. Amer.*, **42**, 249 (1952).
Tutihasi, S., *J. opt. Soc. Amer.*, **46**, 443 (1956).

ON THE MAGNITUDE OF STRANGE PARTICLE PRODUCTION CROSS-SECTION IN NUCLEON-NUCLEON COLLISIONS AT COSMOTRON ENERGY

By V. S. Barashenkov and V. M. Maltsev

Joint Institute for Nuclear Research, Dubna U.S.S.R.

(Received May 12, 1958)

The probabilities of production of different kinds of particles and their momentum distribution for (NN)— collision et $E = 3$ BeV are calculated by the method of statistical theory.

The results of the calculation are compared with the experiment.

The statistical theory of multiple production of strange particles was considered in [1] — [3]. For (πN) — collisions this theory agrees with experiment rather well if the energy of colliding particles is high enough [4], [5].

At present it is possible to compare the theoretical calculations with the experiments for (NN) — collisions as well. The calculated statistical weights of different channels of reaction for (NN) — collisions at the energy $E = 3$ BeV are given in Table I (reference 6). The statistical weights are expressed in percentages. The calculations are made under the same assumptions as in[1] — [3] and in the same symbols.

If it assumed that the effective inelastic cross-section for (pp) — collisions at $E = 3$ BeV is equal to $\sigma_{in} = 26$ mb[7] then the K^+-particle production cross-section in (pp) — collisions is equal to $\sigma_K^+ = 1.0$ mb for the $V = V_2$ case, and $\sigma_K^+ = 0.05$ mb for the $V = V_3$ case, and the cross-section of production of all strange particles is equal to $\sigma_{st} = 1.5$ mb for the $V = V_2$ case and $\sigma_{st} = 0.07$ mb for the $V = V_3$ case.

In paper[8] which is obviously the most detailed one at the present time, the magnitude

$$\frac{d^2\sigma_K^+}{dp\, d\Omega} = (4.5 \pm 0.9) \times 10^{-32} \frac{\text{cm}^2}{\text{ster MeV}}$$

was obtained for the effective K^+-particle production cross-section with the momentum equal to $p = 1.9\,\mu_\pi$ ($\mu_\pi = 140$ MeV) at the angle $\theta = 180°$ (in the c.m. system) for (pp) — collisions at $E = 3$ BeV. In order to integrate over all the momenta we

calculated momentum distribution $W^+ = W^+(p)$ of K^+-mesons produced[1]. The results of calculations for the $V = V_2$ case in the c.m. system are given in Fig. 1. The calculated π-meson spectrum turns out to be somewhat softer than the corresponding spec-

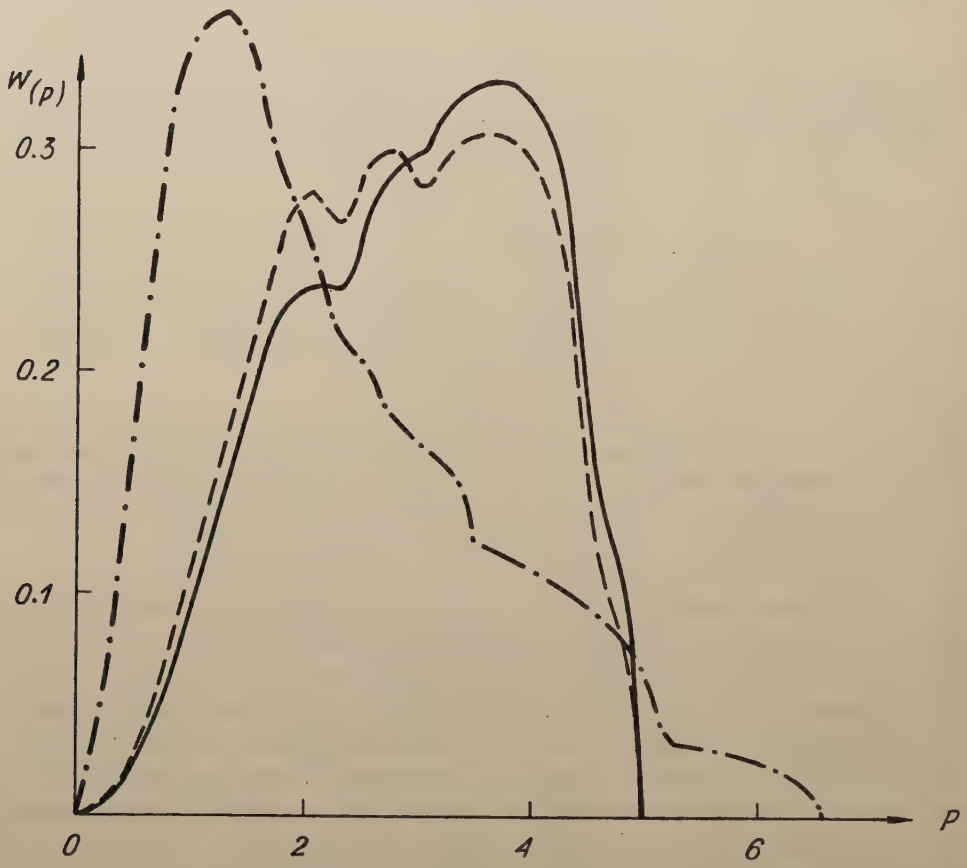

Fig. 1. Momentum distribution ($W^+ = W^+(p)$) of K^+ – particles produced in $(p-p)$ – collisions at $E = 3$ BeV; $V = V_2$ (solid curve). For comparison there are given the total momentum distribution of $K^\pm$ and K^0 – particles (dashed curve) and the momentum distribution of the pions produced in $(p-p)$ – collisions (dash-dots). All the spectra are normalized to unity and reffered to the c. m. s. of the colliding nucleons. The momentum is expressed in the units of the pion mass $\mu_\pi = 140$ MeV.

trum for K-mesons. The softening of π-meson spectrum is due to the pions produced during the decay of the isobar state $p = T = 3/2$ (See the physical meaning of the notion "isobar" in the statistical theory of multiple particle production([11])). Assuming isotropic angular distribution in the c.m. system for the $V = V_2$ case we have

[1] When calculating the spectra we used in part the nomograms of L. G. Zastavenko (to be published).

$$\sigma_K^+ = 4\pi \times 4.5 \times 10^{-32}/\mathrm{W}^+(1.9) = 0.33 \text{ mb} \quad [2]$$

(considering that $\int_0^{P\max} \mathrm{W}^+(p)dp = 1$).

The calculation for the $V = V_3$ case gives almost an equal value of the cross-section. However, this value is different by one order from the cross-section calculated for the $V = V_3$ case by the data of Table I. As well as in case of (πN) collisions, the

TABLE I

Secondary Particles	(pp)-collision		(pn)-collision	
	V_2	V_3	V_2	V_3
$2N$	1.74	1.82	2.70	2.88
$2N\pi$	22.2	23.3	19.6	20.8
$2N2\pi$	44.2	46.3	48.0	51.0
$2N3\pi$	24.3	25.5	21.5	22.8
$2N4\pi$	1.87	1.96	1.75	1.86
$2NK\tilde{K}$	0.00092	0.00096	0.0011	0.0012
$N\Lambda K^+$	1.85	0.0867	1.43	0.0684
$N\Lambda K^0$	0	0	1.43	0.0684
$N\Sigma^+K^+$	0.903	0.0424	0	0
$N\Sigma^+K^0$	0.903	0.0424	0.722	0.0344
$N\Sigma^0K^+$	0.602	0.0282	0.512	0.0242
$N\Sigma^0K^0$	0	0	0.512	0.0242
$N\Sigma^-K^+$	0	0	0.722	0.0344
$N\Sigma^-K^0$	0	0	0	0
$N\pi\Lambda K^+$	0.264	0.0124	0.239	0.0112
$N\pi\Lambda K^0$	0.445	0.0209	0.239	0.0112
$N\pi\Sigma^+K^+$	0.12	0.0056	0.130	0.0050
$N\pi\Sigma^+K^0$	0.12	0.0056	0.102	0.0054
$N\pi\Sigma^0K^+$	0.12	0.0056	0.096	0.0045
$N\pi\Sigma^0K^0$	0.12	0.0056	0.096	0.0050
$N\pi\Sigma^-K^+$	0.16	0.0075	0.102	0.0069
$N\pi\Sigma^-K^0$	0	0	0.130	0.0035

$V = V_3$ case leads to contradictions. For the $V = V_2$ case σ_K^+, which was calculated with the momentum distributions taken into account, is three times less than that calculated by Table I. This discrepancy may be explained by the fact that at low energies $E \leqslant 3$ BeV the energy of the strange particles produced in (NN) — collisions

[2] In([8]) they give $\sigma_K^+ = 0.2$ mb. The difference is due to the fact that we considered a number of additional effects such as resonance (πN) interaction in the $P = T = 3/2$ state and different statistical weights of $N\Lambda K$, $N\Sigma K_1$ ... reactions.

is close to that of the threshold, whereas their number is small. Therefore the statistical methods may yield only the orders of the magnitudes. This circumstance is especially essential for the calculation of spectra, which are very sensitive to the assumption about the form of the matrix element. So it should be expected that $\sigma_K^+ \approx 1.0$ mb, which follows from Table I, will very likely be closer to the experimental data than the value $\sigma_K^+ \approx 0.33$ mb. obtained by integrating the calculated spectrum[3].

If one assumes that there exists a resonance interaction of K-mesons similarly to the case of the pion interaction with nucleons then the spectrum of K-mesons produced in $(p\text{-}p)$-collisions will become softer, whereas the magnitude of the cross-section σ_K^+ calculated in accordance with such a spectrum appreciably increases. This possibility is now, however, purely speculative.

In our opinion one cannot at present state for sure that the cross-section for the production of strange particles in $(p\text{-}p)$-collisions is considerably less than than in (πN)-collisions at equal energy values in c.m.s. (cf.([8]) — ([10])).

The very small magnitude of the cross-section σ_{st} for $(p\text{-}p)$-collisions observed in([9]) is likely to be accounted for by the insufficient statistics.

КРАТКОЕ СОДЕРЖАНИЕ

В. С. Барашенков, В. М. Мальцев, *О величине сечения образования странных частиц в нуклон — нуклонных столкновениях при космотронной энергии.*

Методом статистической теории расчитаны вероятности образования различных сортов частиц и их импульсные распределения для случая (N N) — столкновений при E=3Bev. Результаты расчёта сравниваются с экспериментом.

REFERENCES

1. Barashenkov V. S., Barbashev B. M., Bubelev E. G., Maksimenko V. M., *Nucl. Phys.*, **5**, 17 (1957).
2. Barashenkov, V. S., Barbashev, B. M., Bubelev, E. G., *Nuovo Cim.* Suppl. **7**, 117 (1958)
3. Barashenkov, V. S., Maltsev, V. M., *Acta phys. Polon.*, **17**, 177 (1958)
4. Barashenkov, V. S.; JETP, **34**, 1016 (1958); Nucl. Phys., **7**, 146 (1958)
5. Mikhul, E. K., *Acta phys. Polon.* (to be published).
6. Barashenkov, V. S., Barbashev, B. M., Bubelev, E. G., *The report of L.T.Ph. JINR*, 1957.
7. Block M. M. et al., *Phys. Rev.*, **103**, 1484 (1956).
   Fowler, W. B. et al., *Phys. Rev.*, **103**, 1489 (1956).
8. Baumel, P., Harris, G., Orear, I., Taylor, S., *Phys. Rev.*, **108**, 1322 (1957).
9. *Proceedings of the 7th Rochester Conference and of the Conference in Padova-Venezia* (1957).
10. Cool, R. L., Morris, T. W., Ran, R. R., Thorndike, A. M., Whittemore, W. L., *Preprint.*
11. Belenky, S. Z., *Nucl. Phys.*, **2**, 253 (1956).

[3] The same holds for (πN)-collisions for equal c.m.s. energy (E — 2 BeV).

ON THE RATIO OF PHOTONS TO ELECTRONS IN EXTENSIVE AIR SHOWERS OF COSMIC RADIATION FOUND FROM ANALYSIS OF THE TRANSITION CURVE

By J. M. Massalski and A. Oleś

Institute of Nuclear Research, Polish Academy of Sciences, Cracow
Laboratory of General Physics, Academy of Mining and Metallurgy, Cracow

(Received May 14, 1958)

An analysis is made of the transition curve for particles of extensive air showers of cosmic radiation, at an altitude of 2636 m above sea level. The existing discrepancy between the experimental photon-to-electron ratio (p/e) and theory is explained. In accordance with the predictions of the theory a large number of photons were found with energies below the threshold energy of apparatus for registering electrons. The photon-to-electron ratio found for a threshold energy for electrons of 15 MeV, for photons of 15—30 MeV, $p/e = 1.0 \pm 0.1$ (only the statistical error is given) is below the actual value owing to the influence of the low-energy photons on the transition curve.

1. Introduction

The ratio of the number of photons to the number of electrons p/e in extensive air showers of cosmic radiation was found by various authors while studying the transition curve in lead of extensive air showers (Millar 1951, Bassi et al. 1952, Milone 1952a, 1952b, 1953a, 1953b, 1954, Jurkiewicz 1954, Babecki et al. 1957). The results of the analysis of the transition curve obtained by these authors entailed considerable difficulties of interpretation just in connection with the value obtained by these authors for the ratio of the number of photons to electrons. This refers to photons and electrons of energies $\geqslant$10 MeV, which, in the case of photons, give pairs at a high efficiency and, in the case of electrons, penetrate the walls of the conventional counters without any marked absorption.

It is to be expected that for small distances from the shower core for which the photon-to-electron ratio had been measured the values obtained in experiments should be in accordance with the theory of electron-photon cascades. The theory predicts a value of $p/e = 1.5$ for photon and electron energies > 10 MeV.

In the meantime the transition curves obtained in lead for extensive air showers display a weak maximum above values for zero thickness of absorber, which consequently results in small p/e ratios. The authors of the earliest papers (Millar 1951,

Bassi et al. 1952) obtained values for this ratio as low as $p/e = 0.25$. The authors of later papers (Milone 1952a, 1952b, 1953a, 1953b, Massalski 1954, Babecki et al. 1957) obtained values ($p/e = 0.7$) akin to the theoretical value. The problem arises whether the value of $p/e = 0.7$ obtained by the later authors differs significantly from the theoretical value, or does this difference result from other effects not taken into account by these authors.

The authors of the present paper, on the basis of an analysis of the transition curve measured at an altitude of 2636 m above sea level noted (Dubinsky et al. 1957) that the presence in extensive air showers of large numbers of low-energy photons (of energies below the threshold energy of the apparatus for registering electrons) could influence the results obtained by previous authors reducing the ratio p/e and that in reality there are no experimental grounds for believing that this ratio is less than that given by theory.

This view is supported by the results of Brennan (1957) who measured the p/e ratio by comparing the efficiency of a scintillation counter and a tray of GM counters connected with an extensive air shower detector. For photon and electron energies of 1.5 MeV he obtained the value $p/e = 2.1$.

The purpose of this paper is to analyse the transition curve for particles of extensive air showers of cosmic radiation in lead in order to explain the discrepancy between the experimental results obtained for the p/e ratio and theoretical value.

2. *Apparatus*

The extensive air shower detector which we employed consisted of 3 trays of G.M. counters (trays A, B, C) of areas $S = 0.45$ m^2 each. Trays A, B, C were placed in the corners of an equilateral triangle with sides of 5 m in length. In the central part of the triangle were 2 telescopes (one containing brass counters; the other, aluminium counters) consisting of 3 trays (trays D, E, F and d, e, f, respectively). The aluminium counters were employed in order to avoid the cascade effect in the counter walls. Since in the previous papers (Babecki et al. 1957) it was found that the middle tray of the telescope omits coincidences registered by the lower tray, covered surfaces were now employed for trays D, E and d, e without gaps between counters. The surfaces of trays

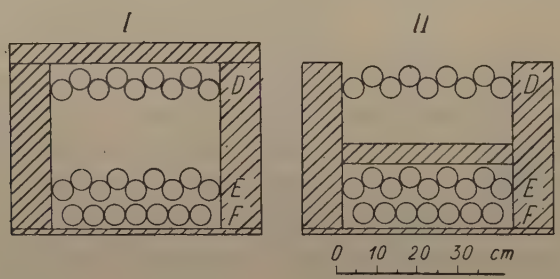

Fig. 1. Position of the lead absorber in both series of measurements

D, E and d, e were $rS = 0.287$ m^2. Tray E was placed directly over tray F, while between trays D and E there was a space making it possible to insert an absorber of up to 15 cm thickness (between trays d and e there was a space of 5 cm). Both telescopes were shielded on the sides by a layer of 10 cm of lead and on the bottom by 1.5 cm of Pb. Measurements were made on Lomnica Peak in the Tatra Mountains at an altitude of 2636 m above sea level. They were made for 2 positions of the lead absorber (Fig. 1):

Position I — above trays D, E, F (or d, e, f) with an absorber thickness of 0 to 20 cm Pb.

Position II — between trays D, E with an absorber thickness of 0 to 15 cm Pb (or 0 to 5 cm Pb between trays d, e).

The coincidence circuit made possible the simultaneous registration of 15 different types of coincidences.

With the absorber in position I the following types of coincidences were registered: coincidences $ABC = T$ and type N coincidences[1]: TD, TE, TF, TDE, TDF, TEF, $TDEF$

With the absorber in position II the following types of coincidences were registered: coincidences T,
type N coincidences: TE, TF, TEF,
and type M coincidences[1] TDE, TDF, $TDEF$

The number of coincidences of type N is expressed by the formula:

$$N = \int_0^\infty K x^{-(\gamma+1)} (1 - e^{-Sx})^3 (1 - e^{-rr'RSx})\, dx \qquad (1)$$

The difference of coincidences N and M obtained for the same telescope trays gives the anti-coincidence number P expressed by the formula

$$P = N - M = \int_0^\infty K x^{-(\gamma+1)} (1 - e^{-Sx})^3 (1 - e^{-\frac{p}{e} P_p rr' Sx})\, e^{-rSx}\, dx \qquad (2)$$

In formulae (1) and (2) we make use of the following notation:

$Kx^{-(\gamma+1)}$ — differential density spectrum of the registered showers.

$rr'S$ — area of the tray equivalent to the telescope in registration of particles from the extensive air showers.

$R = P_e + \frac{p}{e} P_p$, where P_e and P_p are the probabilities that an electron or photon falling on an absorber of a given thickness t creates at least one electron capable of actuating the trays of the counters under the absorber. P_e and P_p were calculated theoretically by Arley (1948). By making use of the values of P_e, P_p or, in the second case only, of P_p calculated by Arley, we determine p/e from the magnitude of R (obtained from the type N coincidences) or $\frac{p}{e} P^p$ (obtained from anti-coincidences).

[1] We shall hereafter omit the letter T.

In the additional measurements the exponent of the density spectrum γ was found by the method of varying the multiplicity of the coincidences and the area of the trays. The mean value obtained by both methods $\gamma = 1.35 \pm 0.03$ was employed in the calculations.

3. Results of Measurements

From the coincidences of the N type we obtained, by formula (1), a value of 0.68 ± 0.07 for the ratio p/e for the brass telescope and 0.60 ± 0.07 for the aluminium telescope.

The results of the anti-coincidence method in which the type N and type M coincidences are combined can be seen in Table I.

TABLE I

thickness of absorber in mm of Pb	2	4	7	10
p/e from the *DEF* coincidences	1.03	1.02	1.01	0.99
mean p/e		1.01	$\pm$ 0.10	

Hence both methods, even for small thicknesses of absorber (0—10 mm Pb), give different values for p/e, the anti-coincidence method giving the larger value.

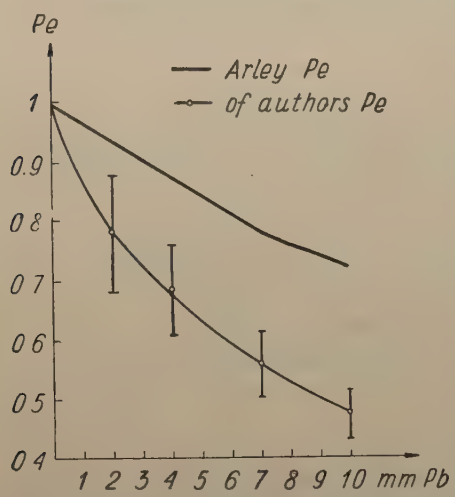

Fig. 2. The curve $P_e(t)$ obtained in the experiment and the theoretical curve according to Arley.

Let us consider the agreement of the obtained curves with the Arley theory. In the anti-coincidence method we obtain $\frac{p}{e}P_p$, and then calculate $P_e = R - \frac{p}{e}P_p$. The fact that in the anti-coincidence method the same value of p/e is obtained for different thicknesses of absorber indicates that P_p calculated by Arley is not inconsistent with P_p obtained from experiment. On the other hand, P_e obtained from experiment differs from the theoretical value (Fig. 2). The experimental curve is much steeper than the theoretical curve. Another fact which should be noted is the loss by the central tray of coincidences recorded by the outside trays of the telescope. In measurements of coincidences of the *DF* and *DEF* type it was found that there are *DF* coincidences of the outer telescope trays which are not accompanied by *DEF* coincidences. Hence the middle tray of the *DEF* telescope operated at an efficiency of less than 1. Table II presents the results of these observations. Such a great loss of coincidences

can not be explained by electronic factors by the inefficiency of the G.M. counters in the registration of ionizing particles. It was found experimentally that the losses due to these factors do not exceed 1%.

The above-mentioned loss of coincidences by the E tray increases with the absorber thickness (Table II). This phenomenon, observed for large thicknesses of absorber,

TABLE II

mm Pb.	$\frac{F-EF}{EF}$	$\frac{DE-DEF}{DEF}$
0	7.4	4.5
2	5.3	4.4
4	4.6	3.5
7	6.0	4.6
10	7.7	4.3
15	11.5	7.5
20	15.5	8.2
30	16.5	8.4
40	21.7	11.5
50	24.2	6.7
75	32.7	9.1
100	40	18
150	32	10
200	33	8.7

is caused by penetrating photons of energies of 2—7 MeV, generated in the Pb, for which the absorption coefficient attains a minimum (Zatsepin 1948, Greison 1956, Jurkiewicz 1954, Babecki et al. 1957, Babecki 1958).

4. Interpretation of Results

In our opinion the experimental facts presented above testify to the existence in the spectrum of extensive air shower particles from cosmic radiation of a large number of photons with energies lower than the threshold energy of apparatus for registering electrons (E_t). The existence of a large number of low energy photons is predicted by the theory of electron-photon cascades (Belenky 1948, Greisen 1956, Ivanenko 1958). The integral spectrum of electron for $E \to 0$ is limited, while the divergency of the spectrum of photons of very low energy is eliminated by the photoelectric effect that takes place in the air (at an energy of ~ 50 KeV).

The relative contribution of the photons to the mean particle density of the registered showers, with zero thickness of lead absorber can be found from the formula:

$$g_1 = \frac{\int_{0,1}^{\infty} \varepsilon(E) f_p(E)\, dE}{F_e(E \geqslant E_t) + \int_{0,1}^{\infty} \varepsilon(E) f_p(E)\, dE} \tag{3}$$

In this formula $f_p(E)$ denotes the differential energy spectrum of photons, $\varepsilon(E)$ — the efficiency of registering photons of energy E, $F_e(E \geqslant E_t)$ — the integral spectrum for electrons above the energy E_t. The spectra of electrons and photons are so normalized that the integral spectrum of electrons $F_e\ (E > 0) = 1$. In calculating formula (3) we used the integral energy spectrum of electrons and photons given in Greisen's article (1956, Fig. 16) and from other data in the book by Belenky. Hence we have for the ratio $F_p(E > 0.1)/F_e(E > 15)$ the value 30, which coincides within the limits of error of the theory with the value which we can obtain for this ratio from the formulae given by Ivanenko (1958). From estimations with formula (3) we find that the amount of photons in the density of the registered showers (for zero thickness of lead absorber) amounts to about 20% for a threshold energy $E_t = 15$ MeV (tray F of the telescope).

Photons contribute to the registration of extensive air showers not only in measurements made by single trays (connected with an extensive air shower detector) but also in the measurements made with a telescope comprised of two or even three trays. In this latter case one or two trays of the telescope (D and E) can be actuated by low energy electrons which do not reach tray F while simultaneously this tray is actuated by photons; coincidences produced entirely by photons are also possible. The photon contribution (g_2 and g_3) to the parricle density of the registered showers for coincidences DF and DEF depends on the number of photons falling on the telescope in each registered shower. This contribution can be estimated by introducing the notion of efficiency for single trays of the telescope for registering a given shower by means of photons: $\eta = 1 - e^{-g_1 \bar{x} s}$ where $\bar{x}$ denotes the mean particle density in the registered showers. The photon contribution to the particle density of the recorded showers for coincidences DF and DEF is expressed by the formulae:

$$g_2 = \frac{\eta^2 + \eta \int_3^{15} f_e(E)\,dE}{\bar{x}s}\ ;\quad g_3 = \frac{\eta^3 + \eta \int_9^{15} f_e(E)\,dE}{\bar{x}s}$$

where $f_e(E)$ is the differential energy spectrum of electrons, and s the area of the telescope tray.

The first expression for the counters in the above formulae give the efficiency of registering a given shower by photons while the second expression denotes the efficiency in the case of mixed coincidences in which one or two trays of the telescope are actuated by electrons of low energy and the lower tray by photons.

These formulae give for g_2 and g_3 the values of 13 and 5% respectively. Employing the values of g_1, g_2, g_3 we can estimate the photon contribution (for zero thickness of absorber) to the coincidences F, DF and DEF. This contribution to the number of coincidences turns out to be 14.5, 8.5 and 4%, respectively. The values obtained are in agreement with the experimental data in Table II. The above effects thus explain the loss of coincidences in the experiment by the middle tray; at the same time they result in the curves $R(t)$ and $P_e(t)$ having too high a value for zero absorber, which leads to the lowering of the value of p/e obtained from experiment.

The above-discussed presence of low energy photons in extensive air showers does not explain in full the differences between the experimental curve P_e and the curve calculated theoretically by Arley. The steep slope of the experimental curve P_e is caused, in part, by the fact that the experimental electron spectrum contains more low energy electrons than assumed by Arley. (Arley 1948, Belenky 1948, Greisen 1956).

From the transition curve for extensive shower particles obtained in our experiment we can determine the ratio of photons to electrons for the following threshold energies. The threshold energy for the electrons in our telescope is 15 MeV. In the measurement of the transition curve the photons are registered by electrons generated in the absorber; hence the threshold energy for photons registered in this way must be contained within the limits 15 MeV $< E_{tp} \leqslant$ 30 MeV. According to the spectrum given by Richards and Nordheim (Greisen 1956, Richards and Nordheim 1948) the ratio p/e for an electron threshold energy of 15 MeV, and photon threshold energy of 15—30 MeV amounts to 2.6—1.7. If we take into account:

1) the spatial distribution in extensive air showers of high energy electrons and photons given by Eyges and Fernbach (Greisen 1956) 2) the fact that the measurements of the p/e ratio refer to the mean distances from the core of the shower of about 1/3 of the scattering unit (Zatsepin 1950), then it is to be expected from the theoretical data of Richards and Nordheim that the ratio p/e has the value 1.5—1.1.

From the measurements with the anti-coincidence method, which we consider to be more correct than the others, we have for a threshold energy for the electrons of 15 MeV, for photons of 15—30 MeV the value 1.0 ± 0.1 (only the statistical error is given). The real value may be greater than that given, since the experimental result is reduced by the presence of a large number of low energy photons and represents the lower limit of the p/e ratio.

The previous paper of the authors (Dubinsky et al. 1957), the papers by Brennan (1957), Dohan et al. (1957) and the present paper eliminate the differences between experiment and theory in regard to the ratio p/e in extensive air showers of cosmic radiation.

We wish to thank Professor M. Mięsowicz, head of the Cracow Branch of the Cosmic Ray Department of the Institute for Nuclear Research and Candidate of Physical Science, I. P. Ivanenko (Moscow) for their valuable discussions. The experiment was performed with the assistence of the Czechoslovac Academy of Sciences and the Slovac Academy of Sciences and the authors are very indebted to them for their hospitality in the course of measurements.

КРАТКОЕ СОДЕРЖАНИЕ

Е. Массальский, А. Олесь, *Об отношении фотонов к электронам в широких атмосферных ливнях космического излучения вычисленного на основе анализа кривой пробега*

На основе анализа кривой пробега частиц широких атмосферных ливней космического излучения полученной на высоте 2636 м над уровнем моря выяснено несогласованность экспериментальных результатотв на отношение фотонов

к элетронам (p/e) с теорией. Подтверждено согласно предположению теории наличие большого числа фотонов с энергией ниже пороговой энергии аппаратуры на регистрацию электронов. Определенное отношение фотонов к электронам для пороговой энергии 15 мев. и фотонов 15—30 мев., $p/e = 1{,}0 \pm 0{,}1$ (дано только статистическую ошибку) является нижним приделом действительной величины по поводу влияния фотонов малой энергии на кривую пробега.

REFERENCES

Arley, N., *On the theory of the stochastic processes*, Copenhagen 1948.

Babecki, J., Jurkiewicz, L., Massalski, J., Mięsowicz, M., *Acta phys. Polon.*, **16,** 119 (1957).

Babecki, J. — *Acta Phys. Polan.*, **17,** 409 (1958)

Bassi, P., Biancki, A. M., Manduchi, C., *Nuovo Cim.*, **9,** 358 (1952).

Belenky, S. Z., *Avalanche processes in cosmic radiation*, Moscow 1948.

Brennan, M. H., *Nuovo Cim.*, **6,** 216 (1957).

Dohán, I., Gemesy, T., Sándor, T., Somogyi, A., *A MTA Központi Fizikai Kutató Intéretének Közlemenyei*, Vol. **5,** 461 (1957).

Dubinsky, J., Massalski, J. M., Mokry, P., Oleś, A., Porębski, J., *Matematicko-Fizikalny Casopis* SAV VII, 4, (1957).

Greisen, K., *Phys. Rev.*, **75,** 1071 (1949).

Greisen, K., *Progress in Cosmic Ray Physics*, edited by J. G. Wilson, Amsterdam 1956.

Ivanenko, I. P. — private communication (in the press).

Jurkiewicz, L., *Bull. Acad. Pol. Sci. Cl.* III, **2,** 329 (1954).

Massalski, J. M., *Bull. Acad. Pol. Sci. Cl.* III, **2,** 335 (1954).

Millar, C., *Nuovo Cim.* **8,** 279 (1951).

Milone, C., *Phys. Rev.*, **87,** 680 (1952a), *Nuovo Cim.*, **9,** 549 (1952b), *ibid*, **10,** 340 (1953a), **10,** 1126 (1953b), **11,** 241 (1954).

Richards, J. A., Nordheim, L. W., *Phys. Rev.*, **74,** 1106 (1948).

Zatsepin, G. T., *Dokl. Akad. Nauk SSSR*, **63,** 243 (1948).

Zatsepin, G. T., *Thesis*, Moscow 1950.

ANALYSIS OF THE INFLUENCE OF LOW ENERGY PENETRATING PHOTONS ON THE ABSORPTION OF EXTENSIVE AIR SHOWERS IN LEAD

By Jan Babecki

Institute of Nuclear Research, Cosmic Ray Department, Cracow.

(Received May 14, 1958)

Continuing the previous work on photons appearing under large thicknesses of lead, we obtained experimental absorption curves from which we calculated for various thicknesses of Pb the mean number of penetrating photons leaving the absorber during one act of coincidence and the number of these photons per electron striking the absorber. The absorption coefficient was found for the photons under study and the value of this coefficient agrees with the theoretical value for an energy range of 1.2—7 MeV. In this manner we obtained a full picture of the phenomenon of the prolongation of the range of electron-photon cascades by photons of energies corresponding to the minimum absorption coefficient.

From experiment it is known that there is a drop in the absorption curve of extensive air showers of cosmic radiation in lead for thicknesses greater than 10 cm (Zatsepin et al. 1948, Babecki et al. 1957). In connection with attempts to explain the mechanism of this phenomenon. Greisen (1949) drew attention to the fact that in measurements of the absorption of extensive air shower particles with very thick lead absorber an important role should be played by photons of an energy of several MeV; these photons are present under the absorber in a far greater number than the electrons. Photons of energies of 1.2—7 MeV, i.e. falling within the range of the "Compton window", correspond to small values of the absorption coefficient; the mean free path of these photons in lead is about 2 cm. It is the low-energy penetrating photons which are responsible for the prolongatnion of the electron-photon cascade in lead.

In calculating the cascade curves for electrons and photons in lead it is therefore necessary to take into account the relation between the photon absorption coefficient and the energy (Zatsepin 1948, Ivanenko 1956, and others). The experimental confirmation of penetrating photons is mentioned in papers by Daudin (1949) and Bassi et al. (1952). This work was continued later at this institute (Jurkiewicz 1954, Babecki et al. 1957.)

In order to establish a final experimental basis for these views a determination

was made in the present work of the number of low energy penetrating photons leaving the absorber with respect to the number of electrons; the absorption coefficient in lead was also determined for these photons.

In the first part of the work the apparatus employed consisted of a detector of extensive air showers (three counter trays: A, B, C, each of an area of $S = 0.468$ m^2 placed in the corners of a triangle having sides 3.4 m in length) and a counter telescope containing three trays: D, E, F (Fig. 1), each of an area of $s = 0.290$ m^2 and placed

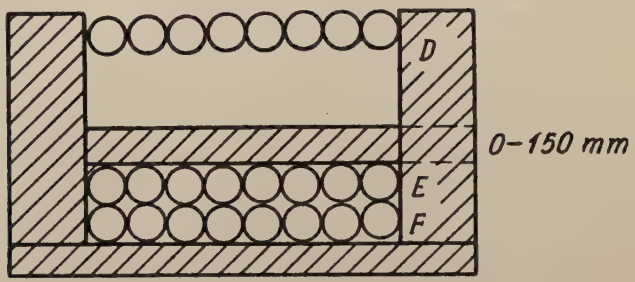

Fig. 1. Counter telescope used in the first series of measurements.

in the centre of the triangle. All G.M. counters were made of brass and had 1 mm walls. Between trays D and E a lead absorber of up to 15 cm could be placed. threefold coincidences $ABC = T$, five-fold coincidences TDF and six-fold coincidences $TDEF$ were counted simultaneously. In analysing the results the ratio of the number of various coincidences to the number of threefold coincidences was taken into consideration. The purpose of this was to eliminate the barometric effect.

The effect of penetrating photons becomes evident upon comparing the number of five-fold TDF and six-fold $TDEF$ coincidences for large thicknesses of absorber (Babecki et al. 1957). The number of five-fold coincidences can be expressed by the formula:

$$TDF(t) = K \cdot \int_0^\infty x^{-(\gamma+1)} (1 - e^{-Sx})^3 (1 - e^{-\mathcal{R}_2(t)Sx})\, dx \qquad (1)$$

where t is the absorber thickness, x the density of the shower particles, $Kx^{-(\gamma+1)}\,dx$ — the differential density spectrum of the recorded showers, and $\mathcal{R}_2(t)$ denotes the relative number of particles actuating trays D and F, i.e. the ratio of the mean number of such particles to the mean number of these particles falling on the detector tray during the same act of coincidence. The term "relative number of particles" will be used in this sense hereafter. We express in a manner identical to the above formula the relation between the number of six-fold coincidences $TDEF$ and the relative number of particles $\mathcal{R}_3(t)$, causing these coincidences. With the help of formula (1) $\mathcal{R}_2$ and $\mathcal{R}_3$ can be found graphically from the ratios of the numbers of coincidences TDF/T and $TDEF/T$.

From the numbers $\mathcal{R}_2$ and $\mathcal{R}_3$ we subtracted the background of the penetrating component measured with an absorber of 25 cm Pb over the entire telescope. The relative numbers of particles of the electron-photon component R_2 and R_3 obtained in this way are given in table I.

TABLE I

Results of the first series of measurements

t mm	R_2	R_3	N_γ	N	n
25	0.180	0:148	2.58	17.4	15.3
50	0.0843	0.0605	1.90	31.4	17.0
75	0.0354	0.0248	0.855	34.5	10.5
100	0.0130	0.0070	0.484	69.2	7.76
150	0.0007	0.0003	0.0323	108	0.69

For all thicknesses of the absorber $R_2 > R_3$. For zero and small thicknesses of Pb this inequality is explained in the paper by Massalski and Oleś (in the press) by the existence in extensive showers of very large numbers of soft photons of energies of the order of several hundred keV.

With greater thicknesses of absorber the inequality $R_2 > R_3$ is caused by the penetrating photons generated in the absorber with an energy of 1.2 to 7 MeV. In view of the low efficiency of the G.M. counters for photons, they contribute to the registration of *TDF* coincidences (one tray beneath the absorber), but they do not contribute to the registration of *TDEF* coincidences (two trays beneath the absorber). The difference R_2—R_3 is caused by such cases in which the upper counter tray D is actuated by particles from the extensive air showers and the lower tray F by photons emitted from the absorber.

The difference $R = R_2 - R_3$ expresses the relative number of electrons produced in the walls of the counters under the absorber by the low-energy photons leaving the absorber. If by ε we denote the efficiency of the counters for photons (here, we assumed $\varepsilon = 2\%$ (Renard 1948), then $N_\gamma = (S/s)\,(R/\varepsilon)$ will express the number of penetrating photons under the absorber per electron falling on the absorber. $N = N_\gamma/R_3$ expresses the number of penetrating photons per electron coming out of the absorber while $n = s\bar{x}N_\gamma$ is the mean number of penetrating photons leaving the absorber in one act of coincidence ($\bar{x}$ is the mean density of particles in the shower). The definitions formulated in the last few sentences are, of course, correct only for large thicknesses of absorber ($t > 2.5$ cm).

Table I gives the values of N_γ, N and n for various thicknesses of Pb. It can be seen that in one act of coincidence there come out of the absorber usually not one but several or up to about fifteen or so penetrating photons. It should be noted that Greisen considered the effect of penetrating photons only from 10 cm of Pb, whereas in the present work it is considered from 2.5 cm of Pb.

Greisen gave a theoretical formula according to which $N_\gamma \sim e^{-\sigma t}$, where σ is the coefficient of photon absorption, corresponding to the minimum of "Compton window" in lead. Greisen, following Hirschfelder and Adams (1948), assumes $\sigma = 0.38\ \mathrm{cm}^{-1}$ (for photon energies of 3 MeV). From the curve $N_\gamma(t)$ (Fig. 2) it is found that $\sigma = (0.39 \pm 0.08)\ \mathrm{cm}^{-1}$, which is in agreement with the theoretical value.

In the above measurements the layer of lead between trays D and E was an absorber for penetrating photons and at the same time their generator. Therefore for

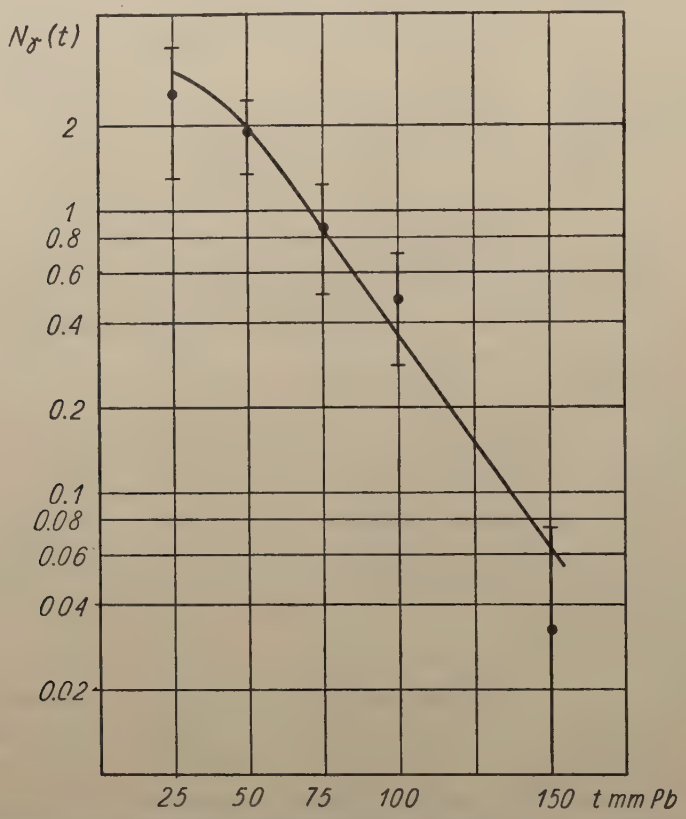

Fig. 2. The absorption curve of the penetratnig photons obtained from the first series of measurements.

each thickness of absorber the photons were produced with a different intensity and, perhaps, with a different energetic constitution. The difference between the numbers of *TDF* and *TDEF* coincidences could have been increased by particles which fell at an angle to tray *D* and then, due to scattering in the side walls of the telescope, actuated tray *F* and by-passed tray *E*.

In order to measure the absorption of penetrating photons in a better geometry we made another series of measurements with trays *A*, *B* and *C* unchanged but with a different telescope (Fig. 3). In trays *D*, *E* and *F* aluminium counters with 1 mm walls

were employed. The areas of trays D and F were 0.295 m^2, while tray E had an area considerably larger (0.528 m^2) in order to eliminate any possible influence of particles scattered from the side walls of the telescope. The coincidences T, TDF and $TDEF$ were counted, each with the aid of four independent numerating systems. The generator of penetrating photons consisted of a layer of lead of a given thickness $T = 50$ mm,

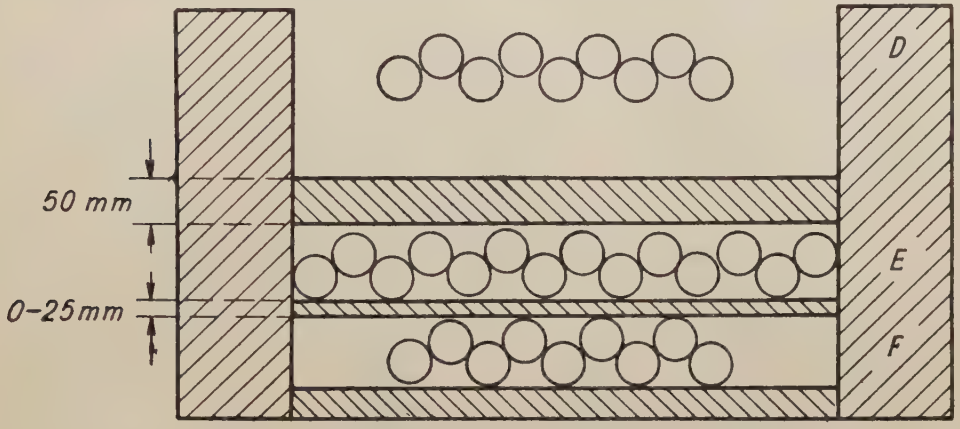

Fig. 3 Counter telescope used in the second series of measurements.

lying between the trays D and E, while photons were absorbed by a layer of lead of a variable thickness ranging from 0 to 25 mm, placed between trays E and F.

Table II gives the relative numbers of particles R_2 and R_3 counted from the second series of measurements and the corresponding values of N_γ. The maximum of the absorption curve $N_\gamma(t)$ (Fig. 4) is caused by the transition effect of the

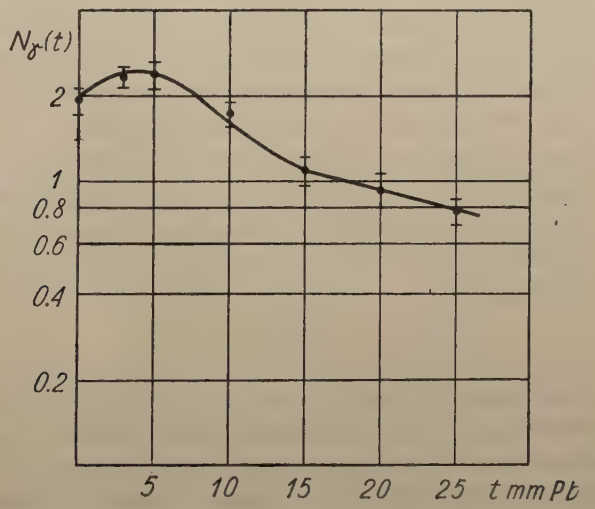

Fig. 4 The absorption curve of the penetrating photons obtained from the second series of measurements.

penetrating photons in the lead. The drop in the curve is at first quite sharp, since the lead generator emits photons of various energies which belong to the "Compton window", and to which there correspond absorption coefficients greater than minimum. As the thickness of the absorber t increases the less penetrating photons are absorbed, so that the last three points now lie on a straight line, from which the minimum coefficient of absorption can be calculated: $\sigma = (0.34 \pm 0.14)$ cm^{-1}.

This result is in agreement with both the value assumed by Greisen and the value calculated from the previous series of measurements. This strengthens the reliability of the results of the first series. It can therefore be concluded that the scattering of particles on the side walls of the telescope does not play a significant role in this type of telescope measurements.

TABLE II

Results of the second series of measurements ($T = 50$ mm Pb)

t mm	R_2	R_3	$N\gamma$
0	0.106	0.0815	1.94
3	0.104	0.0747	2.32
5	0.0990	0.0690	2.38
10	0.0880	0.0662	1.73
15	0.0655	0.0518	1.09
20	0.0675	0.0557	0.935
25	0.0491	0.0393	0.776

On the basis of the work of Babecki et al. (1957) and the present paper it may be concluded that if we make measurements of the absorption of extensive air shower particles with a telescope in which there is only one counter tray under the lead then the curve obtained will be the result of the registration of not only the ionizing particles coming out of the absorber (electrons, muons) but will be increased and extended by penetrating photons of an energy of 1.2—7 MeV. In order to obtain an absorption curve for ionizing particles leaving the absorber it is necessary to use a telescope in which there are two or more counter trays beneath the lead.

I wish to express my gratitude to Professor M. Mięsowicz for suggesting the topic and for guiding the work. I also wish to thank Professor L. Jurkiewicz, Docent J. M. Massalski, Candidate of Science I. P. Ivanenko (Moscow University) Magister A. Oleś and Magister J. Porębski for their valuable discussions and assistance in carrying out the work.

КРАТКОЕ СОДЕРЖАНИЕ

Я. Бабецкий, *Анализ влияния фотонов малых энергии, большой проникающей способности на абсорбцию широких атмосферных ливней космического излучения в свинце*

Продолжая предыдущие работы по фотонам выступающим под большими толщинами свинца, получено экспериментальные кривые поглощения, из которых вычислено для разных толщин *Pb* среднее число фотонов большой проникающей

способности вылетающих из поглотителя во время одного акта совпадения, а также число этих фотонов на один электрон, падающий на поглотитель. Вычислено коэффициент поглощения рассмотриваемых фотонов, величина которого согласуется с теоретической величиной для предела энергии 1,2—7 мэв. Таким образом получено полный вид продолжения пробега электроннофотонной каскады фотонами обладающими энегриями, которые отвечают минимальному коэффициенту поглощения.

REFERENCES

Babecki, J., Jurkiewicz, L., Massalski, J. M., Mięsowicz, M., *Acta phys. Polon.*, **16,** 119 (1957).
Bassi, P., Bianchi, A. M., Manduchi, C., *Nuovo Cimento*, **9,** 358 (1952).
Daudin, J., *C. R. Acad. Sci. (Paris)*, **228,** 1285 (1949).
Greisen, K., *Phys. Rev.*, **75,** 1071 (1949).
Hirschfelder, J. O., Adams, E. N., *Phys. Rev.*, **73,** 863 (1948).
Ivanenko, I. P., *Dokl. Akad. Nauk SSSR*, **107,** 819 (1956).
Jurkiewicz, L., *Bull. Acad. Polon. Sci.*, Cl. III, **2,** 329 (1954).
Massalski, J. M., Oleś, A., *Acta phys. Polon.*, **17**, 401 (1958)
Renard, G. A., *J. Phys. Rad.* **9,** 212 (1948).
Zatsepin, G. T., Kuchai, S. A., Rozental, I. L., *Dokl. Akad. Nauk SSSR*, **61,** 47 (1948).
Zatsepin, G. T., *Dokl. Akad. Nauk SSSR*, **63,** 243 (1948).

THE 13-PARAMETRIC GROUP OF TRANSFORMATIONS OF THE SPINOR SPACE AND ITS REPRESENTATIONS

By Jan Rzewuski

Institute of Theoretical Physics, University of Wrocław; Institute of Physics, Polish Academy of Sciences, Wrocław Branch, Wrocław

(Received May 23, 1958)

The irreducible representations of a 13-parametric group of transformations of the spinor space are constructed. They include all transformation types assumed so far phenomenologically for the fundamental particles including their isotopic spin characterization. An eight-dimensional real spinor space corresponding to the original four-dimensional complex spinor space is introduced. It is shown that the spinor space provides a common geometrical basis for all conservation laws (including charge, isotopic spin and baryon conservation laws). The possible bilinear connexions of the spinor space with the conventional space-time are discussed. These connexions enable one to introduce inversions and to derive the connexion between the differential equations in both spaces.

Introduction

In preceding work[1] we have considered the eightdimensional spinor space as the geometrical basis for a physical theory. In this space a group $\boldsymbol{g}$ of transformations[2] was operating which was a direct product of two six-parametric commuting unimodular groups $\boldsymbol{c}$ and $\boldsymbol{c'}$ and a one-parametric commutative group $\boldsymbol{a}$

$$\boldsymbol{g} = \boldsymbol{c} \cdot \boldsymbol{c'} \cdot \boldsymbol{a} \tag{0.1}$$

The groups $\boldsymbol{c}$, $\boldsymbol{c'}$ and $\boldsymbol{a}$ were defined as the following transformation groups of the four complex coordinates z_α, $z_{\dot\alpha}$ ($\alpha = 1,2$) of a point in the spinor space

$$\boldsymbol{c}: \quad \begin{matrix} z_1' = \alpha z_1 + \beta z_2 & z_{\dot 1}^{*\prime} = \alpha z_{\dot 1}^* + \beta z_{\dot 2}^* \\ z_2' = \gamma z_1 + \delta z_2 & z_{\dot 2}^{*\prime} = \gamma z_{\dot 1}^* + \delta z_{\dot 2}^* \end{matrix} \qquad \alpha\delta - \beta\gamma = 1 \tag{0.2}$$

[1] Jan Rzewuski (1958a, b, c), quoted hereafter as I, II, III respectively.

[2] A subgroup of $\boldsymbol{c'}\,\boldsymbol{a}$ namely the direct product $\boldsymbol{u'}\,\boldsymbol{a}$ where $\boldsymbol{u'}$ is the three-parametric unitary subgroup of $\boldsymbol{c'}$ was considered in another connexion by W. Pauli (1957), C. Enz (1957), D. L. Pursey (1957) and F. Gürsey (1958). Gürsey introduces also the full group $\boldsymbol{c'}$.

$$\boldsymbol{c}': \quad \begin{matrix} z'_\varrho = az_\varrho + bz^*_\varrho \\ z^{*\prime}_\varrho = cz_\varrho + dz^*_\varrho \end{matrix} \qquad ad - bc = 1 \qquad (\varrho = 1,2) \tag{0.3}$$

$$\boldsymbol{a}: \quad z'_\varrho = e^{i\varphi} z_\varrho, \qquad z^{*\prime}_\varrho = e^{i\varphi} z^*_\varrho \qquad (\varrho = 1,2) \tag{0.4}$$

In this paper we want to discuss briefly the representations of the group $\boldsymbol{g}$ in connexion with the classification of fundamental particles (Section 1) and introduce the formalizm of the eight-dimensional real spinor space (Section 2) which is a convenient tool for all considerations involving differential operations in the spinor space. It is shown that the spinor space provides a common geometrical basis for the conservation laws of angular momentum, isotopic spin, charge and number of baryons. Finally (Section 3) we discuss the possible connexions of the coordinates of the spinor space with the coordinates of space-time. These connexions enable one to introduce the notion of inversions and to derive the connexion between differential equations in both spaces.

1. Representations of the group g

The representations of the group g may be easily found by the conventional method of infinitesimal transformations. We shall first consider the representations of $\boldsymbol{c} \cdot \boldsymbol{c}'$

Introducing the 12 parameters

$$\begin{aligned} &\alpha = 1 + \alpha_1 + i\alpha_2 \qquad \beta = \alpha_3 + i\alpha_4 \\ &\gamma = \alpha_5 + i\alpha_6 \qquad \delta = \frac{1 + (\alpha_3 + i\alpha_4)(\alpha_5 + i\alpha_6)}{1 + \alpha_1 + i\alpha_2} \\ &a = 1 + \alpha_7 + i\alpha_8 \qquad b = \alpha_9 + i\alpha_{10} \\ &c = \alpha_{11} + i\alpha_{12} \qquad d = \frac{1 + (\alpha_9 + i\alpha_{10})(\alpha_{11} + i\alpha_{12})}{1 + \alpha_7 + i\alpha_8} \end{aligned} \tag{1.1}$$

we may write for an arbitrary representation u of the group $\boldsymbol{c} \cdot \boldsymbol{c}'$

$$u' = D(\alpha)u = \left[1 + \sum_{i=1}^{12} \left(\frac{\partial D}{\partial \alpha_i}\right)_{\alpha=0} \alpha_i + \ldots\right] u. \tag{1.2}$$

To find the commutation relations between the generators of the infinitesimal transformations

$$I_i = \left[\frac{\partial D(\alpha)}{\partial \alpha_i}\right]_{\alpha=0} \tag{1.3}$$

we take the particular case of the representation $z\,(z_1, z_2, z^*_1, z^*_2)$ of the group $\boldsymbol{c} \cdot \boldsymbol{c}'$ through itself (cf. (0.2—3) and 1.1)) and obtain

$$I_1 = \begin{Vmatrix} 1 & 0 & 0 & 0 \\ 0 & -1 & 0 & 0 \\ 0 & 0 & 1 & 0 \\ 0 & 0 & 0 & -1 \end{Vmatrix}, \quad I_3 = \begin{Vmatrix} 0 & 1 & 0 & 0 \\ 0 & 0 & 0 & 0 \\ 0 & 0 & 0 & 1 \\ 0 & 0 & 0 & 0 \end{Vmatrix}, \quad I_5 = \begin{Vmatrix} 0 & 0 & 0 & 0 \\ 1 & 0 & 0 & 0 \\ 0 & 0 & 0 & 0 \\ 0 & 0 & 1 & 0 \end{Vmatrix}$$

$$I_7 = \begin{Vmatrix} 1 & 0 & 0 & 0 \\ 0 & 1 & 0 & 0 \\ 0 & 0 & -1 & 0 \\ 0 & 0 & 0 & -1 \end{Vmatrix}, \quad I_9 = \begin{Vmatrix} 0 & 0 & 1 & 0 \\ 0 & 0 & 0 & 1 \\ 0 & 0 & 0 & 0 \\ 0 & 0 & 0 & 0 \end{Vmatrix}, \quad I_{11} = \begin{Vmatrix} 0 & 0 & 0 & 0 \\ 0 & 0 & 0 & 0 \\ 1 & 0 & 0 & 0 \\ 0 & 1 & 0 & 0 \end{Vmatrix} \tag{1.4}$$

and

$$I_{2n} = iI_{2n-1} \qquad (n = 1,2, \ldots, 6) \tag{1.5}$$

These operators satisfy certain commutation relations which are independent of the order of representation. The commutation relations are most conveniently expressed by means of the following linear combinations of the operators (1.4):

$$\begin{aligned} I_z^1 &= \tfrac{1}{4}(I_1 + iI_2) & I_z^2 &= \tfrac{1}{4}(I_1 - iI_2) \\ I_+^1 &= \tfrac{1}{2}(I_3 + iI_4) & I_+^2 &= \tfrac{1}{2}(I_3 - iI_4) \\ I_-^1 &= \tfrac{1}{2}(I_5 + iI_6) & I_-^2 &= \tfrac{1}{2}(I_5 - iI_6) \\ I_z^3 &= \tfrac{1}{4}(I_7 + iI_8) & I_z^4 &= \tfrac{1}{4}(I_7 - iI_8) \\ I_+^3 &= \tfrac{1}{2}(I_9 + iI_{10}) & I_+^4 &= \tfrac{1}{2}(I_9 - iI_{10}) \\ I_-^3 &= \tfrac{1}{2}(I_{11} + iI_{12}) & I_-^4 &= \tfrac{1}{2}(I_{11} - iI_{12}) \end{aligned} \tag{1.6}$$

It may now be easily verified that the operators with different upper indices commute, and the operators with the same upper index satisfy the following relations:

$$\begin{aligned} [I_z^i, I_+^i] &= I_+^i \\ [I_z^i, I_-^i] &= -I_-^i \\ [I_+^i, I_-^i] &= 2I_z^i \end{aligned} \tag{1.7}$$

These relations determine uniquely the representation.

Introducing the vectors u_1, u_2, $u_{\dot 1}$, $u_{\dot 2}$ which transform with respect to $\boldsymbol{g}$ contragrediently to (0.2)

$$\begin{aligned} u_1' &= \alpha u_1 + \gamma u_2 & u_{\dot 1}' &= \alpha^* u_{\dot 1} + \gamma^* u_{\dot 2} \\ u_2' &= \beta u_1 + \delta u_2 & u_{\dot 2}' &= \beta^* u_{\dot 1} + \delta^* u_{\dot 2} \end{aligned} \tag{1.8}$$

and the vectors v_1, v_2, $v_{\dot 1}$, $v_{\dot 2}$ which transform with respect to $\boldsymbol{g}$ contragrediently to (0.3)

$$\begin{aligned} v_1' &= av_1 + cv_2 & v_{\dot 1}' &= a^* v_{\dot 1} + c^* v_{\dot 2} \\ v_2' &= bv_1 + dv_2 & v_{\dot 2}' &= b^* v_{\dot 1} + d^* v_{\dot 2} \end{aligned} \tag{1.9}$$

we easily find for an arbitrary representation the basis

$$w^{\mathcal{J}_1,\mathcal{J}_2,\mathcal{J}_3,\mathcal{J}_4}_{M_1,M_2,M_3,M_4} = \tag{1.10}$$

$$= \frac{u_1^{\mathcal{J}_1+M_1} u_2^{\mathcal{J}_1-M_1} u_{\dot{1}}^{\mathcal{J}_2+M_2} u_{\dot{2}}^{\mathcal{J}_2-M_2} v_1^{\mathcal{J}_3+M_3} v_2^{\mathcal{J}_3-M_3} v_{\dot{1}}^{\mathcal{J}_4+M_4} v_{\dot{2}}^{\mathcal{J}_4-M_4}}{\sqrt{(\mathcal{J}_1+M_1)!(\mathcal{J}_1-M_1)!(\mathcal{J}_2+M_2)!(\mathcal{J}_2-M_2)!(\mathcal{J}_2+M_3)!(\mathcal{J}_3-M_3)!(\mathcal{J}_4+M_4)!(\mathcal{J}_4-M_4)!}}$$

The coefficients of the vectors (1.10) corresponding to a fixed representation (fixed $\mathcal{J}_1$, $\mathcal{J}_2$, $\mathcal{J}_3$, $\mathcal{J}_4$) transform contragrediently to (1.10). They may by written, therefore, in the form

$$f_{\alpha\ldots\beta\dot{\gamma}\ldots\dot{\delta};\varrho\ldots\sigma\dot{\lambda}\ldots\dot{\tau}} \,, \tag{1.11}$$

where the indices before the comma transform with respect to $\boldsymbol{g}$ according to $\boldsymbol{c}$ and the indices after the comma according to $\boldsymbol{c}'$. One easily shows (by means of the conventional methods) using relations (1.7) that one obtains in this way all irreducible representations of the group $\boldsymbol{c}\cdot\boldsymbol{c}'$. The representations of the full group $\boldsymbol{g} = \boldsymbol{c}\cdot\boldsymbol{c}'\cdot\boldsymbol{a}$ are easily obtained by Kronecker multiplication of (1.10) with the one-dimensional spaces which transform with respect to $\boldsymbol{g}$ according to one-dimensional representations of the commutative one-parametric group $\boldsymbol{a}$. There appears a 13-th operator of infinitesimal transformations I_{13} corresponding to the parameter $\varphi = \alpha_{13}$ of (0.4). This operator, being a multiple of the unit matrix, commutes, of course, with all the operators $I_1, \ldots I_{12}$.

We note that among the representations given by (1.10) or (1.11) all transformation types occur which were assumed so far for the description of fundamental particles including their isotopic spin characterization. This is easily seen if we consider the transformations of $\boldsymbol{c}$ as corresponding to the ordinary spin and the transformations of $\boldsymbol{c}'$ as corresponding to the isotopic spin (or vice versa).

This result may appear trivial since it could be obtained by simply attaching isotopic spin indices to the conventional representations of the group $\boldsymbol{c}$. This was in fact the phenomenological method used so far in the description of fundamental particles. In this phenomenological method, however, there exists no geometrical space in which the transformations of the isotopic spin indices could operate. Even if such a space was introduced it was disconnected with the geometrical space-time.

In our formulation the isotopic spin transformations operate on the same geometrical space as the ordinary spin transformations, namely on the spinor space of the variables z_α, $z_{\dot{\alpha}}$. The representations (1.11) are to be considered as functions of the coordinates z_α, $z_{\dot{\alpha}}$ of this space, the coordinates x_μ of space-time appearing as a secondary notion (cf. Section 3).

In the present formulation the order of representations is not bounded and, therefore, arbitrary isotopic spins enter into the theory. This is a similar situation as with the ordinary spin. In this connexion we would like to mention a possibility of

restricting the representations of the group $\boldsymbol{g}$ to the lowest with $\mathcal{J}_i \leqslant \frac{1}{2}$ $(i = 1, \ldots 4)$. For this purpose it is sufficient to consider instead of the vectors v_α, $v_{\dot\alpha}$, v_α, $v_{\dot\alpha}$, the operators

$$u_{\dot\alpha}\xi_1, \; u_{\dot\alpha}\xi_2, \; v_\alpha\xi_2, \; v_{\dot\alpha}\xi_4 \tag{12}$$

where the ξ_i satisfy any of the following conditions

$$\xi_i^2 = 0, \quad [\xi_i, \xi_k]_- = 0$$

or (13)

$$[\xi_i, \xi_k]_+ = 0 \; [1]$$

Assumption (12—13) is in agreement with the transformation properties (0.2—4) and yields the desired effect of restricting formally the ordinary as well as the isotopic spin to the lowest values 0, $\frac{1}{2}$, 1. It remains, of course, an open question whether a formal device of this kind possesses any deeper physical or geometrical meaning.

Corresponding to the $6 + 6 + 1 = 13$ parameters of the group $\boldsymbol{g}$ we have 13 conservation laws which possess a common geometrical origin in the transformations of the spinor space. The 6 laws corresponding to $\boldsymbol{c}$ may be considered as the conservation laws of angular momentum, the 6 laws corresponding to $\boldsymbol{c}'$ as conservation laws of isotopic angular momentum and the one conservation law corresponding to $\boldsymbol{a}$ as the conservation law of baryons (cf. reference on page 1).

As far as non-interacting fields are considered charge conservation is a consequence of invariance with respect to $\boldsymbol{c}'$. In the case of interacting fields charge is not necessarily conseved as a consequence of $\boldsymbol{c}'$ and one has to demand invariance with respect to other transformations of the coordinates z_α, $z_{\dot\alpha}$ connected with inversions (cf. Section 3). In the case of the less stringent condition of invariance with respect to the subgroup $\boldsymbol{u}'$ of $\boldsymbol{c}'$ one obtains then results which are analogous to those of d'Espagnat and Prentki (1956). If one demands invariance with respect to the full group $\boldsymbol{c}'$ one gets more stringent conditions upon the possible interaction terms.

2. The real spinor space

If one wants to develop dynamics in the spinor space one has to consider the physical fields as representations of the group $\boldsymbol{g}$ which are functions of the coordinates z of this space. This problem will be treated in a forthcoming paper (cf. also II), here we want to do only some preparatory work. It is namely sometimes more convenient in considerations involving differentiation processes to deal with real variables. We, therefore, introduce in this Section a real spinor space equivalent to the complex space z.

Consider the eight real variables r_μ and s_μ $(\mu = 1, 2, 3, 4)$ connected with the

[1] For another formulation of this type see W. Królikowski (1958). It may be noted, however, that in Królikowskis formulation only the isotopic spin is restricted to the values $0, \frac{1}{2}, 1$ the ordinary spin being as before arbitrary.

variables z by means of the relations

$$\begin{aligned} z_1 &= r_1 + s_4 + i\,(s_1 - r_4) & z_{\dot{1}} &= -r_2 + s_3 + i\,(s_2 + r_3) \\ z_2 &= r_2 + s_3 + i\,(s_2 - r_3) & z_{\dot{2}} &= r_1 - s_4 - i\,(s_1 + r_4). \end{aligned} \tag{2.1}$$

To the infinitesimal transformations of the group $\boldsymbol{c} \cdot \boldsymbol{c}'$ (cf. (0.2—3) and (1.1)) there correspond the following transformations of the r_μ and s_μ.

$$\begin{aligned} r'_\mu &= r_\mu + \varepsilon_{\mu\nu}\, r_\nu + \eta_{\mu\nu}\, s_\nu & \varepsilon_{\mu\nu} &= -\varepsilon_{\nu\mu} \\ s'_\mu &= s_\mu - \eta_{\mu\nu}\, r_\nu + \varepsilon_{\mu\nu}\, s_\nu & \eta_{\mu\nu} &= -\eta_{\nu\mu} \end{aligned} \tag{2.2}$$

The 12 infinitesimal parameters $\varepsilon_{\mu\nu}$, $\eta_{\mu\nu}$ are connected with the parameters $\alpha_1, \ldots \alpha_{12}$ of Section 1 by means of the relations

$$\begin{aligned} \alpha_1 + i\alpha_2 + \alpha_7 + i\alpha_8 &= \eta_{14} + i\varepsilon_{14} \\ -\alpha_1 - i\alpha_2 + \alpha_7 + i\alpha_8 &= \eta_{23} + i\varepsilon_{23} \\ \alpha_3 + i\alpha_4 &= \tfrac{1}{2}\,[\varepsilon_{12} - \varepsilon_{34} + \eta_{13} + \eta_{24} + i(-\eta_{12} + \eta_{34} + \varepsilon_{13} + \varepsilon_{24})] \\ \alpha_9 + i\alpha_{10} &= \tfrac{1}{2}\,[-\varepsilon_{12} - \varepsilon_{34} + \eta_{13} - \eta_{24} + i(\eta_{12} + \eta_{34} + \varepsilon_{13} - \varepsilon_{24})] \\ \alpha_5 + i\alpha_6 &= \tfrac{1}{2}\,[-\varepsilon_{12} + \varepsilon_{34} + \eta_{13} + \eta_{24} + i(\eta_{12} - \eta_{34} + \varepsilon_{13} + \varepsilon_{24})] \\ \alpha_{11} + i\alpha_{12} &= \tfrac{1}{2}\,[\varepsilon_{12} + \varepsilon_{34} + \eta_{13} - \eta_{24} + i(-\eta_{12} - \eta_{34} + \varepsilon_{13} - \varepsilon_{24})]. \end{aligned} \tag{2.3}$$

One easily infers from these formulae that for

$$\begin{aligned} \varepsilon_{12} &= -\varepsilon_{34} = \varepsilon_3 & \eta_{12} &= -\eta_{34} = \eta_3 \\ \varepsilon_{31} &= -\varepsilon_{24} = \varepsilon_2 & \eta_{31} &= -\eta_{24} = \eta_2 \\ \varepsilon_{23} &= -\varepsilon_{14} = \varepsilon_1 & \eta_{23} &= -\eta_{14} = \eta_1 \end{aligned} \tag{2.4}$$

we get $\alpha_7 = \alpha_8 = \ldots \cdot = \alpha_{12} = 0$. This choice of parameters corresponds, therefore, to the transformations of the group c. Similarly for

$$\begin{aligned} \varepsilon_{12} &= +\varepsilon_{34} = \varepsilon_3 & \eta_{12} &= +\eta_{34} = \eta_3 \\ \varepsilon_{31} &= +\varepsilon_{24} = \varepsilon_2 & \eta_{31} &= +\eta_{24} = \eta_2 \\ \varepsilon_{23} &= +\varepsilon_{14} = \varepsilon_1 & \eta_{23} &= +\eta_{14} = \eta_1 \end{aligned} \tag{2.5}$$

we get $\alpha_1 = \alpha_2 = \ldots = \alpha_6 = 0$. This choice corresponds, therefore, to transformations of the group c'. The general transformations (2.2) are transformations of an eight-dimensional real space with the two invariant forms

$$r_\mu^2 - s_\mu^2 \quad \text{and} \quad r_\mu s_\mu \tag{2.6}$$

Here the usual convention about summation (from 1 to 4) is adopted for the indices μ. Note, however, that r_4 and s_4 are real.

One easily verifies that

$$r_\mu^2 - s_\mu^2 = \tfrac{1}{2}(z_\alpha^* z^{\dot\alpha} + z_\alpha z^{\dot\alpha *})$$
$$r^\mu s^\mu = \frac{i}{4}(z_\alpha^* z^{\dot\alpha} - z_\alpha z^{\dot\alpha *}) \tag{2.7}$$

This is the real and imaginary part of the only complex quantity $z_\alpha^* z^{\dot\alpha}$ which is invariant with respect to transformations of the group $\boldsymbol{c}\cdot\boldsymbol{c}'$ (cf. III). Transformations of $\boldsymbol{a}$ multiply $z_\alpha z^{\dot\alpha *}$ by the factor $e^{2i\varphi}$. Therefore, the only real invariant with respect to the full group $\boldsymbol{g}$ is the absolute value $|z_\alpha^* z^{\dot\alpha}|$.

Introducing the vector k with the components $r_1, \ldots, r_4, s_1, \ldots, s_4$ we may write (2.2) in matrix notation

$$k' = k + \tfrac{1}{2}(I_{\mu\nu}\,\varepsilon_{\mu\nu} + \mathcal{J}_{\mu\nu}\,\eta_{\mu\nu})k, \tag{2.8}$$

with

$$I_{\mu\nu} = \begin{pmatrix} \gamma_{\mu\nu} & 0 \\ 0 & \gamma_{\mu\nu} \end{pmatrix}, \quad \mathcal{J}_{\mu\nu} = \begin{pmatrix} 0 & \gamma_{\mu\nu} \\ -\gamma_{\mu\nu} & 0 \end{pmatrix}, \tag{2.9}$$

and

$$\gamma_{12} = \begin{Vmatrix} 0 & 1 & 0 & 0 \\ -1 & 0 & 0 & 0 \\ 0 & 0 & 0 & 0 \\ 0 & 0 & 0 & 0 \end{Vmatrix}, \quad \gamma_{31} = \begin{Vmatrix} 0 & 0 & -1 & 0 \\ 0 & 0 & 0 & 0 \\ 1 & 0 & 0 & 0 \\ 0 & 0 & 0 & 0 \end{Vmatrix}, \quad \gamma_{23} = \begin{Vmatrix} 0 & 0 & 0 & 0 \\ 0 & 0 & 1 & 0 \\ 0 & -1 & 0 & 0 \\ 0 & 0 & 0 & 0 \end{Vmatrix},$$
$$\gamma_{14} = \begin{Vmatrix} 0 & 0 & 0 & 1 \\ 0 & 0 & 0 & 0 \\ 0 & 0 & 0 & 0 \\ -1 & 0 & 0 & 0 \end{Vmatrix}, \quad \gamma_{24} = \begin{Vmatrix} 0 & 0 & 0 & 0 \\ 0 & 0 & 0 & 1 \\ 0 & 0 & 0 & 0 \\ 0 & -1 & 0 & 0 \end{Vmatrix}, \quad \gamma_{34} = \begin{Vmatrix} 0 & 0 & 0 & 0 \\ 0 & 0 & 0 & 0 \\ 0 & 0 & 0 & 1 \\ 0 & 0 & -1 & 0 \end{Vmatrix}, \tag{2.10}$$

An arbitrary representation u of the group $\boldsymbol{c}\cdot\boldsymbol{c}'$ transforms, therefore, according to

$$u' = \{1 + \tfrac{1}{2}\, I_{\mu\nu}\,\varepsilon_{\mu\nu} + \tfrac{1}{2}\,\mathcal{J}_{\mu\nu}\,\eta_{\mu\nu}\}\, u, \tag{2.11}$$

where the 12 generators of infinitesimal transformations $I_{\mu\nu}$ and $\mathcal{J}_{\mu\nu}$ are matrices of the same rank as the rank of the representation u and satisfy the same commutation relations as the particular matrices (2.9) corresponding to the eight-dimensional real space.

To obtain these commutation relations it is sufficient to derive the commutation relations of the six fourth rank matrices $\gamma_{\mu\nu}$. These relations are easily seen to be

$$[\gamma_{\mu\nu}, \gamma_{\varrho\lambda}] = -\delta_{\mu\varrho}\gamma_{\nu\lambda} - \delta_{\nu\lambda}\gamma_{\mu\varrho} + \delta_{\mu\lambda}\gamma_{\nu\varrho} + \delta_{\nu\varrho}\gamma_{\mu\lambda}. \tag{2.12}$$

An interesting property of the space z or k may be mentioned in connexion with the transformation properties of this space with respect to the group $\boldsymbol{c}\cdot\boldsymbol{c}'$ If one puts

into (2.11) relations (2.4) or (2.5) one easily verifies that only the following linear combinations of the matrices $\gamma_{\mu\nu}$ occur

$$m_1 = \frac{1}{2i}(\gamma_{23} \pm \gamma_{14})$$

$$m_2 = \frac{1}{2i}(\gamma_{31} \pm \gamma_{24}) \tag{2.13}$$

$$m_3 = \frac{1}{2i}(\gamma_{12} \pm \gamma_{34})$$

Here the upper sign corresponds to the group $\boldsymbol{c}'$ (2.5) the lower to the group $\boldsymbol{c}$ (2.4). The matrices (2.13) satisfy the following relations

$$[m_i, m_k] = im_j, \tag{2.14}$$

where i, k, j = cyclic permutation of 1, 2, 3, and

$$m_1^2 + m_2^2 + m_3^2 = \frac{3}{4} \tag{2.15}$$

Thus it is seen that the variables z or k transform with respect to $\boldsymbol{c}$ and $\boldsymbol{c}'$ as quantities with spin $\frac{1}{2}$. However, we may also consider other subgroups of $\boldsymbol{c} \cdot \boldsymbol{c}'$, namely the subgroups which are obtained by putting all the $\varepsilon_{\mu\nu}$ and $\eta_{\mu\nu}$ in which a particular fixed index occurs equal to zero. Choosing e.g. $\mu = 4$ we get

$$\varepsilon_{i4} = \eta_{i4} = 0 \qquad (i = 1, 2, 3). \tag{2.16}$$

In this case only the matrices

$$\vartheta_1 = \frac{1}{i}\gamma_{23}, \quad \vartheta_2 = \frac{1}{i}\gamma_{31}, \quad \vartheta_3 = \frac{1}{i}\gamma_{12}, \tag{2.17}$$

occur in (2.11). These matrices satisfy the relations

$$[\vartheta_i, \vartheta_k] = i\vartheta_j, \tag{2.18}$$

where i, k, j = cyclic permutation of *1, 2, 3,* and

$$\vartheta_1^2 + \vartheta_2^2 + \vartheta_3^2 = 2 \begin{Vmatrix} 1 & 0 & 0 & 0 \\ 0 & 1 & 0 & 0 \\ 0 & 0 & 1 & 0 \\ 0 & 0 & 0 & 0 \end{Vmatrix} \tag{2.19}$$

It is seen, therefore, that with respect to the subgroup of rotations of the space k which leaves the axes r_4 and s_4 invariant, the variables k or z transform like quantities with spin 0 or 1. The components of a spinor may behave like the components of a scalar and a three-dimensional vector if the subgroup (2.16) of $\boldsymbol{c} \cdot \boldsymbol{c}'$ is considered. The similar situation appears, of course, also for all representations of $\boldsymbol{c} \cdot \boldsymbol{c}'$. One should

note, however, that (0.1) is the only way of writing $\boldsymbol{g}$ as a product of three commuting groups (apart from isomorphic possibilities). There exists no possibility to split $\boldsymbol{g}$ into a product of groups in such a way that the group (2.16) appears as one of the components. In fact the uniqueness of (0.1) is the necessary condition in constructing a direct product of groups.

The differential operators invariant with respect to $\boldsymbol{c}\cdot\boldsymbol{c}'$ are according to (2.7)

$$\frac{\partial^2}{\partial r_\mu^2} - \frac{\partial^2}{\partial s_\mu^2} \quad \text{and} \quad \frac{\partial^2}{\partial r_\mu\, \partial s_\mu} \tag{2.20}$$

The only differential operator invariant with respect to $\boldsymbol{g}$ is

$$\left(\frac{\partial^2}{\partial r_\mu^2} - \frac{\partial^2}{\partial s_\mu^2}\right)^2 + 4\left(\frac{\partial^2}{\partial r_\mu\, \partial s_\mu}\right)^2. \tag{2.21}$$

The explicit expressions for the quantities which are conserved as a consequence of invariance with respect to the various transformations of $\boldsymbol{g}$ will be given in a forthcoming paper.

3. Connexion of the spinor space with space-time

Let us now consider the correspondence of the above formulation with the conventional formulation of physical laws in space-time. For this purpose we must postulate some connexion between the coordinates z (or k) of the spinor space and the coordinates (or better the coordinate differences) x_μ of space-time. Let us consider a bilinear connexion of the type (cf., however, also I and III)

$$\begin{aligned} x_3 - x_0 &= c_{1\dot{1}}; & x_1 - ix_2 &= c_{1\dot{2}}; \\ x_1 + ix_2 &= c_{2\dot{1}}; & -x_3 - x_0 &= c_{2\dot{2}}; \end{aligned} \tag{3.1}$$

with

$$c_{\alpha\dot{\beta}} = z_{\alpha;\,\varrho}\, z_{\dot{\beta};\,\dot{\lambda}}\, \varepsilon^{\dot{\lambda}\varrho} \tag{3.2}$$

where, in accordance with the transformation properties,

$$\begin{aligned} z_1 &= z_{1;\,1} & z_2 &= z_{2;\,1} & z^*_{\alpha;\,\beta} &= z_{\dot{\alpha};\,\dot{\beta}} \\ z_{\dot{1}} &= z_{\dot{1};\,\dot{2}} & z_{\dot{2}} &= z_{\dot{2};\,\dot{2}} \end{aligned} \tag{3.3}$$

and $\varepsilon^{\dot{\lambda}\varrho}$ is a constant spinor. We easily derive

$$x_\mu^2 = \varepsilon_\mu^2 \left| z^*_\alpha z^{\dot{\alpha}} \right|^2 \tag{3.4}$$

where ε_μ given by the relations

$$\begin{aligned} \varepsilon_3 - \varepsilon_0 &= \varepsilon_{;\,1\dot{1}} & \varepsilon_1 - i\varepsilon_2 &= \varepsilon_{;\,1\dot{2}} \\ \varepsilon_1 + i\varepsilon_2 &= \varepsilon_{;\,2\dot{1}} & -\varepsilon_3 - \varepsilon_0 &= \varepsilon_{;\,2\dot{2}} \end{aligned} \tag{3.5}$$

is a constant vector (with respect to $\boldsymbol{c}'$) which may be normalized to ± 1 ($+1$ corresponding to space-like, -1 to time-like vectors).

In an analogous way we may introduce the coordinates y_μ of the isospace with help of the bilinear forms

$$c_{;\,\varrho\dot{\lambda}} = \varepsilon^{\alpha\dot{\beta};}\, z_{\alpha;\,\varrho}\, z_{\dot{\beta};\,\dot{\lambda}}\,. \tag{3.6}$$

One should note, however, that the coordinates y_μ are not independent of the x_μ.

Given a bilinear connexion of the type (3.2) one easily derives the connexion between the differential operations in both spaces (cf. II).

$$\frac{\partial}{\partial z_{\alpha;\,\varrho}} = -\frac{1}{2}\, z_{\dot{\beta};\,\dot{\lambda}}\, \varepsilon^{;\varrho\dot{\lambda}}\, \partial^{\alpha\dot{\beta};}$$

$$\frac{\partial}{\partial z^{\cdot}_{\alpha;\,\dot{\lambda}}} = -\frac{1}{2}\, z_{\beta;\,\varrho}\, \varepsilon^{;\varrho\dot{\lambda}}\, \partial^{\beta\dot{\alpha};} \tag{3.7}$$

where

$$\begin{aligned} \partial_{1\dot{1}};&= \partial_3 + \partial_0 & \partial_{1\dot{2}};&= \partial_1 - i\partial_2 \\ \partial_{2\dot{1}};&= \partial_1 + i\partial_2 & \partial_{2\dot{2}};&= -\partial_3 + \partial_0 \end{aligned} \tag{3.8}$$

Relations (3.7) may be solved with respect to $\partial^{\alpha\dot{\beta};}$

$$\partial^{\alpha;}_{\dot{\beta};} = -2\Delta^{-1}\, z_{\dot{\beta};\,\dot{\lambda}}\, \varepsilon^{;\dot{\lambda}}_{;\varrho}\, \frac{\partial}{\partial z_{\alpha;\,\varrho}} \tag{3.9}$$

if

$$\Delta \equiv \varepsilon^2_\mu\, z^*_\alpha\, z^{\dot{\alpha}} \neq 0 \tag{3.10}$$

i.e. outside the light cone.

If $\psi_{\alpha;\ldots}[x_\mu(z)]$, $\psi^{\cdot}_{\dot{\alpha};\ldots}[x_\mu(z)]$ is a spinor with respect to $\boldsymbol{c}$ possessing arbitrary transformation character with respect to $\boldsymbol{c}'$ (dotts) and if this spinor depends on z only by the intermediary of x_μ (3.1—2), we may write the Dirac equations in the form

$$\begin{aligned} \partial^{\alpha\dot{\beta};}\, \psi_{\alpha;\ldots} &= -\varkappa\, \psi^{\dot{\beta};}_{;\ldots} \\ \partial^{\alpha\dot{\beta};}\, \psi_{\dot{\beta};\ldots} &= -\varkappa\, \psi^{\alpha;}_{;\ldots} \end{aligned} \tag{3.11}$$

Introducing (3.11) into (3.7) we get the equivalent equations in the spinor space

$$\frac{\partial \psi_{\alpha;\ldots}}{\partial z_{\alpha;\,\varrho}} = \frac{\varkappa}{2}\, z_{\dot{\beta};\,\dot{\lambda}}\, \varepsilon^{;\varrho\dot{\lambda}}\, \psi^{\dot{\beta};}_{;\ldots}$$

$$\frac{\partial \psi^{\cdot}_{\dot{\alpha};\ldots}}{\partial z^{\cdot}_{\alpha;\,\dot{\lambda}}} = \frac{\varkappa}{2}\, z_{\beta;\,\varrho}\, \varepsilon^{;\varrho\dot{\lambda}}\, \psi^{\beta;}_{;\ldots} \tag{3.12}$$

In general, however, the representation ψ may depend on z also explicitly

$$\psi = \psi\,[x_\mu(z), z]. \tag{3.13}$$

In this case relations (3.7) and (3.9) hold only for the implicit dependence of ψ on z Equations (3.12) are then equivalent to generalized Dirac equations in which besides

the conventional Dirac differential operator also additional terms occur. These terms contain derivatives with respect to those of the variables $z_{\alpha;\beta}$ which occur explicitly in (3.13) (cf. II).

It may be interesting to point out a consequence of the connexion (3.1), (3.2) on inversions. One easily finds out that inversions of space-time are in this formulation always connected with inversions in the isotopic space. (3.6). E.g. the transformation

$$z'_{\alpha} = a z^{\dot{\alpha}*}, \qquad z'_{\dot{\alpha}} = a^{-1} z^{\alpha *}, \qquad |a| = 1, \tag{3.14}$$

is an inversion $x'_i = -x_i$, $(i = 1, 2, 3)$, $x'_0 = x_0$ of space-time and at the same time an inversion of the isotopic space: $y'_1 = y_1$, $y'_2 = -y_2$, $y'_3 = y_3$, $y'_0 = y_0$. The problem of representations of the full group $\boldsymbol{G}$ consisting of $\boldsymbol{g}$ and of the inversions will be treated in a forthcoming paper.

Finally we should like to remark that a bilinear connexion of an eight-dimensional spinor space with a four-dimensional vector space allowes some movements of the spinor space which do not change the coordinates x_μ. Considering in (3.1—2) the $c_{\alpha\dot{\beta}}$ as constants we get four equations for four second order hypersurfaces in the eight-dimensional space of the variables r_μ, s_μ. The cut of these four surfaces is a four-dimensional manifold and any movement inside this manifold is without influence on the x_μ.

It is convenient to consider these movements in a particularly simple frame of reference. E.g. for a vector in the future light-cone we may consider a frame of reference in which $\varepsilon_i = 0$, $\varepsilon_0 = 1$. In this case $\varepsilon_{;1\dot{1}} = \varepsilon_{;2\dot{2}} = -1$, $\varepsilon_{;1\dot{2}} = \varepsilon_{;2\dot{1}} = 0$, and

$$\begin{aligned} |z_1|^2 + |z_{\dot{1}}|^2 &= -c_{1\dot{1}}, \\ |z_2|^2 + |z_{\dot{2}}|^2 &= -c_{2\dot{2}}, \\ z_1 z_2^* + z_{\dot{1}}^* z_{\dot{2}} &= -c_{1\dot{2}}, \end{aligned} \tag{3.15}$$

One easily finds out that any two points z_α, $z_{\dot{\alpha}}$ and $z^{(0)}_\alpha$, $z^{(0)}_{\dot{\alpha}}$ connected by any of the relations

$$z_\alpha = e^{i\varphi} z^{(0)}_\alpha, \qquad z_{\dot{\alpha}} = e^{-i\varphi} z^{(0)}_{\dot{\alpha}} \tag{3.16}$$

or

$$\begin{aligned} z_\alpha &= a z^{(0)}_\alpha + b z^{(0)*}_{\dot{\alpha}} \\ z^*_{\dot{\alpha}} &= -b^* z^{(0)}_\alpha + a^* z^{(0)*}_{\dot{\alpha}} \end{aligned} \qquad |a|^2 + |b|^2 = 1 \tag{3.17}$$

belong to the same manifold (the same x_μ). The same relations hold also for vectors in the past light-cone. For the outside of the light-cone one gets in a properly chosen frame of reference some other linear relations (cf. I and III).

КРАТКОЕ СОДЕРЖАНИЕ

Я. Жевуский, *13-параметровая группа трансформации в спиноровом пространстве и её представления*

Выведено все неприводимые представления 13-параметровой группы трансформации в спиноровом простанстве. Содержат они все типы трансформации, какие до сих пор феноменологически принимались для описания элементарных

частиц вместе с их изотоповой характеристикой. Введено восьмимерное спиноровое действительное пространство соответствующие первотному четырехмерному спиноровому комплексному пространству. Показано, что спиноровое пространство становит общую геометрическую базу для всех законов сохранения (вместе с законом сохранения заряда, изотопного спина и числа барионов). Рассмотрено вероятные билинейные связи между спиноровым а временным простанством.

REFERENCES

Enz, C., *Nuovo Cimento*, **6**, 250 (1957).
Gürsey, F., *Nuovo Cimento*, **7**, 411 (1958).
Królikowski, W., *Bull. Acad. Pol. Sci. Cl.* III, **6**, 523 (1958).
Pauli, W., *Nuovo Cimento*, **6**, 204 (1957).
Pursey, D. L., *Nuovo Cimento*, **6**, 266 (1957).
Rzewuski, J., *Bull. Acad. Polon. Sci.* Cl. III, **6**, 261 (1958a).
Rzewuski, J., *Bull. Acad. Polon. Sci.* Cl. III, **6**, 339 (1958b).
Rzewuski, J., Nuovo Cimento, **9**, 942 (1958).

ON THE BILOCAL THEORY OF THE ELECTRON

By E. Minardi

Istituto Nazionale di Fisica Nucleare — Sezione di Torino-Torino, Italy

(Received June 23, 1958)

The bilocal theory of the electron presented in previous works is developed in such a way that a Majorana neutrino, instead on an ordinary neutrino, is introduced in the zero approximation of the perturbation calculation for that part of the mass due to the virtual photons interacting with the internal part of the bilocal field. Morever the contribution to the mass due to photons which interact with the part of the bilocal field describing the observable motion is calculated. The total mass obtained with the above calculation agrees with a considerable accuracy with the experimental mass of the electron if the 2.30×10^{-13} cm. value of the universal lenght is used, i.e. the value with which the masses of other particles were previously obtained.

We shall develop here the bilocal theory of the electron previously proposed[1] in such a way that a Majorana neutrino, instead of an ordinary neutrino, is introduced in the zero approximation of the perturbation calculation of that part of the electron mass due to the virtual photons interacting with the internal part of the bilocal field. In the case of a classical internal field the electromagnetic interaction is not vanishing and gives rise to a purely electromagnetic mass. Moreover the contribution to the mass due to photons which interact with the part of the bilocal field describing the observable motion will be calculated.

It will be shown that the total mass obtained by means of the above calculation agrees with considerable accuracy with the experimental mass of the electron if the 2.30×10^{-13} cm value of the universal lenth is used, i.e. the value with which the masses of the bosons, of the neutron and of the hyperons have been previously obtained[2].

We have assumed[1] that the physical states, with spin 1/2 of the matter interacting with the electromagnetic field are described by the following eight-dimensional equation, symmetrical in the x and η variables,

$$\alpha_\nu \left(\frac{\partial}{\partial x_\nu} - ieA_\nu (x + \eta) + \frac{\partial}{\partial \eta_\nu} \right) \psi (x, \eta) = 0, \qquad (\nu = 1, 2, 3, 4) \tag{1}$$

[1] E. MINARDI: Nuovo Cimento 3.968 (1956); 4, 1127 (1956); the last work will be referred to as I.
[2] E. MINARDI: Nuovo Cimento 4, 715, 898 (1958).

with the supplementary condition

$$\frac{\partial^2}{\partial x_\nu \partial \eta_\nu} \psi(x, \eta) = 0, \tag{2}$$

where

$$A_\nu(x') = \exp[i H_0 t'] A_\nu(\vec{x}') \exp[-i H_0 t'], \tag{3}$$

and H_0 is the hamiltonian operator of the vacuum electromagnetic field.

An important feature of the theory is that two kinds of virtual processes can arise from eq. (1), as it was shown in detail in I. One can first separate the x and η variables of the equation, operating in the rest system of the particle (where $\vec{p}^{(x)} = 0$, $\eta_4 = 0$, see I) to obtain an "internal equation" in the $\vec{\eta}$ variable only, the separation constant being the mass. Perturbation calculation of the mass, starting from a zero approximation solution of the internal equation, gives rise to matrix elements describing the emission or the absorption of photons whose momentum $\vec{k}$ is conserved with respect to the momentum distribution obtained with the expansion in plane waves of the internal function. Then, in the intermediate state the particle remains fixed in the observable space x, the variation of momentum being absorbed by the internal field. Then the absence of recoil is not an approximation, as in the usual local theory, but a consequence of the existence of the internal field.

Once the contribution m_{int} to the mass due to the photons interacting with the internal field only has been calculated, one can sum up to eq. (1) a term $i \cdot \beta \cdot m_{int}$ to take into account the contribution of the preceding virtual processes. Then by separating the time variable (with the energy as separation constant) but not the x and η variables, one can set up from eq. (1) a perturbation calculation of the self-energy. The resulting matrix elements describe a second kind of virtual processes because in this second case conservation of momentum holds between the momentum of the photon and the momentum of the motion of the particles in the observable space. In this way one calculates the contribution to the mass due to photons which interact with the external part of the bilocal field only.*

As zero approximation bilocal function we choose

$$\psi_0(x, \eta) = V_x^{-1/2} u_p f(\eta_\nu^2) \exp[-i x_\nu p_\nu^{(x)}] \exp[-i \eta_\nu p_\nu^{(\eta)}], \tag{4}$$

(for the meaning of symbols see I, pg. 1130) which is a discontinuous solution of eq. (1) without interaction. We assume (cfr. (2)) that the internal function of leptons is discontinuous at $r = l$, while the internal function of all other particles is always continuous; in eq. (4) the $p_\nu^{(\eta)}$ satisfy the condition $p_\nu^{(\eta)2} = m_0^2$, $p_4^{(\eta)} = 0$ if $\vec{p}^{(x)} = 0$, and are otherwise arbitrary; $\psi_0(x, \eta)$ is the bilocal function of a lepton with m_0 mass and in the limit $m_0 \to 0$ describes a neutrino.

We note however that, if there is interaction, m_0 has not the physical meaning of a mass of a particle because the physical mass is determined by the interaction itself. One can then consider m_0 as a fictitious parameter which is different from zero

during the calculation in order that a rest system of the unperturbed particle exists, in which the separation between the x and η variables can be performed. After the calculation it seems plausible that the limit $m_0 \to 0$ can be performed. This limit is consistent only if the physical mass remains finite.

If we assume that the zero approximation bilocal function (4) describes a Majorana neutrino[3], instead of an ordinary one, it will be necessary to put that the momentum $\vec{p}^{(x)} + \vec{p}^{(\eta)}$ be parallel or antiparallel to the spin. Since this condition must be satisfied for each $\vec{p}^{(x)}$ and particularly for $\vec{p}^{(x)} = 0$, the arbitrariness of $p_\nu^{(\eta)}$ $(\nu = 1, 2, 3)$ is eliminated, as we must have $p_1^{(\eta)} = p_2^{(\eta)} = 0$, $p_3^{(\eta)} = m_0$.

On neglecting those transitions in intermediate states with a mas different from the initial one (see I), the electron mass is given by the following equation (see. I, eq. (12)).

$$\mp m_{\text{int}} = \sum_{1}^{+} \sum_{\alpha} \sum_{k} \frac{(H'_{0/0k\alpha})^\eta \, (H'_{0k\alpha/0})^\eta}{-k} \tag{5}$$

where $(H')^\eta$ describes the interaction of the electromagnetic field with the internal part of the bilocal field and a summation on each possible intermediate state having a mass equal to the initial one is understood.

If we assume a z axis parallel to the momentum direction $p_3^{(\eta)} = p$ (we are in the rest system, $\vec{p}^{(x)} = 0$) it follows that in the Majorana "gauge" the terms having $\alpha = 1$ and $\alpha = 2$ are zero. Therefore, eq. (5) becomes:

$$\pm m_{\text{int}} = -$$

$$\frac{e^2}{4\pi^2} \sum_{1}^{4} \sum_{\tau} \int_0^\infty \int_0^\pi \int_0^{2\pi} |f(\vec{\eta}^2) \exp\,[-i\vec{\eta}\vec{k}]\, d^3\eta|^2 e_3 u^*_{+,1} \alpha_3 u_\tau \, e_3 u^*_\tau \alpha_3 u_{+,1} \, dk \sin\vartheta d\vartheta d\varphi + \tag{6}$$

$$+ \frac{e^2}{4\pi^2} \sum_{1}^{4} \sum_{\tau} \int_0^\infty \int_0^\pi \int_0^{2\pi} |f(\vec{\eta}^2) \exp\,[-i\vec{\eta}\vec{k}]\, d^3\eta|^2 u^*_{+,1} u_\tau \, u^*_\tau \, u_{+,1} \, dk \sin\vartheta \, d\vartheta \, d\varphi,$$

where ϑ and φ are the polar angles of vector $\vec{k}$ and $e_3 = -\operatorname{sen}\vartheta/\sqrt{2}$ is the component along the z axis of the electromagnetic field polarization versor. Eq. (6) is independent on m_0. Since in the Majorana "gauge" the matrix $u_{-,i}$ is equal to matrix $u_{+,i}$ and in eq. (6) the matrix elements corresponding to transitions with spin inversion are zero, we have that the summation of eq. (7) is twice the term of eq. (6) having the intermediate state equal to the initial one. On integrating the angular variables, we get:

$$\mp m_{\text{int}} = \frac{2e^2}{\pi l}\left(-\frac{1}{3} + 1\right) \int_0^\infty G^2(\varrho)\, d\varrho = \frac{4e^2}{5l} \qquad (\varrho = kl) \tag{7}$$

where G is the Wataghin cut-off factor[4].

[3] E. MAJORANA: *Nuovo Cimento*, **14**, 171 (1937).

[4] G. WATAGHIN: Suppl. *Nuovo Cimento*, **1**, 103 (1954) and previous works

Therefore, according to eq. (7), the electron mass due to virtual photons interacting with the internal part of the bilocal field is equal to 4/3 of the mutual electrostatic energy of a homogeneous distribution of total charge e in a spatial sphere having radius $= l$. This result agrees with that from the Lorentz non relativistic classical theory, in the case of a charge homogeneously distributed in a sphere.

To the mass m_{int} due to virtual photons interacting with the internal field we must add the contribution due to the virtual photons which conserve the momentum with the observable motion of the particle. Such contribution is calculated by applying the perturbation procedure to the equation

$$\alpha_\nu \left(\frac{\partial}{\partial x_\nu} - ie A_\nu (x + \eta) + \frac{\partial}{\partial \eta_\nu} \right) \psi (x, \eta) + i \beta m_{\text{int}} \psi (x, \eta) = 0, \tag{8}$$

and by assuming in zero approximation a bilocal function of the form (4), in which the $p_\nu^{(\eta)}$ are made to tend towards zero and u_p is an ordinary spinor of the Dirac theory, corresponding to a "bare" particle with a m_{int} mass. Let us neglect the transitions in intermediate states with a mass different from the initial one (see I) so that the self-energy can be immediately calculated in a relativistic form in the second order by following the usual procedure[5]; the only difference is the appearance of a cut-off factor having the form proposed by Wataghin[4], which, according to the procedure described in the previous works[1], is estimated in the rest system and then put in an invariant form with the help of the Wataghin invariant (see I, page 1131). In view of the relativistic invariance of the theory, in order to obtain the numerical value of the contribution to the mass at rest due to the considered virtual processes, it is sufficient to perform the calculation in the rest system of the initial state of the particle, where calculations are simplified. In this reference the invariant variable[4] is given by:

$$\varepsilon = \frac{1}{m_{\text{int}}} \left[(m_{\text{int}}^2 + k^2) \frac{1}{2} + k \right], \tag{9}$$

where k is the momentum of the virtual photon. On recalling eq. (7), the m_{int} contribution to the rest mass is given by the formula:

$$\Delta m = \frac{m_{\text{int}} e^2}{2\pi} \int_1^\infty G^2(kl) \frac{3\varepsilon^2 - 1}{\varepsilon^3} d\varepsilon = \frac{2e^2}{5\pi l} \int_1^\infty G^2 \left(\frac{2e^2}{5} \frac{\varepsilon^2 - 1}{\varepsilon} \right) \frac{3\varepsilon^2 - 1}{\varepsilon^3} d\varepsilon =$$

$$= 1.037 \int_1^\infty G^2 \left(0.0029 \frac{\varepsilon^2 - 1}{\varepsilon^3} \right) \frac{3\varepsilon^2 - 1}{\varepsilon^3} d\varepsilon \cdot 10^{-30} g \tag{10}$$

where

$$G(kl) = 3 \sqrt{\frac{\pi}{2}} (kl)^{-3/2} \tau_{3/2} (kl) \tag{11}$$

[5] See for example: W. HEITLER: Quantum theory of radiation (Zürich, 1953) pg. 293.

is the Wataghin cut-off factor[6]. By evaluating numerically the integral we obtain that the rest mass of the electron $m_e = m_{int} + \Delta m$ is 9.115×10^{-28} g, with an error in the numerical calculation which is certainly less than 0.04% of the total mass. The obtained result must be compared with experimental results $m_e = (9.1083 \pm \pm 0.0003)\ 10^{-28}$ g. A conclusion on the agreement between the two data from the second decimal figure and forward may be drawn only when the value of the universal length is available with adequate accuracy. As for now, the obtained result can be regarded as quite satisfactory.

*(Note added in proof): It must be noted that the new Ψ wchich is a solution of the equation with the mass term is not required to satisfy condition (2). The system of Egs. (1) and (2) concerns exlusively the problem of the internal structure of a particle interacting with its own electromagnetic field only, while the solution of the eqnation with the mass term describes the observable motion of a particle in any electromagnetic field.

КРАТКОЕ СОДЕРЖАНИЕ

Е. Минарди, *Билокальная теория электрона*

Бинокальная теория электрона представленная в предыдущих работах, разработанная здесь таким образом, что вместо обыкновенного нейтрина введено нейтрино маерани в нулевом приближении пертурбационных расчётов для части массы происходящей из виртуальных фотонов взаимодействуюищх в внутренней частью билокального поля. Кроме того подсчитано вопрос о массе происходящей от фотонов взаимодействующих с той частью билокального поля, которая описывает наблюдаемое движение. Полная масса полученная этим расчетом согласуется с большой точностью с экспериментальной массой электрона, при предположени, что универсальная длина равняется $2{,}30 \cdot 10^{-13}$ см, т. е. тому значению, с помощью которого раньше были получены массы других частиц.

REVERSIBLE SUSCEPTIBILITY UNDER STRESS

By Janusz Morkowski

Department of Ferromagnetics, Institute of Physics of the Polish Academy of Sciences

(Received June 23, 1958)

The reversible susceptibility in polycrystalline nickel was measured by the alternating field method for magnetic field values up to about 68 oersteds. During the measurements the specimen was subjected to external stress — compression and tension, the values of which varied from about — 14 kG/mm² to 21 kG/mm². The results obtained show that application of tension lowers the value of reversible susceptibility in weak fields and increases it at more intense fields as compared with the unstressed specimen. At small compressive stresses down to about — 3 kG/mm² the picture is the reverse; at larger values of compressive stress, however, the reversible susceptibility is smaller for all values of magnetic field intensity than in the unstressed specimen.

The results obtained are interpreted theoretically on the basis of statistical considerations.

1. Introduction

For a ferromagnetic specimen in a magnetic field H, having magnetization I, we define the reversible susceptibility $\varkappa_r$ in the state (H, I) as the limit of the ratio dI/dH as dH decreases to 0, with the additional condition that the direction of dH is opposite to that of H. The physical meaning of this definition is discussed in the book of Vonsovski and Shur (1948).

As is well known, the reversible susceptibility $\varkappa_r$ was introduced by R. Gans (1908, 1909, 1910, 1920), who carefully measured $\varkappa_r$ in polycrystalline Fe and Ni. Although the values of $\varkappa_r$ as a function of the magnetic field strength H showed hysteresis, Gans observed that the plot of $\varkappa_r$ vs. the magnetization does not appreciably depend on the previous magnetic history of the specimen. Gans (1911) formulated therefore the hypothesis that $\varkappa_r$ is a single-valued function of the magnetization and that the dependence of $\varkappa_r/\varkappa_0$ on I/I_s ($\varkappa_0$ being the reversible susceptibility in the demagnetized state and I_s the technical saturation magnetization) fulfils the empirical universal equation (given in parametric form).

$$\frac{\varkappa_r}{3\varkappa_0} = \frac{1}{x^2} - \frac{1}{\sinh^2 x}$$

$$\frac{I}{I_s} = \coth x - \frac{1}{x}$$

The results of many measurements by Gans and other authors (Erhardt 1917, Sizoo 1929) showed very good agreement with the Gans curve. In rather satisfactory agreement are measurements by Kirkham (1937) on Ni over a large range of temperature. Measurements by Grimes and Martin (1954) performed on ferrites showed that the dependence of $\varkappa_r$ on I is very similar to the Gans curve, and some deviations were explained theoretically. Certain authors, however, found remarkable deviations from Gans' law. Samuel (1928) observed that for polycrystalline Co the dependence of $\varkappa_r$ on I — although approximately single valued — was definitely different from Gans' curve. A different dependence of $\varkappa_r$ on I than the one predicted by Gans was observed by Goldschmidt (1930). The measurements by Tebble and Corner (1950) demonstrated even than in some cases the dependence on I may not be single valued.

A successful theoretical explanation of Gans' law was given by Brown (1938), whose theory also explains the deviations from Gans' curve for Co.

The influence of stresses on the reversible susceptibility was investigated by several authors (Kondorski 1940, Shur 1947 and also Tebble et al. 1951), but these investigations are not systematic and empirical material in this respect is very scarce. Only the influence of stress on the initial susceptibility is better known (Vonsovski and Shur 1948), especially in Ni subjected to tension (Kersten 1931).

It is the aim of the present paper to investigate the effect of stresses (tensile as well as compressive) on the reversible susceptibility of Ni. For the results obtained we shall also give a simplified theoretical interpretation generalizing Brown's theory of reversible susceptibility.

2. *Experimental*

Fig. 1 shows the principal parts of the experimental device[1]. To a brass tripod A is fastened a brass tube B carrying a hollow glass cylinder C with the magnetising and primary measuring coils D. The ferromagnetic specimen is mounted in the brass tube coaxially in the form of a long wire of 0.48 mm diameter. The specimen is held by two clamps, (E_1, E_2) the upper one being fastened to the tube by a screw and the lower one transferring stress to the specimen from a balance. Inside the tube between the clamps are placed 10 coilcarcasses (K) with a small (0.6 mm in diameter) aperture for the specimen. On the inner four (total length ca 4 cm) the secondary coil is wound, the remaining 6 are there to make possible measurements under a compressive stress. The specimen is introduced into the device through an opening bored along the axis of the clamps and then fastened to them.

The tube carrying the coils is cut along the axis and perforated in order to reduce the effect of eddy currents. In spite of these precautions the eddy current losses play a slight role and the results must be appropriately corrected.

[1] It should be noted that the device described was proposed by Prof. M. Kwiek.

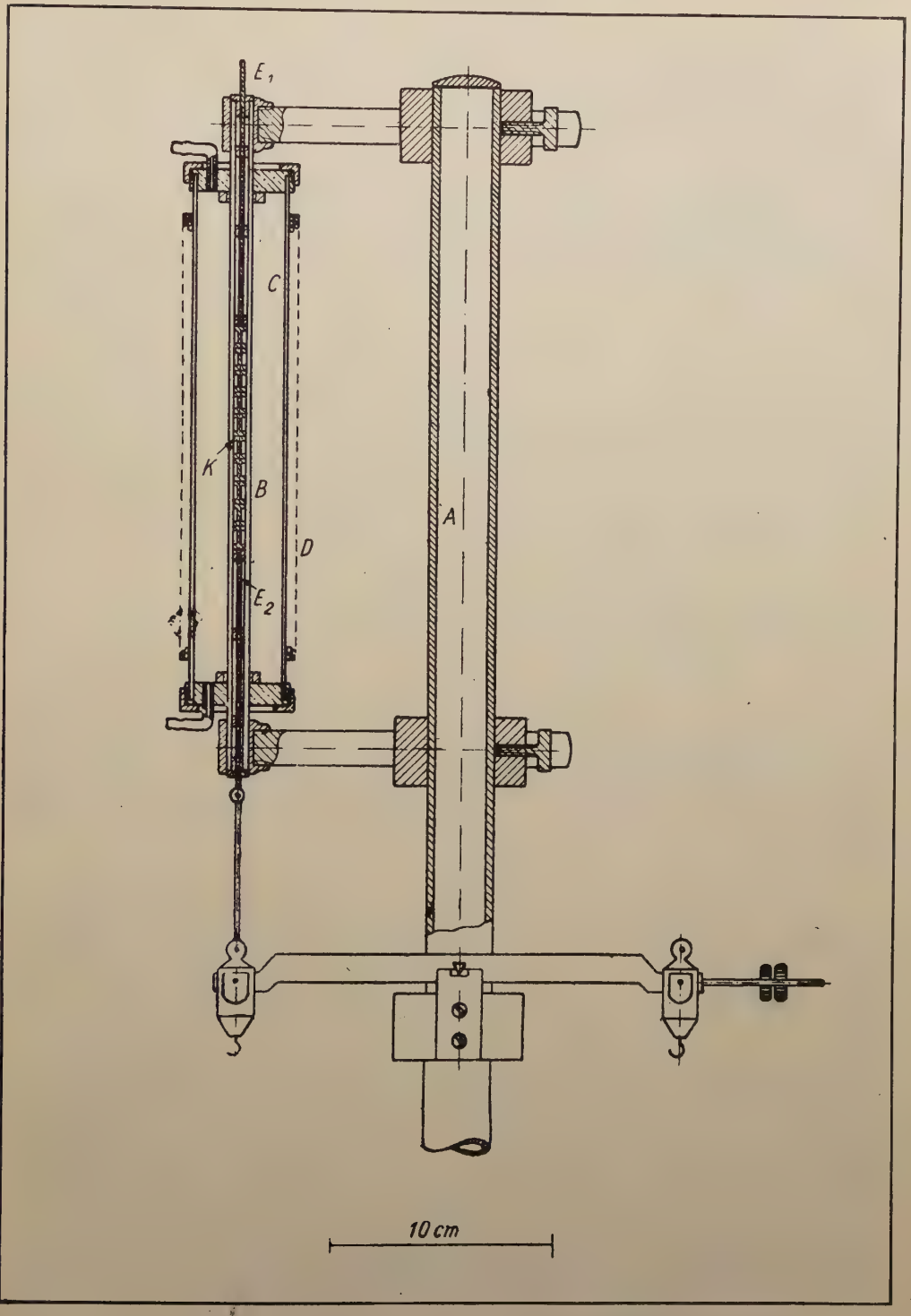

Fig. 1. The apparatus for measurement of reversible susceptibility under stress

The reversible susceptibility was found from measurements of the mutual inductance M_r between the primary measuring coil — II in Fig. 2 — and the secondary coil (III) surrounding the specimen. The mutual inductance was measured by the bridge method (see Kohlrausch 1956), with the help of a known mutual inductance.

The magnetizing coil — I in Fig. 2 — produces the required magnetizing field. The large self inductance "l" is necessary owing to considerable mutual inductance between coils I and II.

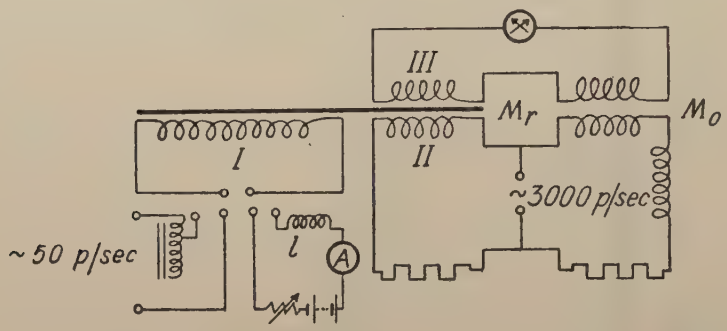

Fig. 2. Diagram of the circuits used to measure the reversible susceptibility

Before starting the measurement the specimens were carefully demagnetized by applying an alternating field (of frequency 50 p/sec) of slowly decreasing amplitude from about 250 oe to 0. The measurements were performed with small alternating currents at a frequency of 3000 p/sec fed from an acoustic generator. It was possible to balance the bridge with an accuracy of about 0.5%.

As is known, measurements of the reversible susceptibility must be performed with very small amplitudes of the alternating magnetic field (cf. Tebble, Corner 1950). The criterion for a sufficiently small amplitude is given by the independence of M_r on this amplitude. In the experiments described here the alternating field amplitude was varied within the limits from 2×10^{-3} oe to about 50×10^{-3} oe. It should be noted that at high compressive stresses (and thus small $\varkappa_r$) in order to obtain a sufficient accuracy of bridge balance the measurements were performed at amplitudes that were somewhat excessive and the results were extrapolated for the amplitude tending to 0; the difference between the true and the uncorrected value did not exceed about 1%. Eddy current losses in the specimen and in the supporting tube lower the value of the "effective" reversible susceptibility found from M_r. The correction for eddy current losses in the specimen was rather high (up to about 10%), but with the help of know formula (Bozorth 1951) it could be accurately determined. The remaining correction — as estimated indirectly — amounted to about 0.4%.

The experimental error of the measured values of $\varkappa_r$, is about 1%, only for the smallest values of $\varkappa_r$ is it somewhat greater.

The measurements were performed on specimens of polycrystalline nickel wire. The principal impurities were[2]:

$$\text{Mg} - 0.82\%, \quad \text{Fe} - 0.21\%, \quad \text{Si} - 0.10\%, \quad \text{Cu} - 0.08\%.$$

Before the measurements the specimens were annealed[3] in hydrogen at 1000°C for 2.5 hours and cooled to room temperature at a mean rate of about 12°C per minute. The specimens were then carefully — in order to avoid strain — introduced into the measuring device.

The reversible susceptibility was measured at 16°C, temperature being kept constant by oil circulating from a thermostate.

The demagnetized specimen was subjected to stress, then demagnetized anew. The reversible susceptibility was measured on the virgin magnetization curve up to magnetic fields of about 68 oe, then the magnetic field was reversed several times and the measurements were continued along the falling branch of the hysteresis curve.

It should be mentioned here that the earth's magnetic field was not compensated, for its component parallel to the specimen axis was about 0.45 oe. Consequently the "demagnetization" was performed at this value of the field. As a result, the values of the reversible susceptibility are — at least for small magnetic fields — different from those obtained on the true "virgin" magnetization curve.

In order to get comparable results and to obtain definite information about the effect of stress upon reversible susceptibility the measurements were repeatedly performed on a given specimen under identical condition but at successively larger stresses.

3. Results

In Figs. 3 to 12 are given the experimental values of the reversible susceptibility $\varkappa_r$ *vs* the external magnetic field strength H obtained for various stresses σ.

All measurements at $\sigma > 0$ were performed on the same specimen (No. I) at $\sigma < 0$ on another (No. II) prepared in the same way (see § 2).

For comparison measurements on specimens from the same material but not annealed (No. III and No. IV) were also performed.

Figs. 3 and 4 show the plot of the $\varkappa_r$ *vs.* H on the "virgin curve" (see § 2) obtained for successively larger values of the tension. As can be seen, an increase of tension causes

---

[2] I am indebted to Mr. S. Downarowicz for the chemical analysis of the specimens.

[3] The annealing was made possible by the kind help of Mr. H. Szydłowski and the use of his apparatus.

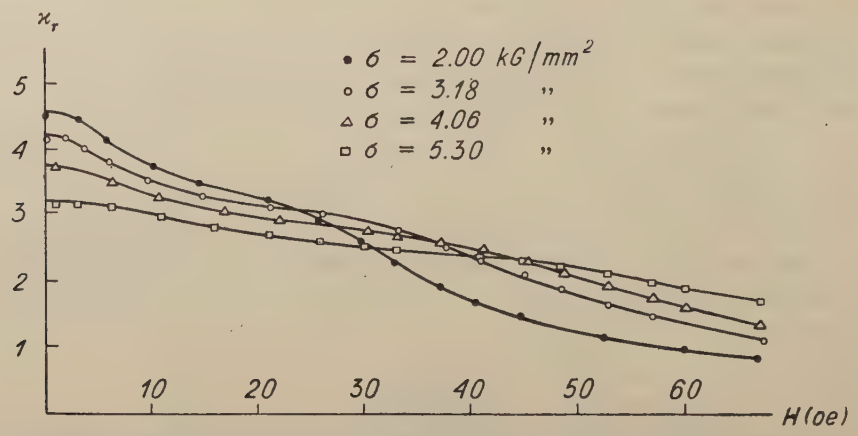

Fig. 3. Plot of the reversible susceptibility vs. external magnetic field strength for tensile stresses

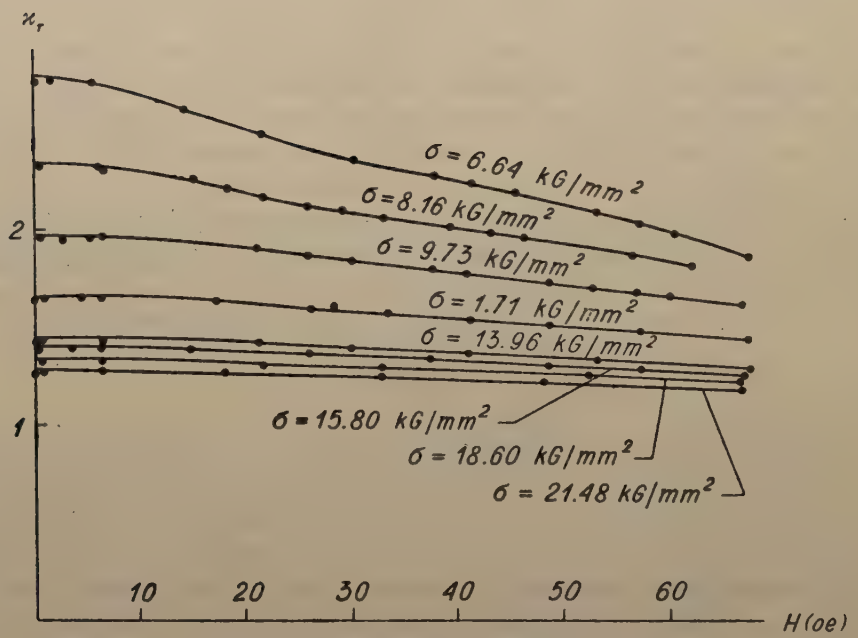

Fig. 4. Plot of the $\varkappa_r$ vs. H for tensile stresses

a decrease of $\varkappa_r$ at small fields H and an increase at high fields. At sufficiently large tensions the dependence of $\varkappa_r$ on H is very slight; this confirms the results of Becker and Kersten (1930). In the Figs. 5 and 6 are given the values of $\varkappa_r$ obtained on the descending branch of the hysteresis loop from +68 to −68 oe. The curves $\varkappa_r$ *vs.* H

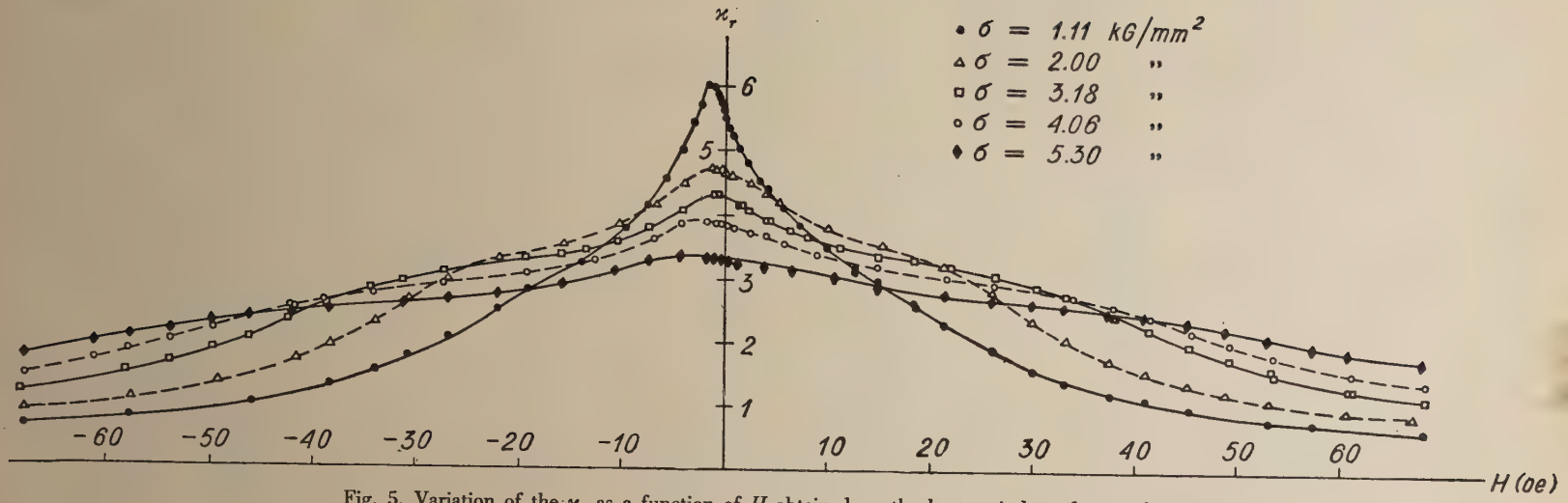

Fig. 5. Variation of the $\varkappa_r$ as a function of H obtained on the hysteresis loop for tensile stresses

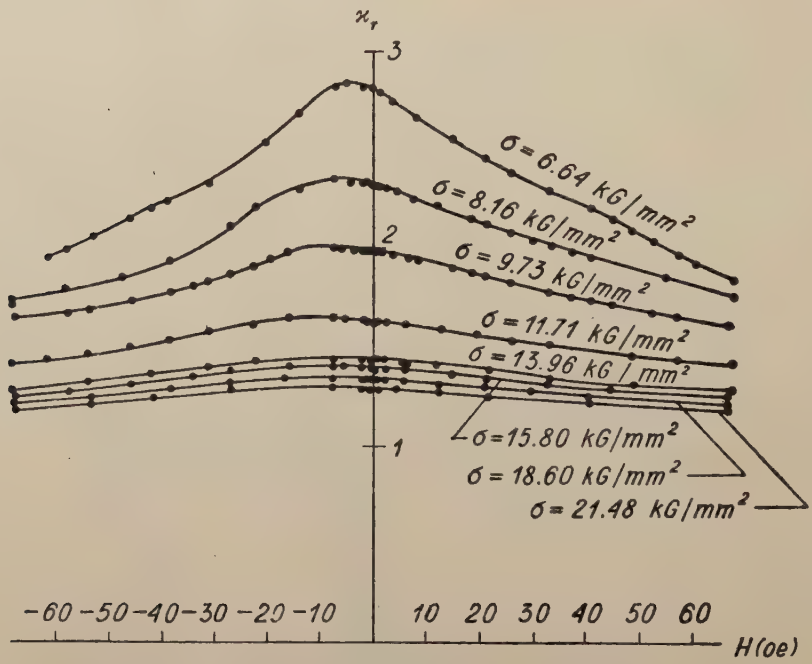

Fig. 6. $\varkappa_r$ vs. H on the hysteresis loop for tensile stresses

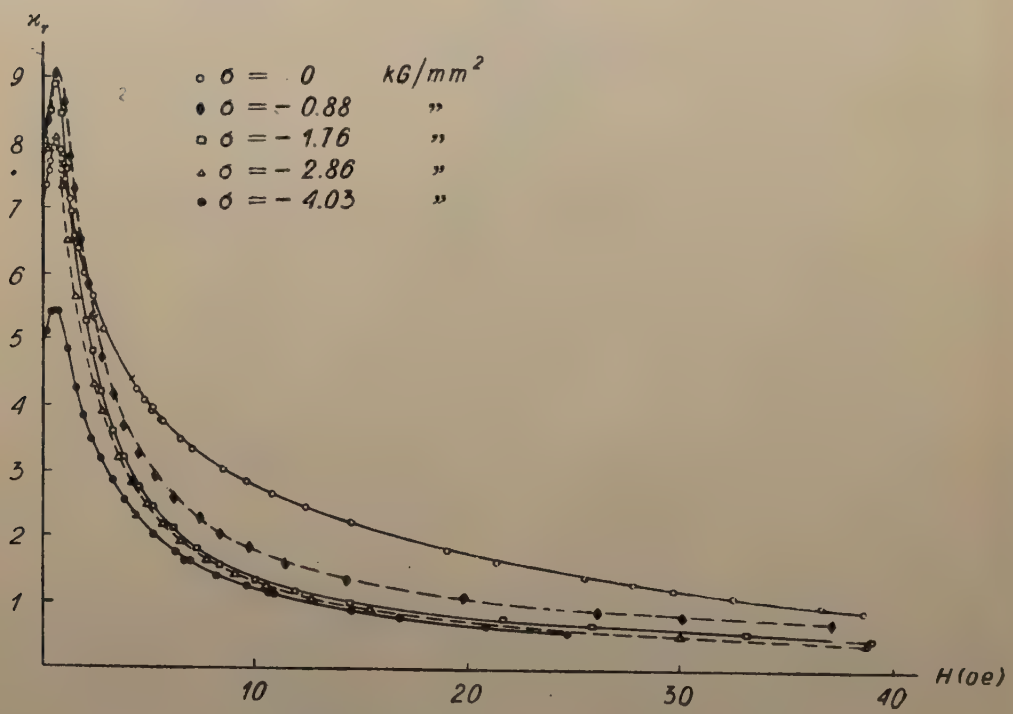

Fig. 7. Results of measurements of $\varkappa_r$ for compressive stresses

show points of inflection in the range of tensions from about 2 kG/mm² to about 6 kG/mm², at which plastic flow probably begins.

The results obtained on the specimen No. II under compression are given in Figs. 7, 8 (on the "virgin curve") and 9*a*, *b*, 10 on the descending branch of the hysteresis loop. It should be noted, that the initial reversible susceptibility increases with increasing compressive stress, reaches the maximum (at $\sigma \cong -1.3$ kG/mm²) and then falls — this observation is in qualitative agreement with the theory of the initial

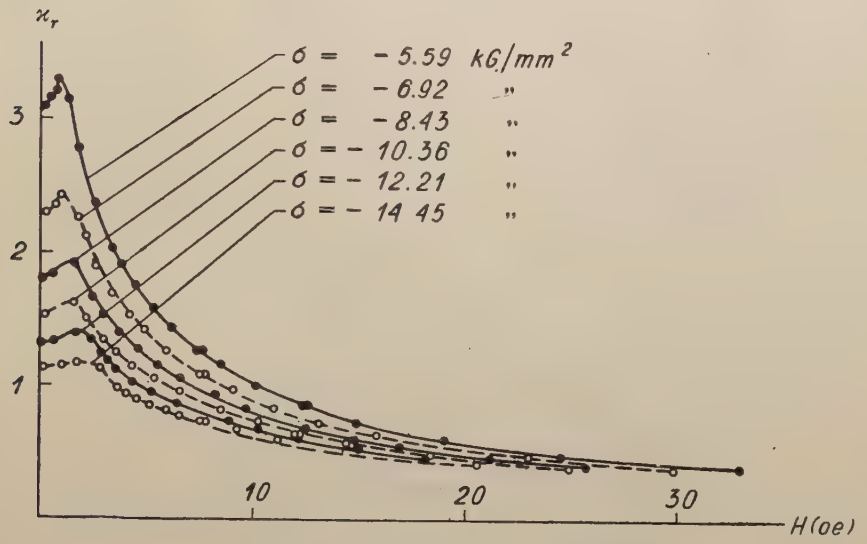

Fig. 8. $\varkappa_r$ vs. H for compressive stresses

susceptibility under stress given by Vonsovski (1947). From Figs. 9*a*, *b*, 10 it is evident that the total reversible change of magnetization when the field runs through values from $H' = +68$ oe to $-H'$, given by $\int_{-H'}^{H'} \varkappa_r \, dH$, rapidly decreases with increasing value of stress. Therefore at large stresses the irreversible magnetization processes play a dominant role in small fields.

The effect of stresses on the reversible susceptibility in unannealed specimens (Nos. III, IV) is rather slight (see Figs. 11 and 12).

It is worth while noting here that annealed specimens under compressive stress exhibit the disaccomodation effect, i.e. a time decrease of initial susceptibility after demagnetization or after imposing stress (after about 20 minutes the decrease of the initial susceptibility amounted to a few % of its stationary value at room temperature).

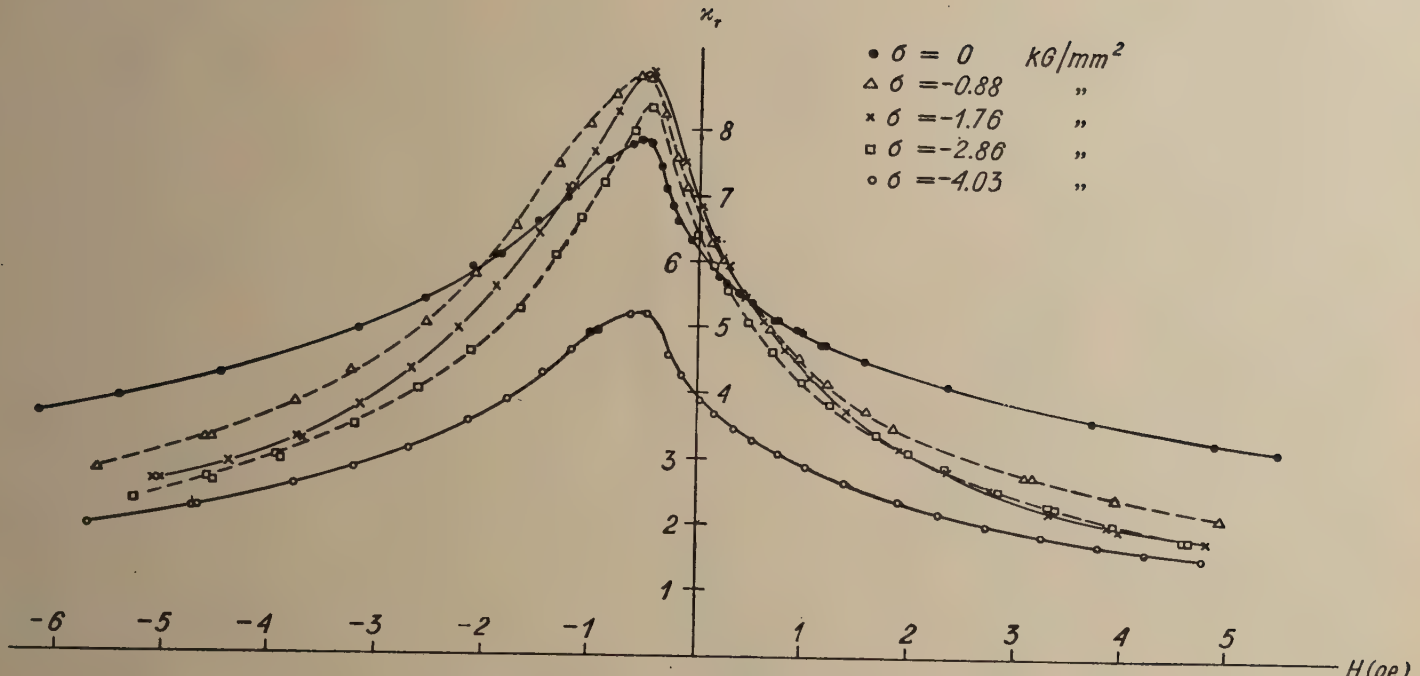

Fig. 9a. Variation of the $\varkappa_r$ with H for compressive stresses

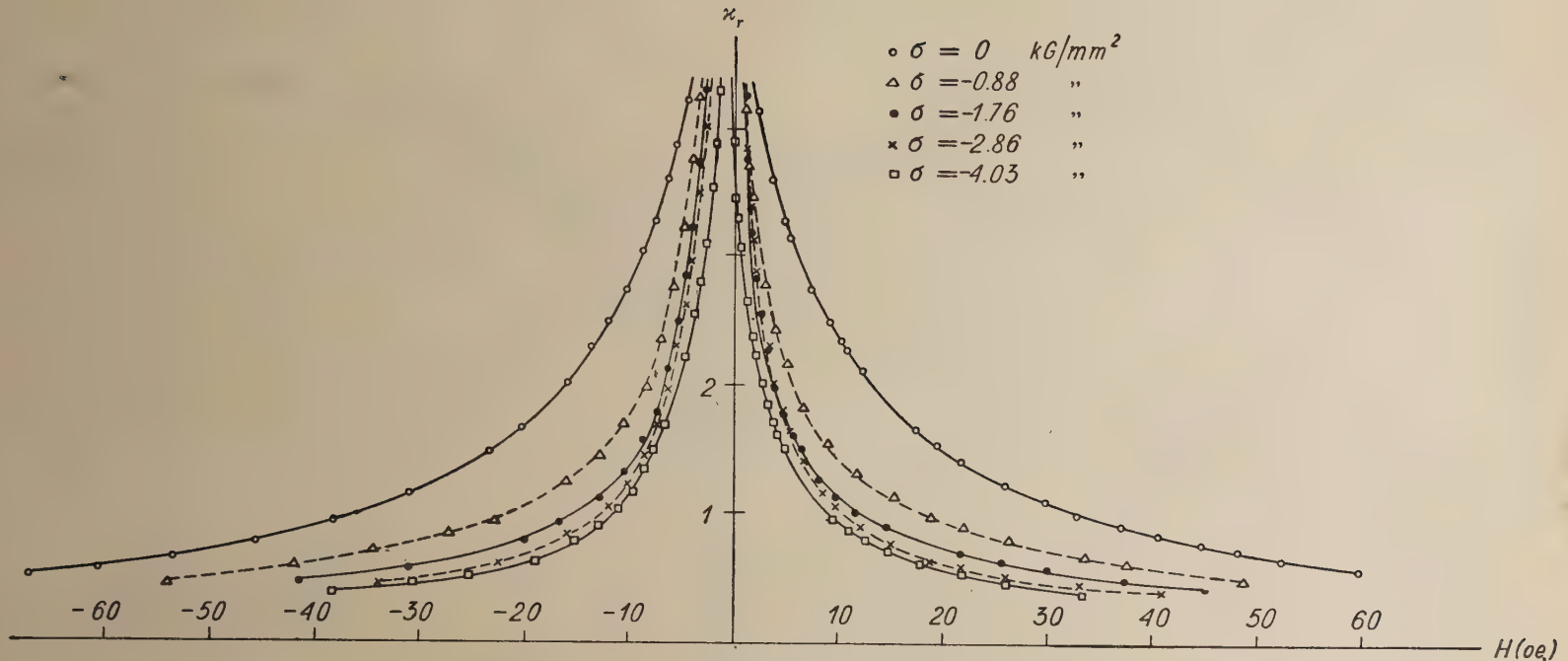

Fig. 9b. Variation of the $\varkappa_r$ with H for compressive stresses

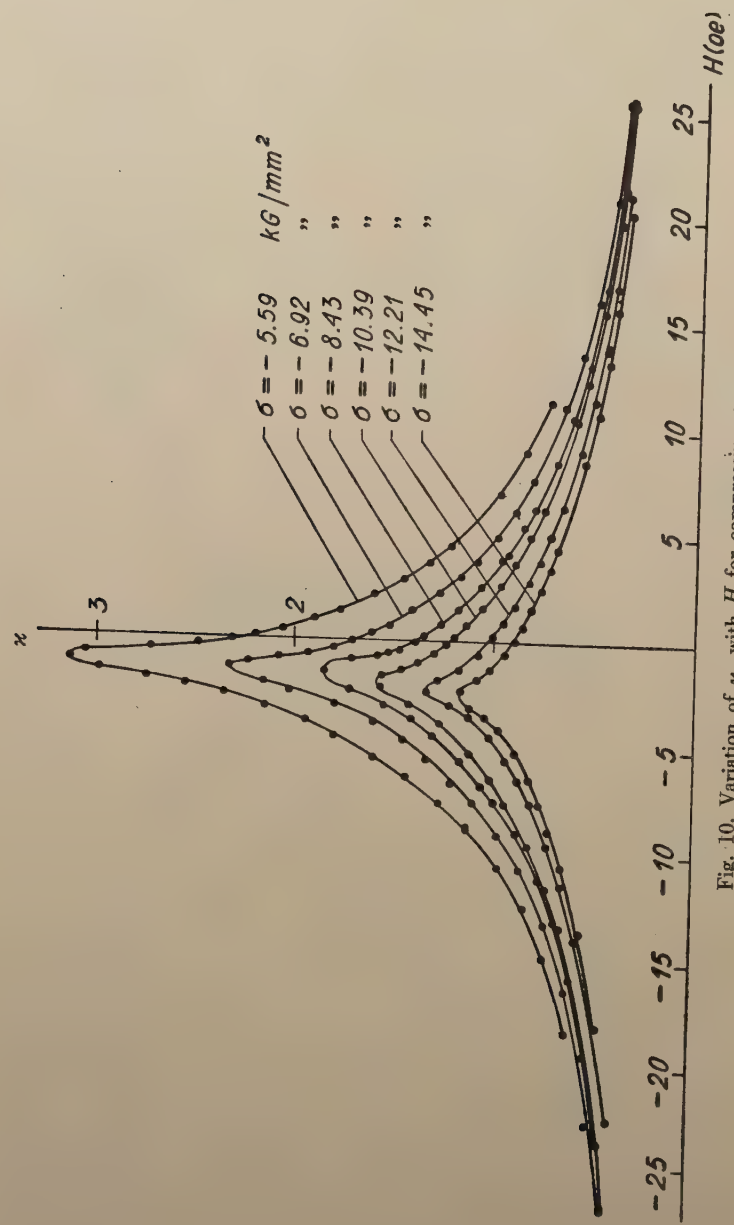

Fig. 10. Variation of $\varkappa_r$ with H for compressive stresses

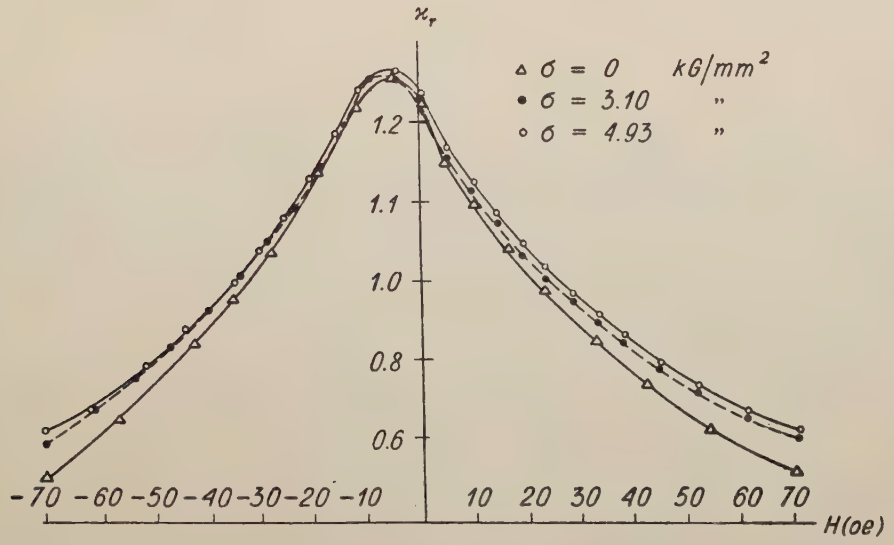

Fig. 11. Plot $\varkappa_r$ vs. H (on the hysteresis loop from −68 oe to +68 oe) for tension, unannealed specimen

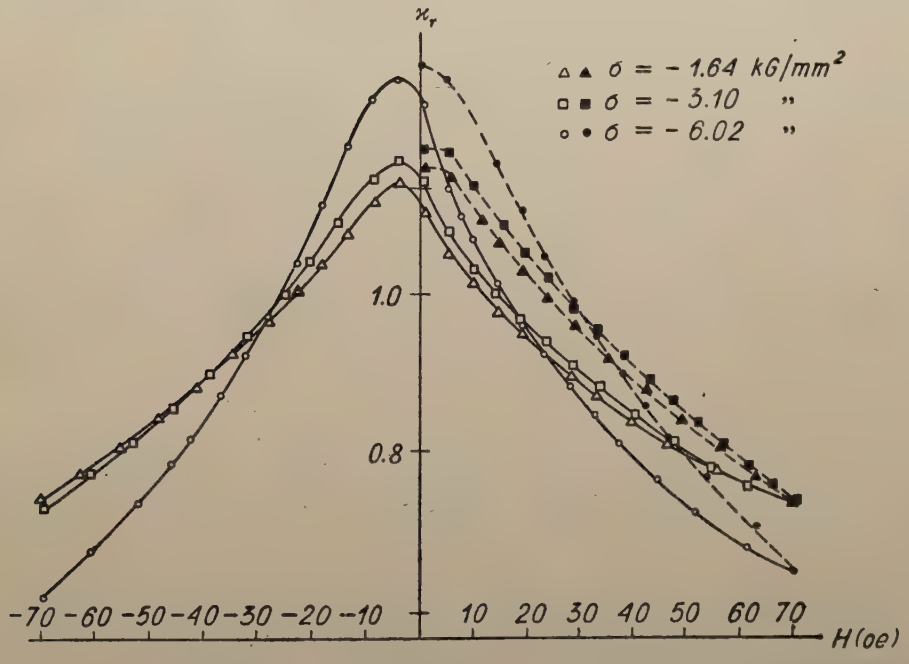

Fig. 12. Influence of compressive stress upon the variation of $\varkappa_r$ with H in unannealed specimen (on the virgin curve and on the hysteresis loop)

4. Theoretical Part

Theoretical investigations of the many quantities depending on domain structure involve considerable difficulties owing to the necessity of taking into account random forces varying irregularly from point to point. On the other hand, it is to be expected that in some cases statistical regularities may appear. Starting from simple statistical considerations Heisenberg (1931) has computed the magnetostriction curves for iron crystals. Heisenberg's statistical method has been extended to other fields by several authors.

A general formulation of statistical domain theory is given in Brown's papers (1937, 1938*a*, *b*, 1939). Brown (1938) has calculated the dependence of the reversible susceptibility on the magnetization on a statistical basis; he achieved good agreement with the experimental data and obtained a satisfactory derivation of Gans' law. Because of the success of Brown's theory the present paper is an attempt to derive the effect of stress on the reversible susceptibility by a suitable modyfication of his considerations. It should be noted here that Brown derived Gans' law by assuming isotropy of the domains. Brown has also ascertained that taking into account the anisotropy of domains does not appreciably alter the results.

Statistical domain theory — which shows close analogies with statistical mechanics — neglects the dissipation of energy accompanying variations of the magnetization. In order to relate such an idealized theory to properties of real ferromagnetics Brown assumes that "so far as a specimen's properties are functions of the magnetization alone, they are the same functions of magnetization as are the properties of an ideal reversible specimen having the same initial susceptibility". It should be stressed here that the justification of this assumption in only empirical, as it is based on the fact that, to a good approximation, the reversible susceptibility depends on the magnetization only, irrespective of previous magnetic history. At large compressive stress, owing to the rectangular form of the hysteresis, loop, the irreversible processes prevail (see, e.g., the paper by Sixtus and Tonks 1931), and it is unlikely that Brown's assumption should be fulfilled.

In view of Brown's results and in order to simplify the theory it is also assumed here, that the domains are isotropic.

We assume also that the internal stresses are small and randomly distributed without the preference of any axis and that this random distribution is not affected by the external stress. The errors connected with this assumption will be discussed later on.

Choosing the common direction of the magnetic field H and the stress σ as the polar coordinate axis, we denote by $n(\vartheta)d\omega$ the volume fraction of the domains having spontaneous magnetization directions within the solid angle $d\omega$ centred about the direction given by the polar angle ϑ. The most probable value of $n(\vartheta)$ — as is shown

in Brown's paper (1937) — is

$$n(\vartheta) = \frac{\exp\left[-LF(\vartheta)\right]}{\int \exp\left[-LF(\vartheta)\right] d\omega} \tag{1}$$

where $F(\vartheta)$ is the free energy per unit volume of the domains whose direction of spontaneous magnetization I_s is specified by the polar angle ϑ, and L is a Lagrange multiplier. The total free energy of a specimen may be considered as consisting of an additive part made up of contributions from the domains and a part due to the random internal forces (free energy of interaction between the domains). By an assumption equivalent to the statement that the part of the free energy due to interaction is independent of the external forces, Brown shows that the Lagrange multiplier is a constant of the material at a given temperature. The value of L, which depends on random forces only, is then assigned from the initial reversible susceptibility.

The free energy of the domains whose direction of spontaneous magnetization I_s subtends the angle ϑ with that of σ and H is — apart from a constant and neglecting the anisotropy energy — the sum of the magnetostatic energy:

$$-HI_s \cos\vartheta$$

and the magnetoelastic energy. Assuming isotropic magnetostriction, the magnetoelastic energy of the external uniform stress σ (Becker, Döring 1939, page 146) is:

$$-\frac{3}{2}\lambda_s\sigma\cos^2\vartheta$$

(λ_s is the mean saturation magnetostriction).

From eq. (1) with $F(\vartheta)$ given by

$$F(\vartheta) = -HI_s\cos\vartheta - \frac{3}{2}\lambda_s\sigma\cos^2\vartheta \tag{2}$$

we find the magnetization

$$I = \frac{\int I_s\cos\vartheta\exp\left[-LF(\vartheta)\right] d\omega}{\int \exp\left[-LF(\vartheta)\right] d\omega}$$

$$= I_s \frac{\int_0^\pi \cos\vartheta\sin\vartheta\exp\left(\alpha\cos\vartheta + \beta\cos^2\vartheta\right) d\vartheta}{\int_0^\pi \sin\vartheta\exp\left(\alpha\cos\vartheta + \beta\cos^2\vartheta\right)} \tag{3}$$

wherein

$$\alpha = LI_sH \qquad \beta = \frac{3}{2}L\lambda_s\sigma$$

The reversible susceptibility is

$$\varkappa_r = \left(\frac{\partial I}{\partial H}\right)_\sigma = LI_s \left(\frac{\partial I}{\partial \alpha}\right)_\beta$$

Introducing

$$S(\alpha, \beta) = \int_{-1}^{+1} \exp(\alpha x + \beta x^2)\, dx \tag{4}$$

the reversible susceptibility may be written as a function of the magnetization in parametric form:

$$\frac{I}{I_s} = \left(\frac{\partial \ln S}{\partial \alpha}\right)_\beta \tag{5}$$

$$\frac{\varkappa_r}{LI_s^2} = \left(\frac{\partial^2 \ln S}{\partial \alpha^2}\right)_\beta \tag{6}$$

It is easy to verify that, for $\beta = 0$ eqs. (5) and (6) yield Gans' function with $L = 3\varkappa_0/I_s^2$ ($\varkappa_0$ is the initial susceptibility at zero stress).

After simple calculations, eqs. (5) and (6) lead to the following explicit form of the dependence of $\varkappa_r$ on I/I_s:

$$\frac{I}{I_s} = \frac{e^\beta \sinh \alpha}{\beta S(\alpha, \beta)} - \frac{\alpha}{2\beta} \tag{5'}$$

$$\frac{\varkappa_r}{LI_s^2} = \left(\frac{I}{I_s} + \frac{\alpha}{2\beta}\right)\left(\coth \alpha - \frac{I}{I_s}\right) - \frac{1}{2\beta} \tag{6'}$$

From eqs. (6') follows the expression for the initial susceptibility at a given stress

$$\varkappa_r(0, \sigma) = \frac{I_s^2}{3(-\lambda_s)\sigma}\left\{1 - 2\frac{e^\beta}{s(0, \beta)}\right\} \tag{7}$$

We note here that — due to the negative value of magnetostriction for Ni — for $\sigma > 0$ i.e. $\beta < 0$ and in the limit $|\beta| \gg 1$ eq. (7) yields the well-known formula of Becker and Kersten (1930)

$$\varkappa_r(0, \sigma) \cong \frac{I_s^2}{3(-\lambda_s)\sigma}$$

Also, from eq. (5) there follows a linear dependence of the magnetization on the magnetic field strength for large tensile stresses and for not very large values of the fields as obtained by Becker. For $\sigma < 0$ eq. (7) predicts an increase of the initial reversible susceptibility with an increase of $|\sigma|$. The measurements show however, that this is really the case for small values of $|\sigma|$ only and after reaching maximum at stress value of about -1.3 kG/mm^2 the initial susceptibility decreases. This strong disagreement with the theoretical results is — as we have mentioned — connected with irreversible changes of magnetization.

Formulae (5) and (6) must be treated merely as a first approximation. Critical remarks about the applicability of statistical domain theory may be found in the literature quoted above (especially see Brown 1938b, 1939), here we shall discuss only the most important simplifying assumptions made in our calculations.

Putting for the $\frac{I_s^2}{3(-\lambda_s)}$ the value 24 kG/mm² (Becker, Döring 1939, p. 131) and determining the Lagrange multiplier L from the initial reversible susceptibility at zero stress we get the theoretical curves $\varkappa_r$ *vs.* I/I_s. Comparison with the experimental curves for several values of tension shows systematic disagreement — the theoretical values are about 10% — 20% too high as compared with the experimental ones. For compression disagreement is also found, but, unfortunately, owing to larger errors in the measurements of the magnetization it is difficult to come to definite conclusions.

A plausible explanation of the disagreement between theoretical and experimental values of $\varkappa_r$ may be given. In deriving our results we have assumed that the distribution of the internal stresses is random, so that it may be considered as isotropic and that this isotropic distribution is not affected by the external stress. The validity of the first assumption in our specimens is difficult to establish, as direct investigations of the internal stresses were not performed. On the other hand is well known that when external stress exceeds the yield-point the mean values of the internal stresses are increased. It can be supposed, therefore that the distribution of the internal stresses will then be anisotropic with the axis of anisotropy parallel to the external stress.

To take into account the anisotropic distribution of the internal stresses we add to the free energy (1) the mean magnetoelastic energy of the internal stresses. As a first approximation we find the former expressions (5′) and (6′), but with β replaced by

$$\beta' = \frac{3}{2} L\lambda_s (\sigma + \sigma_{||} - \sigma_{\perp})$$

($\sigma_{||}$ is the mean value of the internal stresses in the direction of external stress, $\sigma_{\perp}$ in a perpendicular direction). As it was impossible to estimate theoretically the parameter $s = \sigma_{||} - \sigma_{\perp}$ its value was chosen so as to fit the theoretical value of the initial reversible susceptibility at given stress to the experimental one.

The values of s found in this way for external stress varying from about 2 kG/mm² to 6.6 kG/mm² were approximately the same and equal to about 1.5 kG/mm². This result suggests that already at zero external stress the distribution of the internal stresses was probably not isotropic (this may be due to imperfect annealing, not sufficient to remove the internal stresses caused by metallurgical treatment of the wire from which the specimens were cut[4]).

[4] Computation of the mean internal stresses in our specimens I and II from the initial susceptibility by the well known method (Becker, Döring 1939) leads to the value of about 2.2 kG/mm². This value is considerably higher than the lowest possible value resulting from only magnetostrictive stresses, which shows again that the annealing was not sufficient.

In a discussion of the range of validity of the eqs. (5′) and (6′) it must be also taken into account that the neglect of anisotropy energy may cause departures from experimental values, especially at high values of magnetization. The tacit assumption that the Lagrange multiplier L is a constant is also an oversimplification. This can

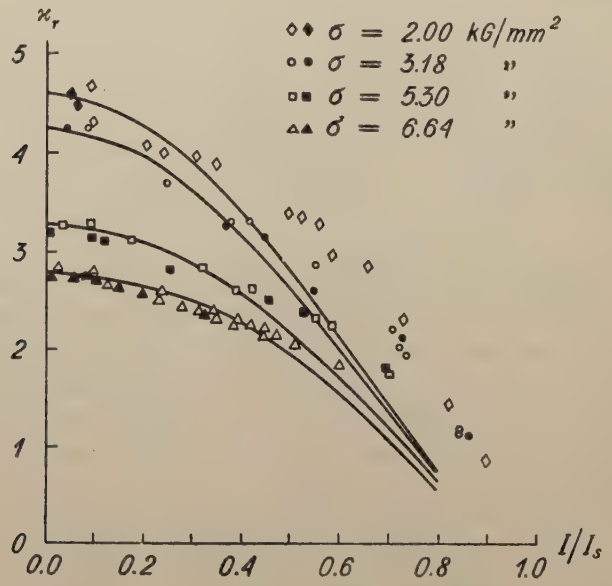

Fig. 13. Theoretical curves $\varkappa_r$ vs. I/Is for several values of the tension and the corresponding experimental points (◊, ○, □, △ values obtained on the hysteresis loop, ◆, ●, ■, ▲ — on the virgin curve). The experimental error in determining I/Is is about 5%.

be seen from the equation $L = 3\varkappa_0/I_s^2$ and from the known fact that $\varkappa_0$ is proportional to the inverse of the mean value of the internal stresses.

The comparison between experimental values of $\varkappa_r$ for several magnetizations with corrected theoretical curves is given in Fig. 13.

The author wishes to express his sincerest gratitude to Professor S. Szczeniowski for his continuous encouragement and helpful advice during this work.

КРАТКОЕ СОДЕРЖАНИЕ

I. Морковски, *Обратимая восприимчивость под напряжением*

Автором измерялась обратная восприимчивость на поликристаллическом никеле, подвергнутом во время измерения растягивающему (до 21 кг/мм²) и сжимающему напряжению (до 14 кг/мм²). Измерения проводились для магнитных полей вплоть до 68 эрстед.

Полученные результаты показывают, что при растягивающем напряжении происходит именьшение обратимой восприимчивости в области слабых магнитных полей и увеличение при более высоких полях. При малых сжимающих на-

пряжениях (до —3 кг/мм²) получаются обратные результаты, более высокие сжимающие нагрузки уменьшают обратную восприимчивость при всех величинах магнитного поля.

Автор произвел сравнение опытных данных с исчисленными на основании простой статистической теории.

REFERENCES

Becker, R., and Döring W., *Ferromagnetismus*, J. Springer 1939.
Becker, R. and Kersten, M., *Z. Phys.*, **64,** 660 (1930).
Bozorth, R. M., *Ferromagnetism*, Van Nostrand Co. New York 1951.
Brown, W. F., *Phys. Rev.*, **52,** 325 (1937); **53,** 484 (1938a); **219** (1938b); **55,** 568 (1939).
Erhardt, F., *Ann. Phys.* **54,** 41 (1917).
Gans, R., *Ann. Phys.* **27,** 1 (1908); **29,** 301 (1909); **33,** 1065 (1910); **61,** 379 (1920); *Phys. Zeits.* **12,** 1053, (1911).
Goldschmidt, R., *Phys. Zeits.* **31,** 1059 (1930).
Grimes, D. M. and Martin, D. W., *Phys. Rev.* **96,** 889 (1954).
Heisenberg, W., *Z. Phys.* **69,** 287 (1931).
Kersten, M., *Z. Phys.* **71,** 553 (1931).
Kirkham, D., *Phys. Rev.* **52,** 1162 (1937).
Kohlrausch, F., *Praktische Physik*, B. G. Teubner, Stuttgart 1956.
Kondorski, E., *Zh. eksper. teor. Fiz.*, **10,** 420 (1940).
Samuel, M. *Ann. Phys.* **86,** 798 (1928).
Sixtus, K. and Tonks, L., *Phys. Rev.* **37,** 930 (1931).
Shur, J., *Izv. Akad. Nauk SSSR, Ser. fiz.*, **11,** 570 (1947).
Tebble, R. S. and Corner, W. D., *Proc. Phys. Soc.* **63** B, 1005 (1950).
Tebble, R. S., Corner, W. D. and Wood, J. E., *Proc. Phys. Soc.* **64** B, 753 (1951).
Vonsovski, S. W., *Zh. eksper. teor. Fiz.*, **17,** 1094 (1947).
Vonsovski, S. W. and Shur, J. S., *Ferromagnetizm*, OGIZ, Moscow 1948.

RAPPORTS DES INTENSITÉS DES RAIES SPECTRALES DANS CERTAINS DOUBLETS DES SÉRIES II ET I SECONDAIRES DES SPECTRES D'ARC D'ALUMINIUM ET D'INDIUM

Par Maria D. Kunisz

Institut de Physique Experimentale de l'Université Jagellon, Cracovie

(Reçu le 28 juin 1958)

On a mesuré les rapports des intensités des composantes des 8 doublets des séries II et I Secondaires d'aluminium et d'indium, en vue de vérifier si la règle des sommes était satisfaite. On s'est sérvi de la méthode de la spectrophotomètrie photographique. Comme source on a utilisé l'arc électrique, l'étincelle et la cathode creuse. Les résultats indiquent qu'il y a une dépendence de la grandeur des écatrs à la règle des sommes de la position du doublet dans la série spectrale.

Introduction

Il est bien connu, depuis une trentaine d'années, que dans un multiplet, selon la règle d'Ornstein, Burger, Dorgelo (la règle des sommes), les rapports des sommes des intensités (éventuellement divisées par ν^4, où ν est la fréquence de la raie) des raies spectrales commençant (finissant) à des niveaux énergétiques communs sont égaux aux rapports des poids statistiques de ces niveaux. Cette règle est valable dans les conditions suivants:

Il faut, que:

1°. Le multiplet considéré ne soit pas lié par des raies d'intercombinaison à d'autres multiplets.

2°. Les intensités des raies examinées ne soient pas modifiées par la réabsorption.

3a. Les raies composantes du multiplet aient le même niveau supérieur, ou

3b. L'équilibre soit thermodynamique et, par conséquent, la population N_m du niveau initial E_m d'une raie spectrale dépende de la population N_0 du niveau fondamental d'atome E_0, de la température T et des poids statistiques g_m et g_0 des niveaux E_m et E_0, selon la relation:

$$N_m = N_0 \frac{g_m}{g_0} e^{\frac{E_0 - Em}{kT}}$$

Dans le can général, la population N_m du niveau E_m peut dépendre également: 1. des collisions des atomes rayonnants avec d'autres atomes, ions et électrons, 2. de la re-

combinaison, 3. de la réabsorption et 4. des transitions spontanées et forcées à partir des niveaux électroniques plus élevés. Quand tous ces effets ont lieu, la règle des sommes n'est pas valable et les rapports des intensités des raies spectrales dans les multiplets se modifient avec les conditions d'excitation, telles que l'intensité du courant électrique ou la pression.

4°. a. Les différences des longueurs d'onde des raies examinées ne soient pas très grandes ou

b. la température T de la décharge soit assez haute pour qu'on puisse admettre que l'expression $exp\ [-(E_m - E_n)/kT] = 1$, où E_m et E_n sont les niveaux d'énergie initiaux des raies.

Il n'y a pas beaucoup de travaux expérimentaux concernant la mesure des intensités des raies spectrales dans les doublets des éléments de la troisième colonne de la table périodique des éléments. Les seuls résultats que l'auteur ait trouvés sont donnés dans le tableau I.

Tableau I

Rapports des intensités des composants de certains doublets des spectres d'arc des éléments de la troisième colonne de la table périodique des éléments

Série principale

Thallium	$I_{6550} : I_{6714}$	$I_{5528} : I_{5584}$	$I_{5109} : I_{5137}$	$I_{4891} : I_{4906}$
O. Vonwiller (1930)	4,5 ± 0,44	5,7 ± 0,92	6,4	7 ± 1
S. E. Williams (1932)	4,4	6,6 ± 0,25	6,0 ± 0,2	5,2 ± 0,2
J. Harlichy				

Série II Secondaire

Aluminium	$I_{3962} : I_{3944}$	$I_{2660} : I_{2652}$
P. G. Voorhoeve (1946)	2,0 ± 0,3	2,0 ± 0,3
Gallium	$I_{4172} : I_{4033}$	
R. Payne-Scott (1933)	1,55 ± 0,07	
Indium	$I_{4511} : I_{4102}$	
R. Payne-Scott (1933)	2,35 ± 0,09	
Thallium	$I_{5350} : I_{3776}$	
L. S. Ornstein (1927)	0,5	
O. Vonwiller (1930)	2,57 ± 0,03	

Série I Secondaire

Aluminium	$I_{3093} : I_{3083}$	$I_{2575} : I_{2568}$	
P. G. Voorhoeve (1946)	1,9 ± 0,3	2,2 ± 0,3	
Thallium	$I_{3519} : I_{3529}$	$I_{2918} : I_{2921}$	$I_{2709} : I_{2711}$

I. P. Bogdanowa (1956) On a mesuré les rapports des intensités pour la décharge dans les vapeurs du thallium avec une addition du gaz rare. On a constaté une dépendence de ces rapports de la pression du gaz rare.

Remarque: En donnant les valeurs des rapports des intensités on a tenu compte de la correction d'Einstein.

Les résultats de ces travaux semblent indiquer, que la règle des sommes pour les spectres de ces éléments n'est pas valable, non seulement pour les doublets de la série principale, mais aussi pour ceux de la série II Secondaire.

Il faut remarquer, qu'on constate dans plusieurs travaux expérimentaux, que les rapports des intensités des raies spectrales dans les doublets de la série principale des métaux alcalins dépendent essentiellement du numéro d'ordre du doublet dans la série et qu'ils augmentent quand on passe du sodium, ou la règle des sommes est valable, par le potassium et le rubidium, jusqu'au coesium, où les écarts à cette règle sont les plus grands. Ce fait est expliqué théoriquement par E. Fermi (1930). Mais, pour les séries II et I Secondaires des spectres des métaux alcalins on n'observe pas de grands écarts de la règle des sommes.

Le présent travail a eu pour but de mesurer les intensités relatives dans certains doublets des séries II et I Secondaires des spectres d'aluminium et d'indium en vue de vérifier si, dans ces séries, la règle des sommes n'était jamais valable ou si les deux doublets ci-dessus constituaient des exceptions.

I. Dispositif experimental

Ce travail a été exécuté par la méthode de la spectrophotométrie photographique.

Le dispositif expérimental était composé des instruments suivants:

1. Un spectrographe Q-24 de C. Zeiss Jena.
2. Un affaiblisseur à 7 marches de Hilger.
3. Une lampe à arc du courant continu.
4. Un générateur d'étincelles (tension jusqu'au 6 kV).
5. Une lampe à cathode creuse type Schüler remplie d'argon ou d'hélium.
6. Une lampe à filament de tungstène étalonnée par les soins du G.U.M. à Varsovie et employée comme étalon secondaire de rayonnement.
7. Un microphotométre photoélectrique MΦ-2 de la production de l'U.R.S.S.

On a employé les plaques photographiques Agfa suivantes: 1) Ultravioletplatten, 2) Spektral-Platten Blau Rapid, 3) Spektral-Platten Gelb Rapid et des plaques photographiques Film Polski 1) Ultrapan-Super et 2) G-2,2.

II. Quelques remarques sur les conditions d'excitation du spectre et sur la méthode de travail

A. Comme le but du présent travail était de vérifier la validité de la régle des sommes, il fallait exciter le spectre de façon, que 1°. les raies spectrales examinées ne soient pas réabsorbées dans la source, 2° la décharge soit thermique.

A cet effet: 1°. L'émission des éléments étudiés a été excitée dans a) l'arc électrique à courant continu, dans l'air sous la pression atmosphérique, b) l'étincelle sous la tension de 6 kV dans une atmosphère d'azote ou de bioxyde de carbone sous la pression d'une atmosphère et c) la lampe à cathode creuse type Schüler remplie d'argon ou d'hélium. Dans les deux dernières sources on n'a pas observé de réabsorption dans nos conditions expérimentales. Par contre, dans l'arc électrique on avait d'ordinaire

une réabsorption assez forte. En vue d'éviter cette réabsorption on n'a pas fait les électrodes directement en métaux dont les spectres étaient examinés, mais on les a construites en tige d'argent percée d'un canal cylindrique dans lequel se trouvait le métal. On a constaté que la réabsorption, pour une certaine valeur de l'intensité du courant électrique, dépendait du rapport du diamètre de la tige d'argent au diamètre du métal. Pour chacun des métaux on avait choisi ces valeurs de telle façon, que la réabsorption n'intervenait pratiquement pas. Par example, pour examiner le spectre d'indium, on utilisait des électrodes d'argent de 4.0 mm de diamètre extérieur et ceux d'indium de 1.2 mm de diamètre pour le courant 1.5 amp. On vérifiait l'absence de la réabsorption en mesurant d'une part le profil de la raie spectrale et d'autre part en examinant si les rapports de leurs intensités dans les multiplets ne dépendaient pas de l'intensité du courant de l'arc (dans les limites 1.5—5.0 amp.), ce qui serait possible seulement dans le cas où la réabsorption n'existerait pas.

2°. D'autre part, il fallait éviter que les collisions de seconde espèce des atomes rayonnants avec des atomes et des ions, la recombinaison, l'absorption et les transitions spontanées et forcées à partir des niveaux plus élevés n'exerçassent d'influence sur la population du niveau initial de la raie spectrale examinée et par conséquent sur son intensité. Dans nos conditions expérimentales cela avait lieu dans le spectre de l'arc et de l'étincelle. Cette condition a été aussi réalisée dans le spectre de la cathode creuse, mais seulement pour les doublets plus élevés de la série. C'est que, pour ces doublets, on pouvait négliger l'influence sur la population du niveau initial de la raie des transitions à partir des niveaux plus élevés. D'autre part, on pouvait aussi négliger dans la lampe de Schüler les collisions des atomes rayonnants avec d'autres atomes et ions, par rapport aux collisions avec les électrons. C'est pourquoi la cathode creuse a été utilisée uniquement pour la mesure des intensités relatives dans les doublets plus élevés.

B. Élimination du spectre continu

Dans la plupart des doublets, il était possible de choisir les conditions d'excitation du spectre de manière qu'il n'y ait pas de fond continu. On réalisait cela, soit en utilisant une électrode auxiliaire convenable, à l'intérieur de laquelle se trouvait le métal dont le spectre était examiné dans l'arc électrique, soit par un changement de la self-induction dans le circuit de l'étincelle. Seul, le premier doublet de la série II Secondaire d'aluminium n'a pas pu être obtenu sans le spectre continu. Comme l'intensité de ce fond était variable, on appliquait dans la photométrie de ce doublet la méthode décrite par l'auteur dans un travail précédent (Kunisz 1953).

C. Application de la méthode ee spectrophotométrie monochromatique photographique

Tous les doublets des séries II et I Secondaires d'aluminium et d'indium ont été mesuré par la méthode monochromatique de la photométrie photographique. Dans le cas de l'aluminium, où les différences des longueurs d'onde des raies examinées

dans le doublet ne dépassaient pas 18 Å, cette méthode était bien fondée. Pour les doublets de l'indium, par contre, ces différences étaient de 179 Å, 154 Å et 134 Å. Pour cette raison on a choisi pour chaque doublet des plaques photographiques dont les courbes caractéristiques pour les longueurs d'onde des raies de ce doublet étaient parallèles. Ainsi, on travaillait d'ordinaire avec des plaques dont la sensibilité dans le domaine examiné du spectre n'était pas maximum. Pour chaque doublet, on a fait des mesures sur différentes sortes de plaques photographiques.

Le doublet visible d'indium a été photométré par la méthode de la spectrophotométrie hétérochromatique et ensuite par la méthode de la spectrophotométrie monochromatique de la façon décrite ci-dessus. On a obtenu des résultats identiques dans les limites des erreurs expérimentales.

III. Les résultats des mesures expérimentales

On a mesuré les rapports des intensités pour 7 doublets des séries II et I Secondaires d'aluminium et d'indium. On a appliqué la correction Einstein. Dans les calculs des erreurs on a tenu compte des erreurs de la photométrie et pour les doublets de la série I Secondaire des erreurs provenants de la différente population des niveaux superieurs $^2D_{s/_2}$, $^2D_{s/_2}$ des raies. Les résultats de ce travail, ainsi que ceux des travaux précedents, déjà mentionnés, sont présentés dans le tableau II. Selon la règle des sommes, le rapport des intensités des raies spectrales dans tous les doublets examinés doit être le même et égal à 2.

Tableau II

La comparaison des rapports des intensités des composantes des doublets des séries II et I Secondaires donnés dans la littérature pour la décharge en équilibre thermique avec ceux de l'auteur

	Série II Secondaire		Série I Secondaire	
Aluminium	$I_{3962} : I_{3944}$	$I_{2660} : I_{2652}$	$I_{3093} : I_{3083}$	$I_{2575} : I_{2569}$
P. G. Voorhoeve (1946)	2,0 ± 0,3	2,0 ± 0,3	1,9 ± 0,3	2,2 ± 0,3
l'auteur	1,66 ± 0,04	2,03 ± 0,03	1,67 ± 0,05	2,14 ± 0,05
Gallium	$I_{4172} : I_{4033}$			
R. Payne-Scott (1933)	1,55 ± 0,07			
Indium	$I_{4511} : I_{4102}$	$I_{2933} : I_{2754}$	$I_{2710,2714} : I_{2560}$	$I_{2521,2523} : I_{2390}$
R. Payne-Scott (1933)	2,35 ± 0,09			
l'auteur	2,44 ± 0,04	3,33 ± 0,05	2,73 ± 0,10	5,56 ± 0,50
Thallium	$I_{5350} : I_{3776}$			
L. S. Ornstein (1927)	0,5			
O. Vonwiller (1930)	2,57 ± 0,03			

Remarque: En donnant les valeurs des rapports des intensités on a tenu compte de la correction d'Einstein.

IV. Conclusions

La comparaison des résultats de ce travail avec ceux des autres auteurs montre un bon accord pour les deuxièmes doublets des séries II et I Secondaires de l'aluminium et pour le premier doublet de la série II Secondaire de l'indium. Par contre on constate que pour les premiers doublets des séries II et I Secondaires de l'aluminium la régle des sommes n'est pas valable tandis que d'après P.G. Voorhoeve (1946) elle est assez bien accomplie. Comme, dans le present travail c'etait bien verifié qu'il n'yavait pas de la réabsorption dans la source de rayonnement, ces resultats semblent être plus sûrs que ceux de P. G. Voorhoeve, qui devait tenir compte de la réabsorption.

En tenant compte de ces remarques on peut faire des conclusions:

1. La règle des sommes pour les doublets des séries II et I Secondaires du spectre d'aluminium et d'indium n'est pas valable, excepté pour le deuxième doublet de ces séries du spectre d'aluminium. Ce fait est d'autant plus remarquable, que dans les doublets de la série II Secondaire les deux raies proviennent de transitions ayant le même nivau initial.

2. La comparaison des valeurs du rapport d'intensité des composantes des doublets de la même série montre, que, dans tous les cas, il est plus grand pour le deuxième doublet de la série, que pour le premièr.

3. La comparaison des valeurs du rapport d'intensité des composantes du même doublet de la série II Secondaire de l'aluminium, du gallium, d'indium et du thallium (mesurées dans le présent travail ainsi que celles données dans la littérature), montre une dépendance de ce rapport de la position de l'élément dans la table périodique

Les deux dernières dépendances sont représentées sur le diagramme 1.

Dans ce travail on a fait aussi des mesures des rapports des intensités dans les doublets de la série principale d'indium, qui ont montré une dépendance régulière

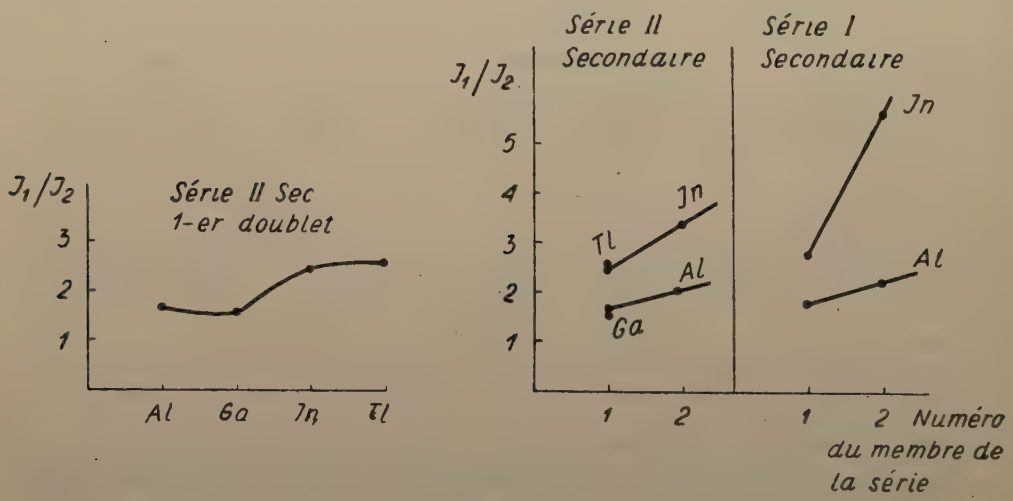

Fig. 1

des rapports des intensités du numéro d'ordre du doublet dans la série. L'auteur se propose de publier ces résultats après avoir fini les mesures sur les doublets de cette série pour le gallium et l'aluminium.

D'après les résultats de ce travail et des données de la littérature, on peut supposer, qu'en général la règle des sommes n'est pas valable dans le spectre d'arc d'aluminium, de gallium, d'indium et de thallium, aussi bien pour la série principale, que pour les séries II et I Secondaires.

L'auteur tient à remercier Monsieur le Professeur H. Niewodniczański pour le sujet du travail et pour les précieux conseils qu'il lui a prodigués au cours de ce travail.

КРАТКОЕ СОДЕРЖАНИЕ

М. Куниш, "*Относительные интенсивности спектральных линий в нескольких дублетах серий II и I побочных дугового спектра алюминия и индия*"

Измерено отношения интенсивностей компонент 8 дублетов серий I и I побочных алюминия и индия. Применено метод фотографической спектральной фотометрии. В качестве источника света использовано электрическую дугу, искру а также разрядную трубку с полым катодом. Результаты настоящей работы показывают зависимость отступлений от правила сумм в дублетах от места дублета в спектральной серии.

BIBLIOGRAPHIE:

Bogdanowa, I. P., *Wiestnik L.T.U.*, **4,** 41 (1956).
Fermi, E., *Zs. f. Phys.*, **59,** 680 (1930).
Frisz, S. E., *Usp. Fiz. Nauk.*, **61,** 461 (1957).
Kunisz, M. D., *Acta phys. Polon.*, **12,** 3 (1953).
Ornstein, L. S., *Phys. Zs.*, **27,** 688 (1927).
Williams, S. E., a. Harlichy, J. *Phys. Rev.* (2), **39,** 802 (1932).
Vonwiller, O. U., *Phys. Rev.*, **35,** 802 (1930).
Voorhoeve, P. G., „Onderzoekingen in het Spectrum van Aluminium" Diss. Utrecht 1946.
Payne-Scott, R., *Nature*, **131,** 365 (1933).

MODIFIED BOHM AND PINES COLLECTIVE DESCRIPTION OF ELECTRON INTERACTIONS IN CRYSTALS. I.

By Jan Śledzik

Institute of Physics of Polish Academy of Sciences, Department of Ferromagnetics in Poznań

(Received July 2, 1958)

The generalized Bohm — Pines theory of electron interactions in translation lattices is formulated. In order to remove the difficulties in normalizing the state vectors a set of new subsidiary conditions is proposed. As a result it is shown that the Bohm — Pines theory may be taken as correct for any desired degree of accuracy. In this treatment the electrons are supposed to be bound with ion — cores (tight binding approximation). The ion — core polarisation is not taken into account because of the complications which the consideration of this phenomenon introduces.

1. Introduction

The Bohm — Pines theory of electron plasma oscillations has been developed in two variants. The first is in the form of a second quantisation hamiltonian and no subsidiary conditions are introduced. In the other, which is formulated in a special mixed representation, the authors introduce new field variables, called "longitudinal degrees of freedom." Since the total number of these degrees for a whole system must remain unchanged, the new variables are subjected to a set of supplementary conditions. It turns out, however, that there cannot be found a normalizable state vector satisfying the conditions in question (Adams 1955b, Kanazawa 1957b).

Kanazawa in the quoted paper proposes to modify the subsidiary conditions to make them less stringent. In principle, this can be done, but in doing to we must bear in mind that simultaneously the equations of motion are changed, since, as Z. Galasiewicz has shown (1958c), the subsidiary conditions, given in the form proposed by Bohm and Pines, secure the identity of the quantum equations of motion both in many electron Schrödinger theory and in the Bohm — Pines collective description.

In the present paper a new term is added to a set of supplementary conditions. This term can be made as small as desired and thus the Bohm — Pines theory of electrons may be approximated to any accuracy.

It is to be noted that Zubarev (1953) and Bogolyubow — Zubarev (1955) have developed a theory of electron gas quite similar to that of Bohm — Pines. Galasiewicz (1956b) proved the equivalence of both theories.

2. The modified supplementary conditions

Suppose we have a system composed of n electrons and N ion-cores. These last are slowly moving (compared to electrons) around their equilibrium positions in nodes of translation lattices. We treat the ion-cores approximately as material points bearing electric charge of density $+Z\varepsilon\delta(\vec{r}-\vec{r}_\alpha)$. Here Z is the number of valence electrons, $-\varepsilon$ the charge of electron, $\vec{r}_\alpha$ position vector of α-th ion-core. We do not take into account the effects of ion-core polarisation. All particles are considered to move in a basic space with volume V.

Thus we have for the hamiltonian of the system the following expression

$$\hat{H}=\sum_{i=1}^{n}\hat{p}_i^2/2m+\sum_{\alpha=1}^{N}\hat{p}_\alpha^2/2M+\frac{\varepsilon^2}{2}\sum_{i\neq j}\frac{1}{r_{ij}}+\frac{Z^2\varepsilon^2}{2}\sum_{\alpha\neq\beta}\frac{1}{r_{\alpha\beta}}-Z\varepsilon^2\sum_{i,\alpha}\frac{1}{|\vec{r}_i-\vec{r}_\alpha|}. \tag{2.1}$$

The first and second term represent the kinetic energies of electrons and ion-cores respectively, the third, the Coulomb electron interaction energy etc. The Roman indices are reserved for electrons, the Greek ones for ions.

Instead of using the hamiltonian (2,1) we transform it introducing the well known expressions:

$$\delta(\vec{r})=\frac{1}{V}\sum_{\vec{\lambda}}e^{i\vec{\lambda}\cdot\vec{r}}, \tag{2,2a}$$

$$\frac{1}{r}=\frac{4\pi}{V}\sum_{\vec{\lambda}}\frac{e^{i\vec{\lambda}\cdot\vec{r}}}{\lambda^2}, \tag{2,2b}$$

and for the charge density and its Fourier components

$$\varrho(\vec{r})=\frac{1}{V}\sum_{\vec{\lambda}}\varrho_\lambda e^{i\vec{\lambda}\cdot\vec{r}}=-\varepsilon\sum_{i=1}^{n}\delta(\vec{r}-\vec{r}_i)+Z\varepsilon\sum_{\alpha=1}^{N}\delta(\vec{r}-\vec{r}_\alpha), \tag{2,2c}$$

$$\varrho_\lambda=-\varepsilon\sum_{i=1}^{n}e^{-i\vec{\lambda}\cdot\vec{r}_i}+Z\varepsilon\sum_{\alpha=1}^{N}e^{-i\vec{\lambda}\cdot\vec{r}_\alpha}. \tag{2,2d}$$

In the above expressions the summation over $\vec{\lambda}$ extends over all reciprocal lattice vectors $\vec{\lambda}=\frac{2\pi}{\sqrt[3]{N}}\sum_{i=1}^{3}s_i\vec{b}^i$, where $\vec{b}^i=\sum_{k=1}^{3}g^{ik}\vec{a}_k$, g^{ik} are contravariant components of the fundamental lattice tensor, $\vec{a}_k$ — three lattice vectors, $s_i=0,\pm1,\pm2,\ldots,\pm\frac{\sqrt[3]{N}-1}{2}$.

The hamiltonian (2,1) rewritten in new terms ϱ_λ takes the form

$$\hat{H}=\sum_{i=1}^{n}\hat{p}_i^2/2m+\sum_{\alpha=1}^{N}\hat{p}_\alpha^2/2M+\frac{2\pi}{V}\sum_{\vec{\lambda}}\frac{\varrho_\lambda\varrho_{-\lambda}}{\lambda^2}-\frac{2\pi Z(1+Z)N\varepsilon^2}{V}\sum_{\vec{\lambda}}\frac{1}{\lambda^2}. \tag{2,3}$$

The last term in (2,3) eliminates the self-energy of electron-electron and ion-ion Coulomb interactions in the third member of the hamiltonian. In the sums over $\vec{\lambda}$ in equation (2,3) we exclude the value $\vec{\lambda} = 0$ because of the charge neutrality of the system. On the other hand this value leads to false resulte in (2,2b) and therefore must be omitted.

Following Bohm and Pines we introduce now a longitudinal vector potential $\vec{A}(\vec{r})$, but let this expression be cut off in its Fourier expansion at $\vec{\lambda} = \vec{\lambda}_c$,

$$\vec{A}(\vec{r}) = \sqrt{\frac{4\pi}{V}}\, c^2 \sum_{\vec{\lambda},\lambda \leqslant \lambda_c} q_\lambda \vec{\varepsilon}_\lambda e^{i\vec{\lambda}\vec{r}}; \qquad \vec{\varepsilon}_\lambda = \frac{\vec{\lambda}}{\lambda}. \tag{2,4}$$

Here q_λ are new variables describing a long-range Coulomb electron-electron, ion-ion and electron-ion interactions. $\vec{\lambda}_c$ is a quantity of order 1 Å^{-1} and must be deduced from the condition of minimum energy for the system.

The electric field may be written as

$$\vec{E}(r) = \sqrt{\frac{4\pi}{V}} \sum_{\vec{\lambda},\lambda \leqslant \lambda_c} p_{-\lambda} \vec{\varepsilon}_\lambda e^{i\vec{\lambda}\vec{r}}. \tag{2,5}$$

The corresponding extended hamiltonian including the electrostatic field can be represented in the form

$$\hat{H}_{\text{ext}} = \frac{1}{2m}\sum_{i=1}^{n}\left(\vec{p}_i + \frac{\varepsilon}{c}\vec{A}_\alpha\right)^2 + \frac{1}{2M}\sum_{\alpha=1}^{N}\left(\vec{p}_\alpha - \frac{Z\varepsilon}{c}\vec{A}_\alpha\right)^2 + \frac{1}{8\pi}\int_V E^2\, d\vec{r} +$$

$$+ \frac{2\pi}{V}\sum_{\vec{\lambda},\lambda > \lambda_c}\frac{\varrho_\lambda \varrho_{-\lambda} - Z(1+Z)N\varepsilon^2}{\lambda^2} - \frac{2\pi Z(1+Z)N\varepsilon^2}{V}\sum_{\vec{\lambda},\lambda \leqslant \lambda_c}\frac{1}{\lambda^2} - \sum_{\vec{\lambda},\lambda \leqslant \lambda_c} \nu_\lambda \left\langle \frac{\hbar\omega_\lambda}{4} \right\rangle \tag{2,6}$$

This form of hamiltonian differs from that of Bohm — Pines by the explicitly written Coulomb short-range interactions — a consequence of taking a cut off vector potential — and by adding the term $-\sum_{\vec{\lambda},\lambda \leqslant \lambda_c} \nu_\lambda \left\langle \frac{\hbar\omega_\lambda}{4} \right\rangle$ whose significance will be given later on.

The subsidiary conditions are now postulated in the form

$$[(div\vec{E} - 4\pi\varrho)_\lambda + \alpha_\lambda (div\vec{A})_\lambda]\, \Psi = 0; \quad \vec{\lambda},\, \lambda \leqslant \lambda_c, \tag{2,7a}$$

or

$$\sqrt{\frac{4\pi}{V}}\left[ip_{-\lambda}\cdot\lambda + i\alpha_\lambda \cdot c\cdot\lambda\cdot q_\lambda - \sqrt{\frac{4\pi}{V}}\varrho_\lambda\right]\Psi = 0; \quad \vec{\lambda},\, \lambda \leqslant \lambda_c \tag{2,7b}$$

We choose a Lagrange multiplier α_λ so as to have

$$\alpha_\lambda = i\frac{\nu_\lambda \omega_\lambda}{c}, \quad \omega_\lambda = \omega_{-\lambda}, \quad \nu_\lambda = \nu_{-\lambda}. \tag{2,7c}$$

Then the relations (2,7b) become

$$\left(p_\lambda + i\omega_\lambda \nu_\lambda q_{-\lambda} + i\sqrt{\frac{4\pi}{V\lambda^2}}\varrho_{-\lambda}\right)\Psi = 0; \qquad \vec{\lambda},\ \lambda \leqslant \lambda_c\,. \tag{2,8}$$

Here ν_λ is a positive number fulfilling the condition

$$0 < \nu_\lambda \leqslant 1, \tag{2,9}$$

and ω_λ signifies a frequency of electron oscillations in a nearly periodic field of the lattice.

Keeping in mind that $\frac{1}{8\pi}\int_V E^2 d\vec{r} = -\frac{1}{2}\sum_{\vec{\lambda},\lambda\leqslant\lambda_c} p_\lambda p_{-\lambda}$ we can now rewrite the hamiltonian (2,6) in the form of several separate terms:

$$\hat{H}_{\text{ext}} = \hat{H}_{\text{part}} + \hat{H}_{s,r} + \hat{H}_{\text{coll}} + \hat{H}_{\text{inter}} + \hat{U} - \\ - \frac{2\pi Z(1+Z)N\varepsilon^2}{V}\sum_{\vec{\lambda},\lambda\leqslant\lambda_c}\frac{1}{\lambda^2} - \sum_{\vec{\lambda},\lambda\leqslant\lambda_c}\nu_\lambda\left\langle\frac{\hbar\omega_\lambda}{4}\right\rangle, \tag{2,10}$$

with

$$\hat{H}_{\text{part}} = \frac{1}{2m}\sum_{i=1}^{n}\hat{p}_i^2 + \frac{1}{2M}\sum_{\alpha=1}^{N}\hat{p}_\alpha^2, \tag{2,11a}$$

$$\hat{H}_{s,r} = \frac{2\pi}{V}\sum_{\vec{\lambda},\lambda>\lambda_c}\frac{\varrho_\lambda\varrho_{-\lambda} - Z(1+Z)N\varepsilon^2}{\lambda^2}, \tag{2,11b}$$

$$\hat{H}_{\text{coll}} = -\frac{1}{2}\sum_{\vec{\lambda},\lambda\leqslant\lambda_c}(p_\lambda p_{-\lambda} + \omega_\lambda^2 q_\lambda q_{-\lambda}) + \frac{1}{2}\sum_{\vec{\lambda},\lambda\leqslant\lambda_c}(\omega_\lambda^2 - \omega_p^2)\,q_\lambda q_{-\lambda}, \tag{2,11c}$$

where $\omega_p^2 = \frac{4\pi n\varepsilon^2}{mV} + \frac{4\pi NZ^2\varepsilon^2}{MV}$ denotes the Langmuir frequency of electron — ion oscillations, and further

$$\hat{H}_{inter} = \sqrt{\frac{4\pi}{V}}\frac{\varepsilon}{m}\sum_{i=1}^{n}\sum_{\vec{\lambda},\lambda\leqslant\lambda_c} q_\lambda \vec{\varepsilon}_\lambda\cdot\left(\vec{p}_i - \frac{\hbar\vec{\lambda}}{2}\right)e^{i\vec{\lambda}\cdot\vec{r}_i} - \\ - \sqrt{\frac{4\pi}{V}}\frac{Z\varepsilon}{M}\sum_{\alpha=1}^{N}\sum_{\vec{\lambda},\lambda\leqslant\lambda_c} q_\lambda \vec{\varepsilon}_\lambda\cdot\left(\vec{p}_\alpha - \frac{\hbar\vec{\lambda}}{2}\right)e^{i\vec{\lambda}\cdot\vec{r}_\alpha}, \tag{2,11d}$$

$$\hat{U} = \frac{2\pi\varepsilon^2}{V}\sum_{\substack{\vec{\lambda},\lambda\leqslant\lambda_c\\ \vec{\sigma},\sigma\leqslant\lambda_c\\ \vec{\lambda}+\vec{\sigma}\neq 0}}\vec{\varepsilon}_\lambda\cdot\vec{\varepsilon}_\sigma\, q_\lambda q_\sigma\left[\frac{1}{m}\sum_{i=1}^{n}e^{i(\vec{\lambda}+\vec{\sigma})\cdot\vec{r}_i} + \frac{Z^2}{M}\sum_{\alpha=1}^{N}e^{i(\vec{\lambda}+\vec{\sigma})\cdot\vec{r}_\alpha}\right]. \tag{2,11e}$$

We transform the Hamilton function (2.10) using the unitary operator

$$\hat{S} = \exp\left(\frac{1}{\hbar}\sum_{\vec{\lambda},\lambda\leqslant\lambda_c}\sqrt{\frac{4\pi}{V\cdot\lambda^2}}\,\varrho_{-\lambda}q_\lambda\right). \tag{2,12}$$

A simple calculation gives

$$\hat{S}^{-1}\hat{H}_{\text{ext}}\hat{S} = \mathcal{H}_{\text{ext}} = \hat{H} - \frac{1}{2}\sum_{\vec{\lambda},\lambda\leqslant\lambda_c} p_\lambda p_{-\lambda} + i\sum_{\vec{\lambda},\lambda\leqslant\lambda_c}\sqrt{\frac{4\pi}{V\cdot\lambda^2}}\,\varrho_\lambda p_\lambda - \sum_{\vec{\lambda},\lambda\leqslant\lambda_c} v_\lambda\left\langle\frac{\hbar\omega_\lambda}{4}\right\rangle, \tag{2,13}$$

and the associated set of subsidiary conditions takes the form

$$(p_\lambda + i\omega_\lambda v_\lambda q_{-\lambda})\,\Phi = 0; \quad \vec{\lambda},\ \lambda\leqslant\lambda_c, \tag{2,14}$$

where

$$\Phi = \hat{S}^{-1}\Psi. \tag{2.15}$$

When we replace p_λ and q_λ by the oscillator annihilation and creation operators a_λ, a_λ^* by means of the well-known relations

$$p_\lambda = i\left(\frac{\hbar\omega_\lambda}{2}\right)^{1/2}(a_{-\lambda} + a_\lambda^*), \tag{2,16a}$$

$$q_\lambda = \left(\frac{\hbar}{2\omega_\lambda}\right)^{1/2}(a_\lambda - a_{-\lambda}^*), \tag{2,16b}$$

the hamiltonian (2,13) becomes

$$\hat{\mathcal{H}}_{\text{ext}} = \hat{H} + \frac{1}{4}\sum_{\vec{\lambda},\lambda\leqslant\lambda_c}\hbar\omega_\lambda(a_\lambda^* a_\lambda + a_\lambda a_\lambda^* + a_\lambda a_{-\lambda} + a_\lambda^* a_{-\lambda}^*) -$$

$$-\sum_{\vec{\lambda},\lambda\leqslant\lambda_c} h_\lambda\hbar\omega_\lambda\varrho_\lambda(a_{-\lambda} + a_\lambda^*) - \frac{1}{4}\sum_{\vec{\lambda},\lambda\leqslant\lambda_c} v_\lambda\,\langle\hbar\omega_\lambda\rangle; \qquad h_\lambda = \sqrt{\frac{2\pi}{V\hbar\omega_\lambda\cdot\lambda^2}}, \tag{2,17}$$

and the supplementary conditions take the form

$$[(1+v_\lambda)\,a_{-\lambda} + (1-v_\lambda)\,a_\lambda^*]\,\Phi = 0; \quad \vec{\lambda},\ \lambda\leqslant\lambda_c, \tag{2,18a}$$

or

$$(a_{-\lambda} + x_\lambda a_\lambda)\,\Phi = 0; \quad \vec{\lambda},\ \lambda\leqslant\lambda_c, \tag{2,18b}$$

with

$$x_\lambda = \frac{1-v_\lambda}{1+v_\lambda}, \quad 0 < v_\lambda \leqslant 1, \quad 0 \leqslant x_\lambda < 1. \tag{2,18c}$$

A state vector satisfying the relations (2,18a), (2,18b) may be written as

$$\Phi = \prod_{\substack{\vec{\lambda},\lambda \leqslant \lambda_c \\ \lambda_z > 0}} \Phi_\lambda \cdot \chi (\ldots \vec{r}_i \ldots; \ldots \vec{r}_\alpha \ldots), \tag{2,19a}$$

with

$$\Phi_\lambda = \sqrt{1 - x_\lambda^2}\, e^{-x_\lambda a_\lambda^* a_{-\lambda}^*}\, \Phi_0, \tag{2,19b}$$

where Φ_0 is an eigen vector of operator $a_\lambda^* a_\lambda$ with an eigen value zero, that is $a_\lambda \Phi_0 = 0$, $\Phi_0^* a_\lambda^* = 0$, $\Phi_0^* \Phi_0 = 1$. It will be shown later that the Φ_0 is an oscillator ground state vector. A product $\prod_{\substack{\vec{\lambda},\lambda \leqslant \lambda_c \\ \lambda_z > 0}} \ldots$ means a multiplication over half a sphere $\lambda \leqslant \lambda_c$, and $\chi (\ldots \vec{r}_i \ldots; \ldots \vec{r}_\alpha \ldots)$ is an eigen function of Hamilton operator (2,1) or (2,3) e.g.

$$\hat{H} \cdot \chi (\ldots \vec{r}_i \ldots; \ldots \vec{r}_\alpha \ldots) = E \chi (\ldots \vec{r}_i \ldots; \ldots \vec{r}_\alpha \ldots). \tag{2,19c}$$

It is easy to verify that

$$\Phi_\lambda^* (a_{-\lambda} + a_\lambda^*)\, \Phi_\lambda = 0, \tag{2,20a}$$

$$\Phi_\lambda^* a_\lambda^* a_\lambda \Phi_\lambda = \Phi_\lambda^* a_{-\lambda}^* a_{-\lambda} \Phi_\lambda = \frac{x_\lambda^2}{1 - x_\lambda^2}, \tag{2,20b}$$

$$\Phi_\lambda^* a_\lambda a_\lambda^* \Phi_\lambda = \Phi_\lambda^* a_{-\lambda} a_{-\lambda}^* \Phi_\lambda = \frac{1}{1 - x_\lambda^2}, \tag{2,20c}$$

$$\Phi_\lambda^* a_\lambda a_{-\lambda} \Phi_\lambda = \Phi_\lambda^* a_\lambda^* a_{-\lambda}^* \Phi_\lambda = - \frac{x_\lambda}{1 - x_\lambda^2}. \tag{2,20d}$$

Taking all the above relations into consideration we get

$$(\Phi^*, \hat{\mathcal{H}}_{\text{ext}} \Phi) = (\chi^*, \hat{H} \chi). \tag{2.21}$$

This means that the extended hamiltonian (2,13), or (2,17) is equivalent to the Schrödinger many electron energy operator having identical spectrum of energy values.

Now we see that the term $-\frac{1}{4} \sum_{\vec{\lambda},\lambda \leqslant \lambda_c} \nu_\lambda \langle \hbar \omega_\lambda \rangle$ introduced into equation (2,6) secures the identical eigen values of both hamiltonians.

We return to the relations (2,10) — (2,11e) and rewrite them in form

$$\hat{H}_{\text{ext}} = \hat{H}_{\text{part}} + \hat{H}_{s,r} + \hat{H}_{\text{coll}} + \hat{H}_{\text{inter}} + \hat{U} - \frac{1}{4} \sum_{\vec{\lambda},\lambda \leqslant \lambda_c} \frac{1 - x_\lambda}{1 + x_\lambda} \langle \hbar \omega_\lambda \rangle, \tag{2,22}$$

with

$$\hat{H}_{\text{part}} = \frac{1}{2m}\sum_{i=1}^{n}\hat{p}_i^2 + \frac{1}{2M}\sum_{\alpha=1}^{N}\hat{p}_\alpha^2, \tag{2,23a}$$

$$\hat{H}_{s,r} = \frac{2\pi}{V}\sum_{\vec{\lambda},\,\lambda>\lambda_c}\frac{\varrho_\lambda\varrho_{-\lambda} - Z(1+Z)N\varepsilon^2}{\lambda^2}, \tag{2,23b}$$

$$\hat{H}_{\text{coll}} = \frac{1}{2}\sum_{\vec{\lambda},\lambda\leqslant\lambda_c}\hbar\omega_\lambda(a_\lambda^* a_\lambda + a_\lambda a_\lambda^*) - \frac{1}{4}\sum_{\vec{\lambda},\lambda\leqslant\lambda_c}\hbar\frac{\omega_\lambda^2-\omega_p^2}{\omega_\lambda}(a_\lambda^* a_\lambda + a_\lambda a_\lambda^* -$$

$$- a_\lambda a_{-\lambda} - a_\lambda^* a_{-\lambda}^*) - \frac{2\pi}{V}Z(1+Z)N\varepsilon^2\sum_{\vec{\lambda},\lambda\leqslant\lambda_c}\frac{1}{\lambda^2}, \tag{2,23c}$$

$$\hat{H}_{\text{inter}} = \frac{\hbar\varepsilon}{m}\sum_{i=1}^{n}\sum_{\vec{\lambda},\lambda\leqslant\lambda_c} h_\lambda\cdot\lambda[\vec{\varepsilon}_\lambda\cdot(\hat{\vec{p}}_i - \hbar\vec{\lambda}/2)\,e^{i\vec{\lambda}\vec{r}_i}\,a_\lambda + a_\lambda^* e^{-i\vec{\lambda}\vec{r}_i}\vec{\varepsilon}_\lambda\cdot(\hat{\vec{p}} - \hbar\vec{\lambda}/2)] -$$

$$- \frac{\hbar Z\varepsilon}{M}\sum_{\alpha=1}^{N}\sum_{\vec{\lambda},\lambda\leqslant\lambda_c} h_\lambda\cdot\lambda[\vec{\varepsilon}_\lambda\cdot(\hat{\vec{p}}_\alpha - \hbar\vec{\lambda}/2)\,e^{i\vec{\lambda}\cdot\vec{r}_\alpha}\,a + a_\lambda^* e^{-i\vec{\lambda}\cdot\vec{r}_\alpha}\vec{\varepsilon}_\lambda\cdot(\hat{\vec{p}}_\alpha - \hbar\vec{\lambda}/2)], \tag{2,23d}$$

$$\hat{U} = \frac{\pi\hbar\varepsilon^2}{V}\sum_{\substack{\vec{\lambda},\lambda\leqslant\lambda_c\\ \vec{\sigma},\sigma\leqslant\lambda_c\\ \vec{\lambda}+\vec{\sigma}\neq 0}}\frac{\vec{\varepsilon}_\lambda\cdot\vec{\varepsilon}_\sigma}{\sqrt{\omega_\lambda\cdot\omega_\sigma}}(a_\lambda - a_{-\lambda}^*)(a_\sigma - a_{-\sigma}^*)\left[\frac{1}{m}\sum_{i=1}^{n}e^{i(\vec{\lambda}+\vec{\sigma})\cdot\vec{r}_i} +\right.$$

$$\left. + \frac{Z^2}{M}\sum_{\alpha=1}^{N}e^{i(\vec{\lambda}+\vec{\sigma})\cdot\vec{r}_\alpha}\right]. \tag{2,23e}$$

The subsidiary conditions will be

$$(a_{-\lambda} + x_\lambda a_\lambda^* + f_{-\lambda})\,\Psi = 0; \qquad \vec{\lambda},\ \lambda\leqslant\lambda_c, \tag{2,24}$$

where

$$f_\lambda = (1+x_\lambda)\,h_\lambda\varrho_\lambda, \qquad h_\lambda = \sqrt{\frac{2\pi}{V\hbar\omega_\lambda\cdot\lambda^2}}.$$

The normalized state vector satisfying (2,24) becomes

$$\Psi = \prod_{\substack{\vec{\lambda},\lambda\leqslant\lambda_c\\ \lambda_z>0}}\Psi_\lambda\cdot\chi(\ldots\vec{r}_i\ldots;\ldots\vec{r}_\alpha\ldots), \quad (\chi^*,\chi) = 1, \tag{2,25a}$$

with

$$\Psi_\lambda = \sqrt{1-x_\lambda^2}\;e^{-\frac{f_\lambda f_\lambda}{1+x_\lambda} - f_{-\lambda}a_{-\lambda}^* - f_\lambda a_\lambda^* - x_\lambda a_\lambda^* a_{-\lambda}^*}\Phi_0. \tag{2,25b}$$

We compute now the expectation values of hamiltonian (2.22). After simple but rather lengthy calculations (see Appendix) we obtain

$$(\Psi^*, \hat{H}_{\text{part}}\,\Psi) = \frac{1}{2m}\sum_{i=1}^{n}\langle \hat{p}_i^2\rangle + \frac{1}{2M}\sum_{\alpha=1}^{N}\langle \hat{p}_\alpha^2\rangle + \frac{1}{4}\sum_{\vec{\lambda},\lambda\leqslant\lambda_c}\frac{1+x_\lambda}{1-x_\lambda}\left\langle\frac{\hbar\omega_p^2}{\omega_\lambda}\right\rangle, \tag{2,26a}$$

$$(\Psi^*, \hat{H}_{s,r}\,\Psi) = \frac{2\pi}{V}\sum_{\vec{\lambda},\lambda>\lambda_c}\frac{\langle\varrho_\lambda\varrho_{-\lambda}\rangle - Z(1+Z)N\varepsilon^2}{\lambda^2}. \tag{2,26b}$$

$$(\Psi^*, \hat{H}_{\text{coll}}\,\Psi) = \frac{2\pi}{V}\sum_{\vec{\lambda},\lambda\leqslant\lambda_c}\frac{\langle\varrho_\lambda\varrho_{-\lambda}\rangle - Z(1+Z)N\varepsilon^2}{\lambda^2} +$$

$$+\frac{1}{2}\sum_{\vec{\lambda},\lambda\leqslant\lambda_c}\frac{1+x_\lambda^2}{1-x_\lambda^2}\langle\hbar\omega_\lambda\rangle - \frac{1}{4}\sum_{\vec{\lambda},\lambda\leqslant\lambda_c}\frac{1+x_\lambda}{1-x_\lambda}\left\langle\hbar\,\frac{\omega_\lambda^2-\omega_p^2}{\omega_\lambda}\right\rangle, \tag{2,26c}$$

$$(\Psi^*, \hat{H}_{\text{inter}}\,\Psi) = -\frac{1}{2}\sum_{\vec{\lambda},\lambda\leqslant\lambda_c}\frac{1+x_\lambda}{1-x_\lambda}\left\langle\frac{\hbar\omega_p^2}{\omega_\lambda}\right\rangle \tag{2,26d}$$

$$(\Psi^*, \hat{U}\,\Psi) = 0. \tag{2,26e}$$

The expectation values $\langle\ldots\rangle$ are computed for eigen function $\chi(\ldots\vec{r}_i\ldots;\ldots\vec{r}_\alpha\ldots)$.

Summing all the terms (2,26a)—(2,26e) we get for average values of energy operator (2,22)

$$(\Psi^*, \hat{H}_{\text{ext}}\,\Psi) = (\chi^*, \hat{H}\,\chi). \tag{2,27}$$

We see that the expressions (2,26a), (2,26c) and (2,26d) diverge to infinity with $x_\lambda \to 1$, $v_\lambda \to 0$, although the average value (2,27) remains finite for all x_λ. Moreover the term H_{inter} treated in Bohm — Pines theory as a perturbation member appears as a divergent quantity. The situation can be improved by adding to (2,26d) the expression $+\frac{1}{2}\sum_{\vec{\lambda},\lambda\leqslant\lambda_c}\frac{1+x_\lambda}{1-x_\lambda}\left\langle\frac{\hbar\omega_p^2}{\omega_\lambda}\right\rangle$ (and subtracting simultaneously the same term from whole hamiltonian). Then the newly defined $\hat{H}_{inter}$ will be, on the average, always zero.

After having made the above remarks we conclude that the Bohm — Pines theory is proved to be correct for any degree of accuracy but can not be true in the limit, that is with $x_\lambda = 1$, $v_\lambda = 0$.

In all above calculations we have treated ω_λ as an operator quantity, which depends on electron and ion momentums, as it will be proved in the snbsequent

paper. With respect to the operator character of ω_λ in the expectation values appear the expressions $\left\langle \frac{1}{\omega_\lambda} \right\rangle$ and $\langle \omega_\lambda \rangle$.

If we assume that the values of ϱ_λ are quite small ($\varrho_0 = 0$), and if we suppose $x_\lambda = 0$ we can treat Ψ_λ in first approximation as a vector equal to Φ_0 and thus write Ψ as a product

$$\Psi = \Phi_0 \cdot \chi (\ldots \vec{r}_i \ldots; \ldots \vec{r}_\alpha \ldots),$$

where Φ_0 is an oscillator ground state function (see Kanazawa 1957b).

3. *Oscillator state vectors*

We shall now attempt to derive the correct oscillator state vectors. We take the appropriate hamiltonian in the form

$$\hat{H}_{osc} = -\frac{1}{2} \sum_{\vec{\lambda}, \lambda \leqslant \lambda_c} (p_\lambda p_{-\lambda} + \omega_\lambda^2 q_\lambda q_{-\lambda}) = - \sum_{\substack{\vec{\lambda}, \lambda \leqslant \lambda_c \\ \lambda_z > 0}} (p_\lambda p_{-\lambda} + \omega_\lambda^2 q_\lambda q_{-\lambda}), \quad (3,1)$$

$$\hat{H}_{osc} \Psi_{osc} = E \Psi_{osc}. \quad (3,2)$$

Since $\vec{A}(\vec{r})$, equation (2,4) and $\vec{E}(\vec{r})$ equation (2,5) must be real we obtain

$$q_\lambda^* = -q_{-\lambda}, \quad (3,3a)$$

$$p_\lambda^* = -p_{-\lambda}. \quad (3,3b)$$

Taking for q_λ the expression

$$q_\lambda = q_\lambda^r + i q_\lambda^i, \quad (3,4)$$

where q_λ^r and q_λ^i are the real and imaginary part, respectively of q_λ, we have from (3,3a)

$$q_\lambda^r = -q_{-\lambda}^r, \qquad q_\lambda^i = q_{-\lambda}^i, \quad (3,5)$$

or

$$q_\lambda = q_\lambda^r + i q_\lambda^i, \qquad q_{-\lambda} = -q_\lambda^r + i q_\lambda^i, \quad (3,6)$$

and vice versa

$$q_\lambda^r = \frac{1}{2} (q_\lambda - q_{-\lambda}), \qquad q_\lambda^i = \frac{1}{2i} (q_\lambda + q_{-\lambda}). \quad (3,7)$$

Hence

$$p_\lambda = \frac{\hbar}{i} \frac{\partial}{\partial q_\lambda} = \frac{\hbar}{2i} \left(\frac{\partial}{\partial q_\lambda^r} - i \frac{\partial}{\partial q_\lambda^i} \right), \quad p_{-\lambda} = \frac{\hbar}{i} \frac{\partial}{\partial q_{-\lambda}} = -\frac{\hbar}{2i} \left(\frac{\partial}{\partial q_\lambda^r} + i \frac{\partial}{\partial q_\lambda^i} \right). \quad (3,8)$$

Using the relations (3,6), and (3,8) we rewrite the hamiltonian (3,1) in the form

$$\hat{H}_{osc} = \sum_{\vec{\lambda}, \lambda \leqslant \lambda_c} \left[-\frac{\hbar^2}{4} \frac{\partial^2}{\partial (q_\lambda^r)^2} + \omega_\lambda^2 (q_\lambda^r)^2 \right] + \sum_{\vec{\lambda}, \lambda \leqslant \lambda_c} \left[-\frac{\hbar^2}{4} \frac{\partial^2}{\partial (q_\lambda^i)^2} + \omega_\lambda^2 (q_\lambda^i)^2 \right]. \quad (3,9)$$

The appropriate eigen functions of (3,9) are

$$\Psi_{osc} = \prod_{\substack{\vec{\lambda},\lambda \leqslant \lambda_c \\ \lambda_x > 0}} (\Psi_\lambda^{osc})_{n_\lambda^1,\, n_\lambda^2}\,; \qquad (\Psi_\lambda^{osc})_{n_\lambda^1,\, n_\lambda^2} =$$

$$= e^{\frac{\omega_\lambda}{\hbar} q_\lambda q_{-\lambda}} H_{n_\lambda^1}\left(\sqrt{\frac{2\omega_\lambda}{\hbar}}\, q_\lambda^r\right) \cdot H_{n_\lambda^2}\left(\sqrt{\frac{2\omega_\lambda}{\hbar}}\, q_\lambda^i\right). \tag{3,10}$$

Here $H_{n_\lambda^1}\left(\sqrt{\frac{2\omega_\lambda}{\hbar}}\, q_\lambda^r\right)$, $H_{n_\lambda^2}\left(\sqrt{\frac{2\omega_\lambda}{\hbar}}\, q_\lambda^i\right)$ stand for Hermite polynomials. The energy spectrum will be given by

$$E = \sum_{\substack{\vec{\lambda},\lambda \leqslant \lambda_c \\ \lambda_x > 0}} E_\lambda \qquad E_\lambda = \hbar\omega_\lambda\,(n_\lambda^1 + n_\lambda^2 + 1). \tag{3,11}$$

We get for the ground state function in the "q" representation

$$\Psi_\lambda^{osc} = c_\lambda \cdot e^{\frac{\omega_\lambda}{\hbar} q_\lambda q_{-\lambda}}, \qquad c_\lambda = \text{const.} \tag{3,12}$$

Now we replace the field quantities q_λ and p_λ by a_λ, a_λ^* according to (2,16a), (2,16b). We obtain

$$\hat{H}_{osc} = \sum_{\substack{\vec{\lambda},\lambda \leqslant \lambda_c \\ \lambda_x > 0}} \hbar\omega_\lambda\,(a_\lambda^* a_\lambda + a_{-\lambda}^* a_{-\lambda} + 1), \tag{3,13}$$

$$\Psi_\lambda^{osc} = e^{\frac{1}{2}\cdot(a_\lambda - a_{-\lambda}^*)(a_{-\lambda} - a_\lambda^*)} \cdot \varphi_\lambda, \tag{3,14}$$

where φ_λ is a new vector satisfying the condition

$$p_\lambda \varphi_\lambda = i\left(\frac{\hbar\omega_\lambda}{2}\right)^{\frac{1}{2}} (a_{-\lambda} + a_\lambda^*)\,\varphi_\lambda = 0\,. \tag{3,15}$$

It can easily be seen that

$$\varphi_\lambda = 2 \cdot e^{-a_\lambda^* a_{-\lambda}^*} \Phi_0. \tag{3,16}$$

Here Φ_0 is a quantity well known from previous considerations.

We shall prove that $\Psi_\lambda^{osc} = \Phi_0$. Since Ψ_λ^{osc} is really a ground state vector (as one may readily verify) we ascertain thereby that Φ_0 represents the same quantity.

In order to avoid the divergences which appear when operating with the expression (3,16) we introduce auxiliary functions defined by

$$\varphi_\lambda(x_\lambda) = 2 \cdot e^{-x_\lambda a_\lambda^* a_{-\lambda}^*} \Phi_0, \tag{3,17}$$

with

$$x_\lambda = 1 - \varepsilon_\lambda, \qquad 0 < \varepsilon_\lambda \ll 1.$$

These functions approximate the φ_λ as nearly as desired. We shall use also the following auxiliary relations

$$a_\lambda^l (a_\lambda^*)^s = \begin{cases} \sum_{r=0}^{s} \binom{l}{r} \binom{s}{r} r! \, (a_\lambda^*)^{s-r} a_\lambda^{l-r} & \text{for } l \leqslant s, \\ \sum_{r=0}^{s} \binom{l}{r} \binom{s}{r} r! \, (a_\lambda^*)^{s-r} a_\lambda^{l-r} & \text{for } r \geqslant s \end{cases} \tag{3,18}$$

and

$$(a_{-\lambda} - a_\lambda^*)^s \, e^{-x_\lambda a_\lambda^* a_{-\lambda}^*} = e^{-x_\lambda a_\lambda^* a_{-\lambda}^*} [a_{-\lambda} - (1 + x_\lambda) a_\lambda^*], \tag{3,19a}$$

$$(a_\lambda - a_{-\lambda}^*)^s \, e^{-x_\lambda a_\lambda^* a_{-\lambda}^*} = e^{-x_\lambda a_\lambda^* a_{-\lambda}^*} [a_\lambda - (1 + x_\lambda) a_{-\lambda}^*]^s, \tag{3,19b}$$

$$\frac{1}{(1+x)^{l+1}} = \sum_{s=0}^{+\infty} (-1)^s \binom{s+l}{s} x^s, \qquad |x| < 1. \tag{3,19c}$$

Using all the above relations we get

$$\Psi_\lambda^{osc}(x_\lambda) = 2 \cdot e^{\frac{1}{2}(a_\lambda - a_{-\lambda}^*)(a_{-\lambda} - a_\lambda^*) - x_\lambda a_\lambda^* a_{-\lambda}^*} \Phi_0 =$$

$$= 2 \cdot \sum_{s=0}^{+\infty} \frac{1}{2^s s!} (a_\lambda - a_{-\lambda}^*)^s (a_{-\lambda} - a_\lambda^*)^s \cdot e^{-x_\lambda a_\lambda^* a_{-\lambda}^*} \Phi_0 =$$

$$= 2 \cdot e^{-x_\lambda a_\lambda^* a_{-\lambda}^*} \sum_{s=0}^{+\infty} \frac{1}{2^s s!} [a_\lambda - (1 + x_\lambda) a_{-\lambda}^*]^s \cdot [a_{-\lambda} - (1 + x_\lambda) a_\lambda^*]^s \Phi_0 =$$

$$= 2 \cdot e^{-x_\lambda a_\lambda^* a_{-\lambda}^*} \sum_{s=0}^{+\infty} \frac{1}{2^s s!} (1 + x_\lambda)^s [(1 + x_\lambda) a_{-\lambda}^* - a_\lambda]^s (a_\lambda^*)^s \Phi_0 =$$

$$= 2 \cdot e^{-x_\lambda a_\lambda^* a_{-\lambda}^*} \sum_{s=0}^{+\infty} \frac{(1 + x_\lambda)^s}{2^s \cdot s!} \sum_{l=0}^{s} (-1) \binom{s}{l} [(1 + x_\lambda) a_{-\lambda}^*]^{s-l} a_\lambda^l (a_\lambda^*)^s \Phi_0 =$$

$$= 2 \cdot e^{-x_\lambda a_\lambda^* a_{-\lambda}^*} \sum_{s=0}^{+\infty} \frac{(1 + x_\lambda)^s}{2^s \cdot s!} \sum_{l=0}^{s} (-1)^l \binom{s}{l} \binom{s}{l} l! \, [(1 + x_\lambda) a_\lambda^* a_{-\lambda}^*]^{s-l} \Phi_0 =$$

$$= 2 \cdot e^{-x_\lambda a_\lambda^* a_{-\lambda}^*} \sum_{l=0}^{+\infty} (-1)^l \frac{(1 + x_\lambda)^l}{l!} (a_\lambda^* a_{-\lambda}^*)^l \sum_{s=l}^{+\infty} (-1)^s \binom{s}{l} \left(\frac{1 + x_\lambda}{2}\right)^s \Phi_0 =$$

$$= 2 \cdot e^{-x_\lambda a_\lambda^* a_{-\lambda}^*} \sum_{l=0}^{+\infty} \frac{(1+x_\lambda)^{2l}}{2^l \cdot l!} (a_\lambda^* a_{-\lambda}^*)^l \sum_{s=0}^{+\infty} (-1)^s \binom{s+l}{s} \left(\frac{1 + x_\lambda}{2}\right)^s \Phi_0 =$$

$$= \frac{2}{1+\frac{1+x_\lambda}{2}} e^{-x_\lambda a_\lambda^* a_{-\lambda}^*} \sum_{l=0}^{+\infty} \frac{(1+x_\lambda)^{2l} (a_\lambda^* a_{-\lambda}^*)^l}{2^l \cdot l! \left(1+\frac{1+x_\lambda}{2}\right)^l} \Phi_0 =$$

$$= \frac{2}{1+\frac{1+x_\lambda}{2}} \exp\left\{\left[\frac{(1+x_\lambda)^2}{2\left(1+\frac{1+x_\lambda}{2}\right)} - x_\lambda\right] a_\lambda^* a_{-\lambda}^*\right\} \Phi_0 =$$

$$= \frac{4}{3+x_\lambda} \exp\left[\frac{1-x_\lambda}{3+x_\lambda} a_\lambda^* a_{-\lambda}^*\right] \Phi_0 . \tag{3,20}$$

Hence, passing over to the limit $x_\lambda \to 1$ we obtain

$$\lim_{x_\lambda \to 1} \Psi_\lambda^{osc}(x_\lambda) = \Psi_\lambda^{osc} = \Phi_0 . \tag{3.21}$$

We get the same expression for the ground state vector from the following considerations: Let us assume that this state can be written as

$$\Psi_\lambda^{osc} = \sum_{m,n=0}^{+\infty} c_\lambda (m, n) (a_\lambda^*)^m (a_{-\lambda}^*)^n \Phi_0 . \tag{3.22}$$

Then

$$\hat{H}_\lambda^{osc} \Psi_\lambda^{osc} = \hbar\omega (a_\lambda^* a_\gamma + a_{-\lambda}^* a_{-\lambda} + 1) \Psi_\lambda^{osc} =$$
$$\hbar\omega_\lambda \sum_{m,n=0}^{+\infty} c_\lambda (m, n) (m + n + 1) (a_\lambda^*)^m (a_{-\lambda}^*)^n \Phi_0 . \tag{3,23a}$$

The ground state energy is, according to (3,11) equal to $\hbar\omega_\lambda$. Therefore

$$E_\lambda \Psi_\lambda^{osc} = \hbar\omega_\lambda \sum_{m,n=0}^{+\infty} c_\lambda (m, n) (a_\lambda^*)^m (a_{-\lambda}^*)^n \Phi_0 . \tag{3.23b}$$

Since $\hat{H}_\lambda^{osc} \Psi_\lambda^{osc} = E_\lambda \Psi_\lambda^{osc}$ we obtain

$$\sum_{m,n=0}^{+\infty} c_\lambda (m, n) (m + n + 1) (a_\lambda^*)^m (a_{-\lambda}^*)^n \Phi_0 = \sum_{m,n=0}^{+\infty} c_\lambda (m, n) (a_\lambda^*)^m (a_{-\lambda}^*)^n \Phi_0 . \tag{3,23c}$$

This condition is satisfied if $m = n = 0$, which gives

$$\Psi_\lambda^{osc} = c\ (0, 0)\ \Phi_0 . \tag{3,23d}$$

It is sufficient to choose $c_\lambda (0,0) = 1$ and we have $\Psi_\lambda^{osc} = \Phi_0$.

Returning to the analysis made in sections 1 and 2 we consider the case studed by Kanazawa (1957b). This case is equivalent to assuming $\nu_\lambda = 1$, $x_\lambda = 0$. We obtain the corresponding subsidiary conditions from (2,18b) and (2,19b)

$$a_{-\lambda} \Phi = 0; \quad \vec{\lambda}, \lambda \leqslant \lambda_c, \quad \Phi = \Phi_\lambda = \Phi_0 , \tag{3.24}$$

or from (2,24) and (2,25b)

$$(a_{-\lambda} + f_{-\lambda})\,\Psi = 0; \quad \vec{\lambda},\ \lambda \leqslant \lambda_c, \quad \Psi_\lambda = e^{-h_\lambda^2 \varrho_\lambda \varrho_{-\lambda} - h_\lambda \varrho_{-\lambda} a^*_{-\lambda} - h_\lambda \varrho_\lambda a^*_\lambda}\,\Phi_0. \quad (3,25)$$

It is worth while to point out that the excited state with l plasmons having a momentum $+\hbar\vec{\lambda}$ and s plasmons having momentum $-\hbar\vec{\lambda}$ is of the form

$$(\Psi^{osc}_{\lambda})_{l,s} = \frac{1}{\sqrt{l!\,s!}}\,(a^*_\lambda)^l\,(a^*_{-\lambda})^s\,\Phi_0\,. \quad (3,26)$$

I am indebted to Professor S. Szczeniowski for helpful suggestions during the preparation of this article as well as for reading and commenting upon the text.

Appendix

We shall prove, first of all, that (2,25b) is true. We have from (2,12) and (2,15)

$$\Psi = \hat{S}\,\Phi. \quad (A.1)$$

Since

$$\hat{S} = \exp\left(\frac{1}{\hbar}\sum_{\vec{\lambda},\lambda\leqslant\lambda_c}\sqrt{\frac{4\pi}{V\lambda^2}}\,\varrho_{-\lambda}\,q_\lambda\right) = \exp\left[\sum_{\vec{\lambda},\lambda\leqslant\lambda_c} h_\lambda \varrho_{-\lambda}\,(a_\lambda - a^*_{-\lambda})\right], \quad (A,2)$$

we get for Ψ the expression

$$\Psi = \prod_{\substack{\vec{\lambda},\,\lambda\leqslant\lambda_c \\ \lambda_z>0}} \Psi_\lambda \cdot \chi(\ldots \vec{r}_i \ldots; \ldots \vec{r}_\alpha \ldots), \quad (A,3a)$$

$$\Psi_\lambda = \sqrt{1-x_\lambda^2}\exp\left(h_\lambda \varrho_{-\lambda} a_\lambda - h_\lambda \varrho_{-\lambda} a^*_{-\lambda} + h_\lambda \varrho_\lambda a_{-\lambda} - h_\lambda \varrho_\lambda a^*_\lambda - x_\lambda a^*_\lambda a^*_{-\lambda}\right)\cdot\Phi_0. \quad (A,3b)$$

By (3,18) we obtain

$$a_\lambda e^{l_\lambda a^*_\lambda} = \sum_{p=0}^{+\infty}\frac{l_\lambda^p}{p!}\,a_\lambda (a^*_\lambda)^p = \sum_{p=0}^{+\infty}\frac{l_\lambda^p}{p!}\,[(a^*_\lambda)^p a_\lambda + p\cdot(a^*_\lambda)^{p-1}], \quad (A,4a)$$

$$\exp(g_\lambda a_\lambda + l_\lambda a^*_\lambda) = \exp[l_\lambda a^*_\lambda + g_\lambda (a_\lambda + l_\lambda)], \quad (A,4b)$$

where g_λ and l_λ are arbitrary functions.

Further

$$a_\lambda e^{-x_\lambda a^*_\lambda a^*_{-\lambda}} = \sum_{p=0}^{+\infty}\frac{(-1)^p x_\lambda^p}{p!}\,(a^*_{-\lambda})^p a_\lambda (a^*_\lambda)^p =$$

$$= \sum_{p=0}^{+\infty}\frac{(-1)^p x_\lambda^p}{p!}\,(a^*_{-\lambda})^p\,[(a^*_\lambda)^p a_\lambda + p\,(a^*_\lambda)^{p-1}] = e^{-x_\lambda a^*_\lambda a^*_{-\lambda}}(a_\lambda - x_\lambda a^*_{-\lambda}), \quad (A,5a)$$

hence

$$\exp(g_\lambda a_\lambda - x_\lambda a_\lambda^* a_{-\lambda}^*) = \exp[-x_\lambda a_\lambda^* a_{-\lambda}^* + g_\lambda (a_\lambda - x_\lambda a_{-\lambda}^*)]. \tag{A,5b}$$

Using the already proved relations (A,4b) and (A,5b) we get

$$\exp[h_\lambda \varrho_{-\lambda}(a_\lambda - a_{-\lambda}^*) + h_\lambda \varrho_\lambda (a_{-\lambda} - a_\lambda^*) - x_\lambda a_\lambda^* a_{-\lambda}^*] \cdot \Phi_0 =$$

$$= \exp[h_\lambda \varrho_{-\lambda}(a_\lambda - a_{-\lambda}^*) - h_\lambda \varrho_\lambda a_\lambda^* - x_\lambda a_\lambda^* a_{-\lambda}^* + h_\lambda \varrho_\lambda (a_{-\lambda} - x_\lambda a_\lambda^*)]\, \Phi_0 =$$

$$= \exp[h_\lambda \varrho_{-\lambda}(a_\lambda - a_{-\lambda}^*) - (1 + x_\lambda) h_\lambda \varrho_\lambda a_\lambda^* - x_\lambda a_\lambda^* a_{-\lambda}^*]\, \Phi_0 =$$

$$= \exp[-h_\lambda \varrho_{-\lambda} a_{-\lambda}^* + h_\lambda \varrho_{-\lambda} a_\lambda - (1 + x_\lambda) h_\lambda \varrho_\lambda a_\lambda^* - x_\lambda a_\lambda^* a_{-\lambda}]\, \Phi_0 = \tag{A,6}$$

$$= \exp\{-h_\lambda \varrho_{-\lambda} a_{-\lambda}^* - (1 + x_\lambda) h_\lambda \varrho_\lambda a_\lambda^* + h_\lambda \varrho_{-\lambda}[a_\lambda - (1 + x_\lambda) h_\lambda \varrho_\lambda] -$$

$$- x_\lambda a_\lambda^* a_{-\lambda}^*\}\, \Phi_0 = \exp[-(1 + x_\lambda) h_\lambda^2 \varrho_\lambda \varrho_{-\lambda}] \cdot \exp[-h_\lambda \varrho_{-\lambda} a_{-\lambda}^* -$$

$$- (1 + x_\lambda) h_\lambda \varrho_\lambda a_\lambda^* + h_\lambda \varrho_{-\lambda} a_\lambda - x_\lambda a_\lambda^* a_{-\lambda}^*]\, \Phi_0 =$$

$$= \exp[-(1 + x_\lambda) h_\lambda^2 \varrho_\lambda \varrho_{-\lambda}] \cdot \exp[-h_\lambda \varrho_{-\lambda} a_{-\lambda}^* - (1 + x_\lambda) h_\lambda \varrho_\lambda a_\lambda^* - x_\lambda a_\lambda^* a_{-\lambda}^* +$$

$$+ h_\lambda \varrho_{-\lambda}(a_\lambda - x_\lambda a_{-\lambda}^*)]\, \Phi_0 = \exp[-(1 + x_\lambda) h_\lambda^2 \varrho_\lambda \varrho_{-\lambda}] \times$$

$$\times \exp[-(1 + x_\lambda) h_\lambda \varrho_{-\lambda} a_{-\lambda}^* - (1 + x_\lambda) h_\lambda \varrho_\lambda a_\lambda^* - x_\lambda a_\lambda^* a_{-\lambda}^*]\, \Phi_0$$

Finally we obtain

$$\Psi_\lambda = \sqrt{1 - x_\lambda^2} \exp\left[-\frac{f_\lambda f_{-\lambda}}{1 + x_\lambda}\right] \cdot \exp[-f_{-\lambda} a_{-\lambda}^* - f_\lambda a_\lambda^* -$$

$$- x_\lambda a_\lambda^* a_{-\lambda}^*]\, \Phi_0; \quad f_\lambda = (1 + x_\lambda) h_\lambda \varrho_\lambda. \tag{A,7}$$

In order to simplify all subsequent calculations we write the $\hat{S}$ in the form

$$\hat{S} = \prod_{\substack{\vec{\lambda},\, \lambda \leqslant \lambda_c \\ \lambda_z > 0}} \hat{S}_\lambda \tag{A,8}$$

As a consequence we get

$$\hat{S}_\lambda = \exp[h_\lambda \varrho_{-\lambda}(a_\lambda - a_{-\lambda}^*) + h_\lambda \varrho_\lambda (a_{-\lambda} - a_\lambda^*)],$$

$$\hat{S}_\lambda^{-1} = \exp[h_\lambda \varrho_\lambda (a_\lambda^* - a_{-\lambda}) + h_\lambda \varrho_{-\lambda}(a_{-\lambda}^* - a_\lambda)]. \tag{A,9}$$

We now compute the expression $\hat{S}_\lambda^{-1} a_\lambda \hat{S}_\lambda$. We have

$$\hat{S}_\lambda^{-1} a_\lambda \hat{S}_\lambda = \exp[-h_\lambda \varrho_\lambda (a_{-\lambda} - a_\lambda^*) - h_\lambda \varrho_{-\lambda}(a_\lambda - a_{-\lambda}^*)] \cdot a_\lambda \times$$

$$\times \exp[h_\lambda \varrho_{-\lambda}(a_\lambda - a_{-\lambda}^*) + h_\lambda \varrho_\lambda (a_{-\lambda} - a_\lambda^*)]. \tag{A,10a}$$

We know from (A,4a) that

$$a_\lambda \exp(-h_\lambda \varrho_\lambda a_\lambda^*) = \exp(-h_\lambda \varrho_\lambda a_\lambda^*) \cdot (a_\lambda - h_\lambda \varrho_\lambda), \tag{A,10b}$$

hence

$$\hat{S}_\lambda^{-1} a_\lambda \hat{S}_\lambda = (a_\lambda - h_\lambda \varrho_\lambda), \tag{A,10c}$$

and changing $\vec{\lambda}$ to $-\vec{\lambda}$ we obtain

$$\hat{S}_\lambda^{-1} a_{-\lambda} \hat{S}_\lambda = (a_{-\lambda} - h_\lambda \varrho_{-\lambda}). \tag{A,11}$$

Quite similarly we have

$$\hat{S}_\lambda^{-1} a_\lambda^* \hat{S}_\lambda = \exp\left[- h_\lambda \varrho_\lambda (a_{-\lambda} - a_\lambda^*) - h_\lambda \varrho_{-\lambda} (a_\lambda - a_{-\lambda}^*)\right] \cdot a_\lambda^* \times$$
$$\times \exp[h_\lambda \varrho_{-\lambda}(a_\lambda - a_{-\lambda}^*) + h_\lambda \varrho_\lambda (a_{-\lambda} - a_\lambda)], \tag{A,12a}$$

which together with

$$a_\lambda \exp(h_\lambda \varrho_{-\lambda} a_\lambda) = \sum_{s=0}^{+\infty} \frac{h_\lambda^s \varrho_{-\lambda}^s}{s!} (a_\lambda^*) a_\lambda^s = \sum_{s=0}^{+\infty} \frac{h_\lambda^s \varrho_{-\lambda}^s}{s!} [a_\lambda^s a_\lambda^* - s a_\lambda^{s-1}] =$$

$$= \exp(h_\lambda \varrho_{-\lambda} a_\lambda)(a_\lambda^* - h_\lambda \varrho_{-\lambda}), \tag{A,12b}$$

gives

$$\hat{S}_\lambda^{-1} a_\lambda^* \hat{S}_\lambda = (a_\lambda^* - h_\lambda \varrho_{-\lambda}). \tag{A,12c}$$

Making use of equations (A,10c) and (A,12c) we get finally

$$\Psi_\lambda^* a_\lambda a_\lambda^* \Psi_\lambda = (1 - x_\lambda^2) \Phi_0^* \exp(-x_\lambda a_\lambda a_{-\lambda}) \hat{S}_\lambda^{-1} a_\lambda \hat{S}_\lambda \cdot \hat{S}_\lambda^{-1} a_\lambda^* \hat{S}_\lambda \exp(-x_\lambda a_\lambda^* a_{-\lambda}^*) \Phi_0 =$$
$$= (1 - x_\lambda^2) \Phi_0^* \exp(-x_\lambda a_\lambda a_{-\lambda})(a_\lambda - h_\lambda \varrho_\lambda)(a_\lambda^* - h_\lambda \varrho_{-\lambda}) \exp(- x_\lambda a_\lambda^* a_{-\lambda}^*) \Phi_0 =$$
$$= (1 - x_\lambda^2) \Phi_0^* \exp(- x_\lambda a_\lambda a_{-\lambda})(a_\lambda a_\lambda^* - h_\lambda \varrho_{-\lambda} a_\lambda - h_\lambda \varrho_\lambda a_\lambda^* + \tag{A,13}$$
$$+ h_\lambda^2 \varrho_\lambda \varrho_{-\lambda}) \exp(- x_\lambda a_\lambda^* a_{-\lambda}^*) \Phi_0.$$

On the other hand, by (3,18) and (3,19c) we have

$$\Psi_\lambda a_\lambda a_\lambda^* \Psi_\lambda = (1 - x_\lambda^2) \sum_{s=0}^{+\infty} \sum_{p=0}^{+\infty} \frac{(-1)^{s+p} x_\lambda^{s+p}}{s!\, p!} \Phi_0^* a_\lambda^{s+1} (a_\lambda^*)^{p+1} a_{-\lambda}^s (a_{-\lambda}^*)^p \Phi_0 -$$

$$- (1 - x_\lambda^2) \sum_{s=0}^{+\infty} \sum_{p=0}^{+\infty} \frac{(-1)^{s+p} x_\lambda^{s+p}}{s!\, p!} h_\lambda \varrho_{-\lambda} \Phi_0^* a_\lambda^{s+1} (a_\lambda^*)^p a_{-\lambda}^s (a_{-\lambda}^*)^p \Phi_0 -$$

$$- (1 - x_\lambda^2) \sum_{s=0}^{+\infty} \sum_{p=0}^{+\infty} \frac{(-1)^{s+p} x_\lambda^{s+p}}{s!\, p!} h_\lambda \varrho_\lambda \Phi_0^* a_\lambda^s (a_\lambda^*)^{p+1} a_{-\lambda}^s (a_{-\lambda}^*)^p \Phi_0 +$$

$$+ (1 - x_\lambda^2) \sum_{s=0}^{+\infty} \sum_{p=0}^{+\infty} \frac{(-1)^{s+p} x_\lambda^{s+p}}{s!\, p!} h_\lambda^2 \varrho_\lambda \varrho_{-\lambda} \Phi_0^* a_\lambda^s (a_\lambda^*)^p (a_{-\lambda})^s (a_{-\lambda}^*)^p \Phi_0 =$$

$$= (1 - x_\lambda^2) \sum_{s=0}^{+\infty} \sum_{p=0}^{+\infty} \frac{(-1)^{s+p} x_\lambda^{s+p}}{s!\, p!} (s+1)!\, p!\, \delta_{s,p} + \tag{A,14}$$

$$+ (1 - x_\lambda^2) \sum_{s=0}^{+\infty} \sum_{p=0}^{+\infty} \frac{(-1)^{s+p} x_\lambda^{s+p}}{s!\, p!} h_\lambda^2 \varrho_\lambda \varrho_{-\lambda} s!\, p!\, \delta_{s,p} = (1 - x_\lambda^2) \sum_{s=0}^{+\infty} (s+1) x_\lambda^{2s} +$$

$$+ (1 - x_\lambda^2) h_\lambda^2 \varrho_\lambda \varrho_{-\lambda} \sum_{s=0}^{+\infty} x_\lambda^{2s} = (1 - x_\lambda^2) \left[\frac{1}{(1 - x_\lambda^2)^2} + \frac{h_\lambda^2 \varrho_\lambda \varrho_{-\lambda}}{(1 - x_\lambda^2)} \right]$$

$$= \frac{1}{1 - x_\lambda^2} + h_\lambda^2 \varrho_\lambda \varrho_{-\lambda} = \frac{1}{1 - x_\lambda^2} + \frac{f_\lambda f_{-\lambda}}{(1 + x_\lambda)^2}.$$

In the same way we obtain

$$\Psi_\lambda^* a_\lambda^* a_\lambda \Psi_\lambda = \frac{1}{1 - x_\lambda^2} + \frac{f_\lambda f_{-\lambda}}{(1 + x_\lambda)^2} - 1, \tag{A.15a}$$

$$\Psi_\lambda^* a_\lambda^* a_{-\lambda}^* \Psi_\lambda = \Psi_\lambda^* a_\lambda a_{-\lambda} \Psi_\lambda = \frac{f_\lambda f_{-\lambda}}{(1 + x_\lambda)^2} - \frac{x_\lambda}{1 - x_\lambda^2}, \tag{A,15b}$$

$$\Psi_\lambda^* a_\lambda^* a_\lambda^* \Psi_\lambda = \frac{f_{-\lambda}^2}{(1 + x_\lambda)^2}, \qquad \Psi_\lambda^* a_\lambda a_\lambda \Psi_\lambda = \frac{f_\lambda^2}{(1 + x_\lambda)^2}, \tag{A,15c}$$

$$\Psi_\lambda^* a_\lambda a_{-\lambda}^* \Psi_\lambda = \frac{f_\lambda^2}{(1 + x_\lambda)^2}, \qquad \Psi_\lambda^* a_{-\lambda} a_\lambda^* \Psi_\lambda = \frac{f_{-\lambda}^2}{(1 + x_\lambda)^2}. \tag{A,15d}$$

Recalling that

$$(\hat{\vec{p}}_i \varrho_\lambda) = - \varepsilon \sum_{j=i}^{n} (\hat{\vec{p}}_i e^{-i \vec{\lambda} \cdot \vec{r}_i}) = \varepsilon \hbar \vec{\lambda} e^{-i \vec{\lambda} \cdot \vec{r}_i}, \qquad (\hat{\vec{p}}_\alpha \varrho_\lambda) = - Z \varepsilon \hbar \vec{\lambda} e^{-i \vec{\lambda} \cdot \vec{r}_\alpha}, \tag{A,16a}$$

$$(\hat{p}_i^2 \varrho_\lambda) = - \varepsilon (\hbar \vec{\lambda})^2 e^{-i \vec{\lambda} \vec{r}_i}, \qquad (\hat{p}_\alpha^2 \varrho_\lambda) = Z \varepsilon (\hbar \vec{\lambda})^2 e^{-i \vec{\lambda} \cdot \vec{r}_\alpha}, \tag{A,16b}$$

we can already easily compute all the expectation values (2,26a) — (2,26e).

КРАТКОЕ СОДЕРЖАНИЕ

Я. Следзик, *Смодифицированное колективное описание Бома й Пинеса взаимодействия электронов в кристаллах, I.*

Сформулировано обобщенную теорию Бома—Пинеса взаимодействия электронов в трансляционных кристаллических решётках. Чтобы устанить трудности в нормировани векторов состояния предложено ряд новых добавочных условий. В результате показано, что теория Бома—Пинеса может быть считана верной во всякой степени приближения. В этой обработке предполагается, что электроны связаны с ионами (приближение тесной связи). Поляризации ионных оболочек не учтено по поводу осложнения, которое вводит рассматривание этого явления.

REFERENCES

Adams, E. N., *Phys. Rev.* **98,** 947 (1955a), Ibid. **98,** 1130 (1955b).
Bogoliubow, N. N. and Zubarev, D. N., *Zh. Eksper. Teor. Fiz.* **28,** 129 (1955).
Bohm, D. and Pines, D., *Phys. Rev.* **82,** 625 (1951a), Ibid. **85,** 338 (1952b), Ibid. **92,** 609 (1953a).
Galasiewicz, Z., *Acta phys. Polon.* **14,** 50 (1956a), Ibid. **15,** 79 (1956b), Ibid. **17,** 63 (1953a).
Ichikawa, Y. N., *Prog. Theor. Phys.* **18,** 247 (1957).
Kanazawa, H., *Prog. Theor. Phys.* **13,** 227 (1955a), Ibid. **18,** 247 (1957b).
Langmuir, I. and Tonks, L., *Phys. Rev.* **33,** 195 (1929).
Zubarev, D. N., *Zh. Eksper. Teor. Fiz.* **25,** 548 (1953).

CORRECTIONS AND ADDITIONAL REMARKS TO THE PAPER: SELF-DEPOLARIZATION AND DECAY OF PHOTOLUMINESCENCE OF SOLUTIONS, ACTA PHYS. POLON. **14**, 295 (1955)

By A. Jabłoński

Physics Department, Nicholas Copernicus University, Toruń

(Received July 11, 1958)

My collaborators, M. Frąckowiak, A. Bączyński and M. Czajkowski, linked my attention to an error, which occured in eqs. (35), (35a) and (36) of the above paper, consisting in writing $\frac{\nu^{k-1}}{(k-1)!}$ instead of $\frac{\nu^{k-1}}{k!}$. These equations have to describe the degree of polarization of fluorescence of a solution as a function of concentration of luminescent molecules (ν denoting the concentration multiplied by the volume of the active sphere, i.e. the average number of luminescent molecules within this sphere). I refrain from quoting here the corrected form of all these equations, but should like to quote eq. (36) (in which the effect of quenching or of the self-quenching is neglected), since this equation was compared with experimental results of Mlle Cauchois (1930). It should read:

$$P = 3P_0 \frac{\sum_{k=1}^{\infty} \frac{\nu^{k-1}}{k!} \frac{2k}{k+1}}{\sum_{k=1}^{\infty} \frac{\nu^{k-1}}{k!} \left[k(3-P_0) + \frac{2kP_0}{k+1} \right]}, \tag{1}$$

where P denotes the degree of polarization, and P_0 is the value of P for $\nu = 0$. For $\nu \ll 1$ it becomes approximately

$$\frac{1}{P} - \frac{1}{3} \approx \left(\frac{1}{P_0} - \frac{1}{3} \right) \frac{1+\nu}{1+\frac{2}{3}\nu} \approx \left(\frac{1}{P_0} - \frac{1}{3} \right) \left(1 + \frac{1}{3}\nu \right). \tag{2}$$

Cz. Bojarski and M. Frąckowiak (private communication) pointed out that eq. (1) may be written in a closed form:

$$P = \frac{6P_0}{(3-P_0)\frac{\nu^2}{\nu - 1 + e^{-\nu}} + 2P_0}. \tag{3}$$

Expressions (1) and (3) fit very well to the experimental results of Mlle Gauchois for not to high concentrations of solution (fluorescein sodium in glycerol). However her last point, for the highest concentration (10^{-2} g/cm^3) deviates very considerably from the calculated curve (experimental value $P = 0.16$, calculated value $P = 0.11$). This deviation may be due either to the neglected effect of the self-quenching, or possibly also to some other simplifications introduced by derivation of eqs. (1) and (3).

REFERENCES

Cauchois, Y., *J. Chim. phys.*, **27**, 336 (1930).

ERRATA

A. Jabłoński, Decay of Photoluminescence of Solutions, *Acta Phys. Polon.* **16**, 471 (1957).

p. 474, line 6, the expression

$$A_k = B \frac{\gamma_k}{\Gamma_k} \frac{\nu_k^{k-1}}{(k-1)!}$$

should read

$$A_k = B\gamma_k \frac{\nu^{k-1}}{(k-1)!}$$

LETTERS TO THE EDITOR

THE INFLUENCE OF POLARIZATION OF LIQUID CRYSTAL MOLECULES ON THE SCATTERING OF SLOW NEUTRONS

By J. A. Janik, S. Kraśnicki, A. Murasik

2-nd Laboratory of the Institut of Nuclear Research, Cracow
Physical Institute of the Jagiellonian Univ., Cracow
1-B Laboratory of the Institut of Nuclear Research, Warsaw

(Received October 20, 1958)

1. Introduction

On the basis of existing theories of the scattering of slow neutrons by molecules one should expect an influence of molecular polarization on the scattering cross section. This is due to the fact that the final formulas for the cross section *vs.* energy are the result of an averaging over a random molecular orientation for an unpolarized sample and for a non-random distribution for a polarized one.

The substance we chose, for an investigation of this effect was *p*-azoxyanisol, which belongs to a so called liquid crystal group [1]. The structure of a *p*-azoxyanisol molecule is shown in Fig. 1. Due to a strong diamagnetic anisotropy of these molecules one gets a so called nematic phase in the temperature interval of about 116—134°C. In this phase the molecular interaction is so strong that „swarms" or „domains" of perfectly ordered molecules are formed. An external amgnetic field causes an ordering of these domains so that a liquid of almost complete polarization of molecules can be obtained. The long axes of the molecules are then parallel to the magnetic field.

In the present paper the results of neutron transmission measurements for polarized and unpolarized *p*-azoxyanisol at various temperatures are given together with a simple interpretation of the effect obtained.

2. Apparatus

The neutron beam was obrained in the Polish reactor „EWA" at Świerk near Warsaw. The collimated beam (angular spread 20′) was monochromatized by reflection from an Al crystal. The various energies at which measurements were made were obtained by appropriate crystal settings.

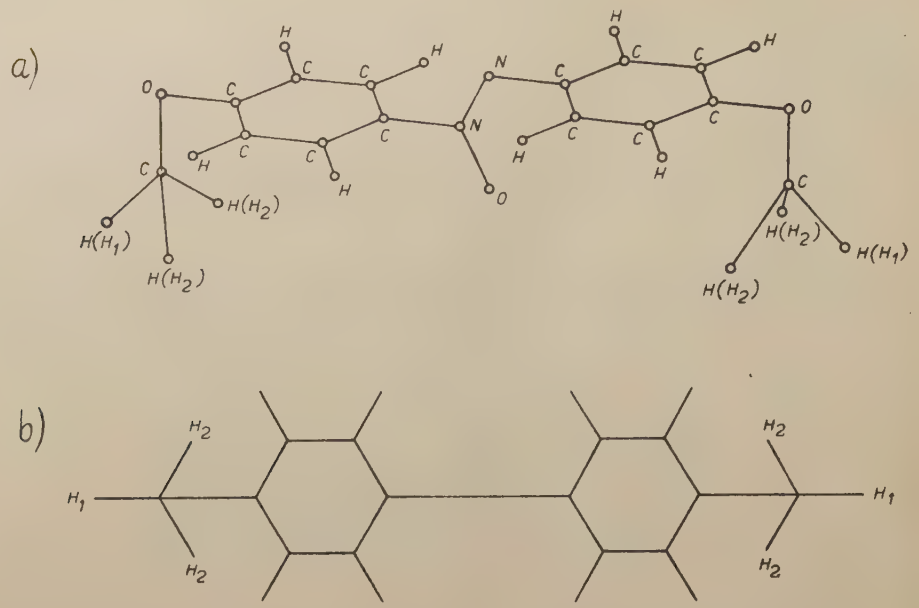

Fig. 1. Geometrical structure of the *p*-azoxyanisol molecule ($CH_3O—C_6H_4—N_2O—C_6H_4—OCH_3$) a. Axenometric view, b. View from above

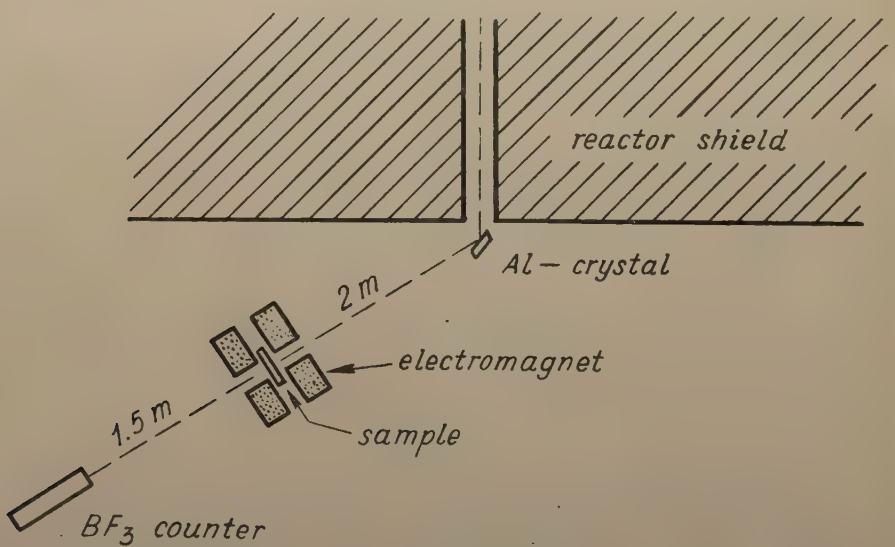

Fig. 2. Geometry of the measurements

As neutron detector a BF_3-counter was used. The scattering sample in a flat Al vessel was placed between the poles of an electromagnet. Neutrons passed through a narrow (0.7 cm of diameter) channel made in the poles, parallel to magnetic field and to the long axes of the polarized molecules. The geometry of measurements is shown in Fig. 2.

The flat Al vessel containing the substance was heated at the edges so that the temperature interval of 116—140°C could be obtained. The temperature gradient between the heated edges and the center of the vessel was less than 0.5°C. The thickness of *p*-azoxyanisol in the vessel was 3 mm.

We had at our disposal three *p*-azoxyanisol samples of different origin. Their polarizibility was tested by measuring the change of dielectric constant when a magnetic field of some thousands of Oe was applied.

The measurements of neutron transmission were made with the magnetic field and without it at low neutron energy (0.037 eV and 0.031 eV) and also at a higher energy (0.25 eV).

3. Experimental results

The experimental results are shown in the Fig. 3. It can be seen that the scatter of experimental data is larger than the limits of statistical errors, the qualitative reproducibility of the observed effect is however evident. In the temperature interval corresponding to the liquid crystal phase a regular transmission decrease of about 1—2% is obrained by applying a magnetic field for the neutron energy of 0.037 eV and 0.031 eV (low energy). For higher neutron energy a transmission increase of this same order of magnitude is observed. Above the transition point (about 134°C) no effect is obtained as the isotropic phase does not allow any polarisation of sample

4. Theory

Our interpretation of the effect is based on the theory of T. J. Krieger and M. S. Nelkin [2]. Not expecting any quatitative agreement looking however for a qualitative one we assume that only two movements in the molecule are responsible for the observed effect. The first is a hindered internal rotation (torsional oscillation) of two CH_3-groups around the CO-axes of the methoxy groups and the other consists in a free rotation of the whole molecule around its long axis. We believe that due to intermolecular interaction a rotation of the molecule around other axes of inertia can not occur and vibrational motions in the molecule (except the torsional oscillation) contribute to the scattering cross section to the same extent in the presence of polarisation as in a disorder.

Assuming additionally that neutron scattering is elastic in our case we get the following basic formula for the scattering cross section per proton of the CH_3-group in the molecule:

$$\sigma_H = \frac{a_{HH}}{2\pi} \int_{-\infty}^{+\infty} dt \int_0^{\pi} d\vartheta \int_0^{2\pi} d\varphi \left\{ \sin\vartheta \exp\left[-\frac{1}{2} (\hat{\varkappa}.\mathfrak{M}^{-1}.\hat{\varkappa}) (it + Tt^2) \right] \exp\left[-\frac{(\hat{\varkappa}.\hat{c}_0)^2}{2\omega_0} \right] \right\}$$

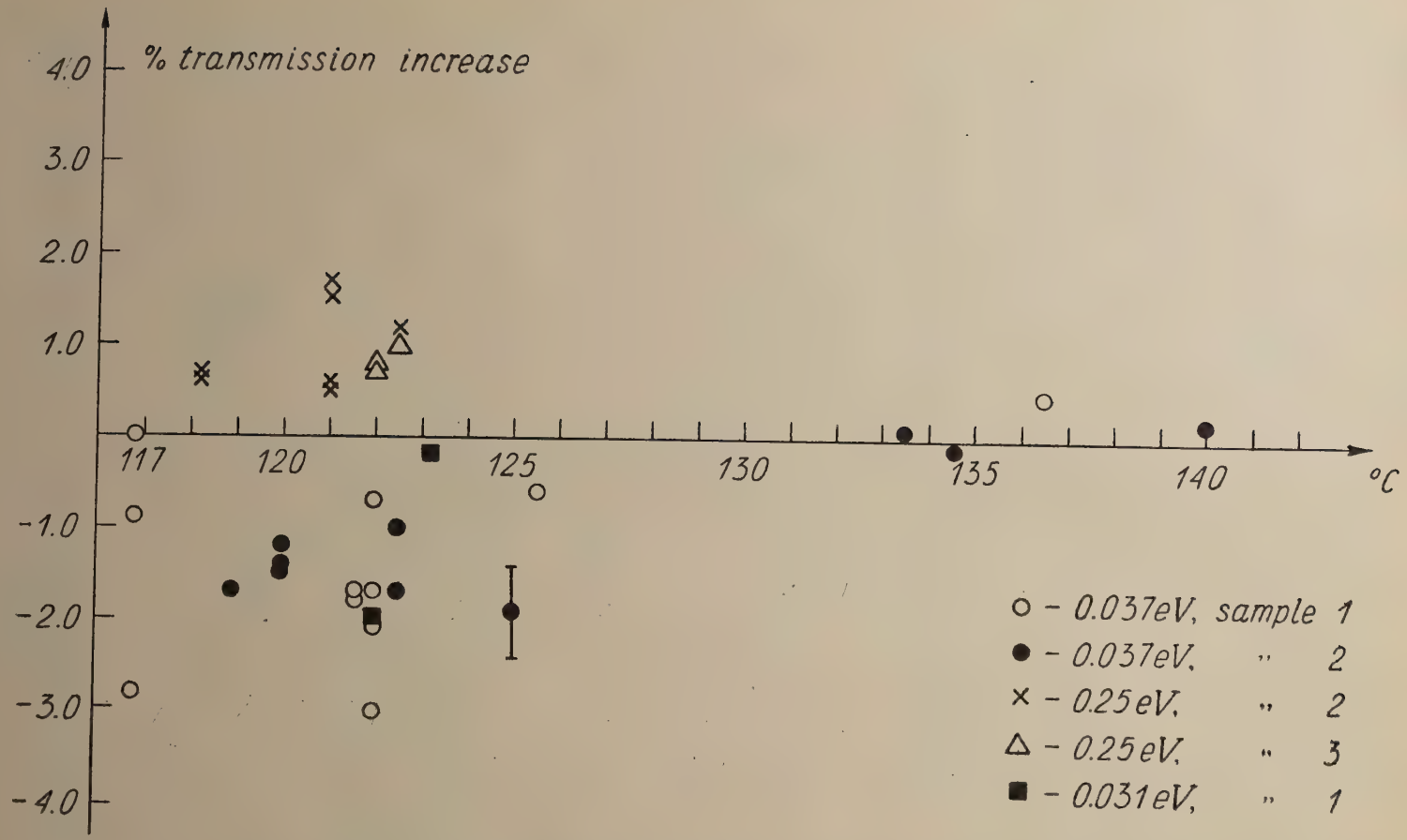

Fig. 3. Experimental results. Per cents of transmission increase due to polarization of sample are plotten *vs.* sample temperature. Negative per cents of transmission increase denote a transmission decrease.

where: a_{HH} — denotes the free proton scattering length,
$\hat{\varkappa}$ — momentum gained by the neutron,
$\mathfrak{M}$ — mass tensor of the molecule,
T — temperature of the sample,
ω_0 — frequency of the torsional oscillation and
$\hat{c}_0$ — amplitude vector of the torsional oscillation.

The assumed torsional oscillation of frequency of 300 cm^{-1} causes a difference in the second exponent of the above formula between the polarized and unpolarized molecules. The assumed free rotation of the molecule around its long axis is responsible for an analogous difference in the first exponent due to the mass tensor $\mathfrak{M}$. Final results of calculations are shown in the Table 1.

Tabele 1.

Neutron energy	Change of the cross section due to polarization			
	per proton H_1	per proton H_2	per 1 proton of the CH_3-group	per 1 proton of the molecule
0.037 eV	+5.59%	−0.90%	+3.69%	+0.53%
0.100 eV	+10.13%	−8.98%	−7.83%	−1.12%

Although we were not able to perform our calculations for 0.250 eV we think the the observed effect is qualitatively explained. In fact for low energy we got an increase of the scattering cross section which corresponds to the decrease of the transmission in agreement with the experimental results. Similarly for higher energy a decrease of the cross section, which we got from calculations, corresponds to the experimentally obtained increase of the transmission.

It should be mentioned here that the possibility of free rotation of the molecule around its long axis causes not only a change of H_1 and H_2 cross sections due to polarization but also a change of the cross sections of protons of benzene-rings. This should be superposed on the values of the Table 1 and should cause a slight increase of the figures of the last column in better agreement with the experiment.

5. *Acknowledgements*

We would like to express our thanks to Prof. Dr H. Niewodniczański, Prof Dr M. Mięsowicz, Prof. Dr M. Jeżewski, Doc. Dr. Piech and Doc. B. Buras for kind interest and valuable discussions as well as to Doc. Dr J. Schoen and Dr Wojciechowski for the preparation of investigated samples.

REFERENCES

[1] „Liquid Crystals and Anisotropic Melts", Trans. Farad. Soc. **29,** (1933)
[2] T. J. Krieger, M. S. Nelkin — *Phys Rev.* **106,** 290 (1957).

THEORETICAL CALCULATION OF THE SLOW NEUTRON SCATTERING CROSS SECTION OF ETHYLEN — MOLECULE

By J. A. Janik, F. Maniawski, H. Rżany

2-nd Laboratory of the Institute of Nuclear Research, Cracow

(Received November 11, 1958)

In 1957 a paper of T. J. Krieger and M. S. Nelkin [1] has appeared in which a formula for the scattering cross section of slow neutrons by gazeous molecules was given. The K-N theory introducing some mathematical approximations in averaging over molecular orientations forms a step forward as compared to Messiah [2] theory which gave an accurate general formula for the cross section, the detailed calculations however were limited to simple molecules of the H_2 and CH_4 — type. The theory of Krieger and Nelkin was proved by them for H_2 and CH_4 — molecules. The calculated cross section *vs.* energy values were in agreement with experimental ones in the energy limits corresponding to the limits of validity of the theoretical assumptions.

It seems to be interesting to prove if the theory is adequate for some other molecules. In the present paper the results of our calculations and a comparison with the experiment are given for C_2H_4 — molecule.

The most troublsome was the evaluation of the quantity $\overline{\omega}$ (of the K-N theory) which contains amplitudes of vibrations for all vibrational modes of the molecule. The amplitudes can be calculated from the normalization condition when their ratios are known from the solutions of the secular equation [3], [4]. For C_2H_4 — molecule we were able to use the solutions of the secular equation obtained by M. Rytel [3].

Results are shown in the Fig. 1. The full line shows the results of the present calculations. Circles represent Melkonians [5] experimental data for gazeous C_2H_4. The agreement is very good in the energy interval of 0.005 eV to about 0.07 eV. Above 0.07 eV (ca 560 cm^{-1}) a deviation between theoretical results and experimental points occurs. This deviation can be understood when one remembers that K-N theory gives a formula for the elastic scattering of neutrons only (in respect to vibrations) and the experimental data contain a contribution of inelastic scattering above a threshold energy. The only fact which we do not understand is this, that the lowest excited vibrational level of C_2H_4 — molecule lies at the 810 cm^{-1} and the discrepancy between the theory and experiment for neutron scattering starts to appear at about 560 cm^{-1}.

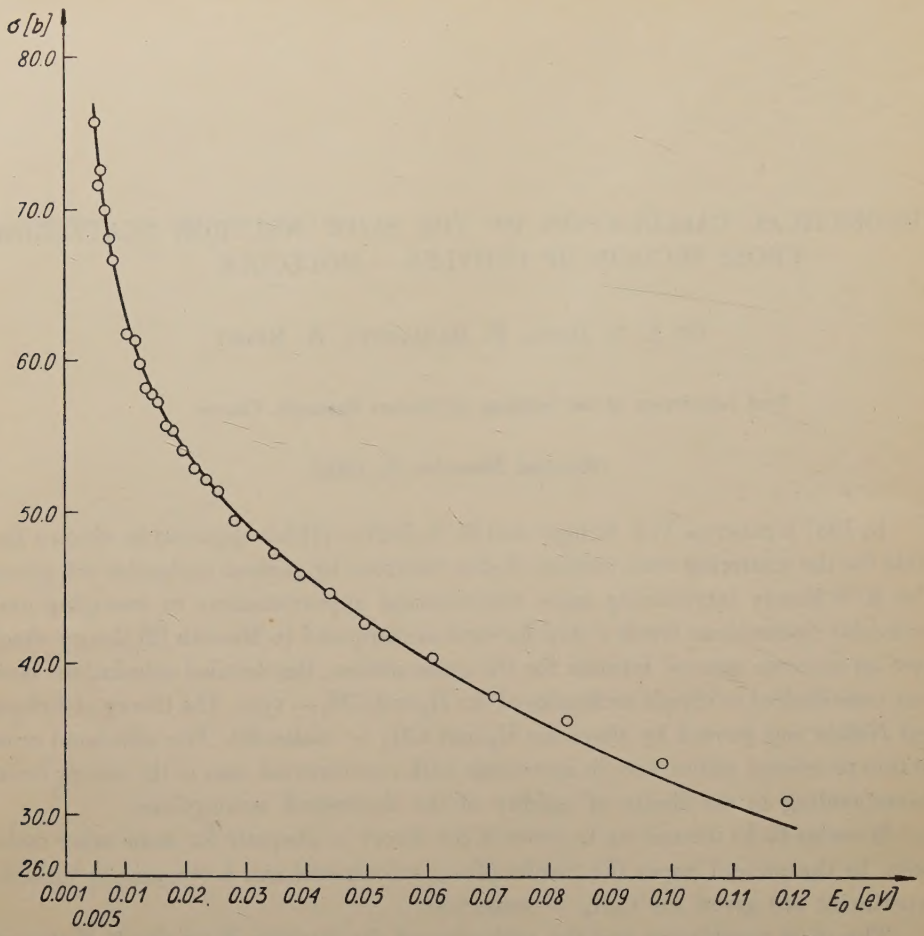

Fig. 1

An assumption of the existence of a lower than 810 cm^{-1} level in ethylen — molecule could be a possible solution of this difficulty.

We would like to express our thanks to Prof. Dr H. Niewodniczański for his kindest interest as well as to Mr. M. Rytel for valuable discusisons and kindest informations about the not yet published solutions of the secular equation for the C_2H_4 — molecule.

REFERENCES

[1] T. J. Krieger and M. S. Nelkin, *Phys. Rev.* **106,** 290 (1957).
[2] A. H. Messiah, *Phys. Rev.* **84,** 204 (1951).
[3] M. Rytel (private communication).
[4] Arnett and Crawford, *J. Chem. Phys.* **18,** 118 (1950).
[5] E. Melkonian, *Phys. Rev.* **76,** 1750 (1949).

REVIEWS OF BOOKS

Wilhelm Macke

Wellen, Ein Lehrbuch der Theoretischen Physik Akademische Verlagsgesellschaft, Leipzig 1958.

Das vorliegende Werk soll den zweiten Band einer Lehrbuchreihe der theoretischen Physik bilden, deren Unterteilung — nach der Ansicht der Verfassers — dem gegenwärtigen Stand der Erkenntnis besser entsprechen wird, als die bisher übliche Einordnung in Mechanik, Akustik, Optik, Thermodynamik usw. Die neue Einteilung soll nach folgenden Themen durchgeführt werden: 1. Teilchen, 2. Wellen, 3. Quanten, 4. Felder, 5. Statistik, 6. Relativität. Es bleibt abzuwarten, ob man in dieser Anordnung und in dieser Reihenfolge alle die Grundbegriffe und Grundgesetze der Physik konsequent und folgerichtig einführen können wird.

Schon im ersten Satz des Vorwortes finden wir die Erklärung, dass „unter 'Wellen' werden in diesem Buche alle physikalischen Vorgänge verstanden und dargestellt bei denen sich Energie ohne gleichzeitigen Materietransport durch den Raum hindurch fortpflanzt". Dadurch werden also prinzipiell alle Arten von „Materiewellen", die ja eben im Materietransport bestehen, von der Betrachtung ausgeschlossen. In der Tat werden diese Wellen in der Folge nirgends systematisch behandelt und nur an einigen Stellen kurz erwähnt. Es werden jedoch verschiedene Eigenschaften mechanischer und elektromagnetischer Wellen derart eingehend untersucht, dass sie als Illustrationen ähnlicher Eigenschaften von „Elektronenwellen", „Schrödinger-Wellen" u dgl. sehr gut dienen können. Schade, dass der Verfasser nach seiner pädagogisch so sorgfältigen, anschaulichen Art auch die charakteristische Besonderheit der „de Broglie-Wellen" nicht besprochen hat, die darin besteht, dass ihre Amplitude nur bis auf eine multiplikative Konstante bestimmt ist.

Die neun Kapitel aus denen der referierte Band besteht zerfallen deutlich in zwei Teile von ziemlich verschiedenem Charakter. Die vier ersten (die zusammen 180 Seiten umfassen) bilden ein abgeschlossenes Ganzes, das nach der bis jetzt üblichen Einteilung der Physik vollständig in der Mechanik (mit Akustik) Platz finden könnte. Der Referent betrachtet es als den wertvollsten, schönsten und originellsten Teil des ganzen Lehrbuchs. Zuerst werden im ersten Kapitel über Schwingungen der harmonische Oszillator und dessen ungedämpfte, gedämpfte und erzwungene Schwingungen, sowie die Fourierschen Reihen und Transformationen besprochen, sodann geht der Verfasser im 2. Kapitel über zur Behandlung zweier gekoppelter Oszillatoren, die

er dann zu „Oszillatorketten" verallgemeinert, d.h. zu Systemen von endlich vielen — im Grenzfall unendlich vielen — gekoppelten linearen Oszillatoren, und untersucht die Eigenschaften mechanischer Wellen, die sich längs dieser Oszillatorketten ausbreiten. Das gibt ihm eine gute Gelegenheit um solche wichtige Begriffe wie Phasengeschwindigkeit, Gruppengeschwindigkeit, Energietransport u. dgl. anschaulich zu erklären. Besonders schön ist der Übergang von dem Paar gekoppelter Oszillatoren mit seinem hin und her pendelnden Energietransport, über die Oszillatorketten mit endlichem N, in welchen dieses Pendeln mit wachsendem N immer langsamer wird, bis zu unendlichen Oszillatorketten, wo der Energietransport endlich ganz in einer Richtung erfolgen kann. Im 3. Kapitel wird die Oszillatorkette durch Grenzübergang zum Seil. Im 4. Kapitel endlich, durch eine Verallgemeinerung der Seiltheorie auf den dreidimensionalen Raum, geht der Verfasser über zur Behandlung der Akustik.

Die nächsten fünf Kapitel (240 Seiten) tragen keinen so einheitlichen Charakter mehr. Es wird in ihnen so viel Stoff verarbeitet, dass sie eher als ein Repetitorium, eine Beleuchtung anderweitigen Kenntnisse vom Standpunkte der Wellentheorie und nicht als Teil eines eigentlichen Lehrbuchs erscheinen. Mit diesem Vorbehalt aber anthalten sie sehr viel Lesenswertes und oft Originelles. Die Kapitel 5—7. handeln hauptsächlich von elektromagnetischen Wellen in allen ihren Erscheinungsformen, einschliesslich der geometrischen Optik, der Abbildungstheorie, des Abbeschen Sinussatzes, der Dispersion, der Metalloptik, der Kristalloptik, der Materie im Magnetfeld und vieles mehr.

Die letzten zwei Kapitel sind der Relativitätstheorie gewidmet. Sie enthalten auch viele interessante und anderswo selten behandelte Einzelheiten, als Ganzes aber gefallen sie dem Referenten viel weniger als der Rest des Buches. Das Bestreben nach möglichst eingehender Anknüpfung an die klassische Mechanik wurde so weit getrieben, dass manche Leser zu der irrigen Meinung geführt werden könnten, dass die Einsteinsche Lehre nichts weiter ist als eine Ergänzung der Newtonschen Mechanik durch Einführung der Fitzgerald-Lorentzschen Längenkontraktion und der Einsteinschen Zeitdilatation. Die genaue Stelle des Übergangs von den vorbereitenden, „vorrelativistischen" Überlegungen zur neuen Auffassung ist nicht deutlich hervorgehoben.

Nach der Meinung des Referenten enthält auch das Buch viele verbeserungsbedürftige Einzelstellen und Ausdrücke, die aber den Wert des ganzen Werkes nur wenig beeinträchtigen. Im Grossen und Ganzen ist das vorliegende Buch zweifellos als ein originelles und sehr lehrreiches Lehrbuch zu betrachten, das allen Lernenden als Hilfslehrbuch beim Studium der theoretischen Physik wärmstens empfolen werden kann. Wie schon hervorgehoben, werden sie dort keinen Lehrgang der Wellenmechanik finden, doch wird ihnen das Mackesche Lehrbuch das nachfolgende Studium der Wellenmechanik sicher sehr erleichtern und vielleicht auch dazu beitragen diese neue Lehre etwas weniger formal anzufassen, als das in den meisten heutigen Lehrbücher geschieht (mit der lobenswerten Ausnahme der Hundschen Darstellung in „Materie als Feld").

Jan Weyssenhoff